# Flexural Behavior of Axially and Laterally Loaded Piles under Liquefied Soil Conditions

A Thesis Submitted

in Partial Fulfillment of the Requirements

for the Degree of

Master of Technology

*by*

Meera R.S

*to the*

Department of Civil Engineering,

Indian Institute of Technology Kanpur

May, 2005

*Dedicated*

*to*

*My Parents*

# CERTIFICATE

This is to certify that the work contained in the thesis entitled "Flexural Behavior of Axially and Laterally Loaded Piles under Liquefied Soil Conditions", by Meera R.S, has been carried out under my supervision and this work has not been submitted elsewhere for a degree.

May, 2005

**Dr. P. K. Basudhar,**
Professor,
Department of Civil Engineering,
Indian Institute of Technology
Kanpur – 208 016.

# ABSTRACT

The present work deals with the prediction of the flexural behaviour of axially and laterally loaded pile foundations under liquefied soil conditions. Pseudo-static analysis has been carried out by taking into consideration the combined effect of axial load and lateral load. Based on the available literature effect of degradation on the modulus of subgrade reaction due to soil liquefaction has been incorporated in the analysis. Using MATLAB, computer program has been developed for the same and the predicted behaviour of the pile has been found to be in good agreement with the observed values in the field. Parametric studies have been carried out to evaluate the influence of pile and soil properties on the flexural response of piles during liquefaction. The obtained results have been presented in dimensionless design charts for various conditions of pile head fixity and ground conditions. The present study highlights the importance of considering the axial load from the superstructure along with the inertia forces from the superstructure and the kinematic forces from the liquefied soil in the design of pile foundations in liquefiable areas. The significance of densification of the soil in the liquefiable areas and provision of an adequate top nonliquefied soil cover in the appreciable reduction of the destruction has been substantiated. The study also points out the necessity of finding the proper design parameters in both normal and liquefied soil conditions.

# ACKNOWLEDGEMENT

I am deeply indebted to my thesis supervisor Prof P.K.Basudhar for his inspiring guidance, valuable suggestions, constant encouragement and overall supervision throughout the progress of my work. The way he made me think and work has an everlasting impact on my career and life. I express my deep sense of gratitude to my thesis supervisor for giving me valuable advices and knowledge and making my life at IIT Kanpur a memorable one. I am expressing my sincere thanks to his family members for their support.

I am thankful to the faculty of Geotechnical Engineering, Prof. Sarvesh Chandra and Dr. Nihar Ranjan Patra for their technical support during the study. I am grateful to the Geotechnnical Engineering Laboratory staff for their cooperation.

I am grateful to my classmates Sutapa, Arindam, Pradipta, Bappa, and Shyam for their immense help and encouragement in all situations. I am thankful to Paritosh, Abhik, Saxena ji and research scholars Priti, Sarat da, Koushik da and Shanker da for their valuable suggestions and cooperation.

It is difficult to find words to express my sincere thanks to my friends Vanitha, Neeraja, Smitha, Lyci, Trishi and Harikrishna who were always there to help and support me, encouraged me in situations of trouble and made my stay at IIT Kanpur a memorable one.

Last but not the least, I am deeply indebted to my father, mother and sister for their love, ceaseless inspiration and constant encouragement which helped me to make all this possible and for that, and everything else, I dedicate this to them.

# CONTENTS

**CHAPTER 4**

# LIST OF SYMBOLS

| | |
|---|---|
| a, b, c, d, e, f, g, h | Coefficients of boundary conditions |
| A | Stiffness matrix |
| B | Force vector |
| C | Modified displacement coefficient matrix |
| D | Diameter of the pile |
| $E_p$ | Modulus of elasticity of the pile |
| $E_s$ | Modulus of elasticity of the soil |
| $E_0$ | Modulus of deformation of the soil |
| F | Displacement coefficient matrix |
| {g} | Ground displacement vector |
| $g_{max}$ | Maximum possible permanent horizontal ground displacement of the liquefied soil |
| $g_{rs}$ | Permanent horizontal displacement of the level ground far away from the water front |
| $g_w$ | Displacement of the quay wall |
| $g_x$ | Horizontal ground displacement at a distance x from the waterfront |
| g (z, x) | Permanent horizontal ground displacement profile with depth, z at a distance, x from the waterfront |
| $g_0$ | Permanent horizontal ground displacement at the waterfront |
| G | Modification factor |
| H | Horizontal load factor |

| | |
|---|---|
| $H_T$ | Horizontal load applied at the pile top |
| $I_p$ | Moment of inertia of the pile |
| J | Coefficient matrix |
| k | Matrix for the modulus of subgrade reaction |
| $k_h$ | Modulus of subgrade reaction |
| $k_{hn}$ | Modulus of subgrade reaction for non-liquefied soils |
| K | Stiffness factor |
| L | Length of the pile |
| $L_s$ | Affected distance of lateral spreading |
| $L_x$ | Location factor |
| $L_1$ | Thickness of the top non-liquefiable soil cover |
| $L_2$ | Thickness of the liquefiable layer |
| $L_3$ | Length of pile further embedded into the bottom non-liquefiable layer |
| L/D | Length to diameter ratio |
| M | Moment factor |
| $M_D$ | Developed bending moment |
| $M_T$ | Moment applied at the pile top |
| M' | Non-dimensional bending moment coefficient |
| M* | Maximum non-dimensional bending moment coefficient |
| n+1 | Number of elements |
| N | Standard penetration test value |
| $N_a$ | Axial load distribution matrix |
| O | Applied force vector |
| p | Soil pressure |

| | |
|---|---|
| $P$ | Axial load applied at the pile top |
| $P_z$ | Axial load variation with depth z |
| $Q$ | Soil modulus to soil strength ratio |
| $r$ | Non-liquefied depth factor |
| $R$ | Pile flexibility factor |
| $s$ | Liquefied depth factor |
| $sl$ | Gradient of the surface topography |
| $S_f$ | Stiffness degradation parameter |
| $S_u$ | Un-drained strength of the soil |
| $t$ | Embedded depth factor |
| $T$ | Lateral soil force vector |
| $U$ | Matrix for the equilibrium conditions |
| $V$ | Vertical load factor |
| $x$ | Distance of the location of the pile from the waterfront |
| $y$ | Deflection of the pile |
| $y_r$ | Relative displacement of the pile and the soil |
| $y_1$ | Reference value for $y_r$ |
| $Y$ | Non-dimensional deflection coefficient |
| $Y^*$ | Maximum non-dimensional deflection coefficient |
| $z$ | Depth |
| $Z$ | Non-dimensional depth coefficient |
| $\infty$ | Axial load distribution ratio |
| $\beta$ | Axial load variation coefficient |

# LIST OF FIGURES

# LIST OF TABLES

# Chapter 1

# INTRODUCTION

## 1.1 General

In seismically active zones, the performance of pile foundations are significantly affected due to soil liquefaction especially when there is lateral movement of the liquefied soil. The lateral spreading of loose saturated sands causes substantial damage to isolated pile foundations. There are several well documented case histories in this regard from the 1964 Niigata earthquake in Japan (Hamada .et al 1986) and the 1995 Kobe earthquake (Tokimatsu and Asaka 1998; Ishihara .et al 1998).The damages which have been observed are the cracking and rupture of piles at shallow and deep elevations, rupture of pile connections, permanent lateral and vertical movements and rotations of pile heads and pile caps with corresponding effects on the superstructure.

Sometimes the deflection at the pile top is equivalent to that of the ground displacement where as in some cases the same is less due to the containments offered by the superstructure. Under such conditions the piles are generally exposed to large lateral soil pressures, including especially passive pressures from the top nonliquefied layer. In some cases the soil has failed even before the piles, with negligible bending stress and very small deformation of the pile head and superstructure, while in other cases, the piles have failed in bending, experiencing excessive permanent deformation and rotation at the pile heads. The observed damage and cracking to piles is often concentrated at the upper and lower boundaries of the liquefied soil layer where there is sudden change in soil properties, or at the connection with the pile cap. More damage tends to occur to piles when the lateral movement is forced by a strong nonliquefied shallow soil layer than when the piles are free to move laterally and the forces acting on them are limited by the strength of the soil.

Two types of lateral displacements are associated with liquefaction. They are the cyclic displacements in the course of dynamic softening of the soil and the permanent ground displacements due to lateral spreading of liquefied deposits. The field studies from the past earthquakes indicate that not only inertia force from the super structure such as the horizontal forces and overturning moments imposed on pile heads by the superstructures but also the forces arising from the dynamic and permanent ground displacements of liquefied and laterally spreading soils play an important role in the flexural behaviour of the pile. Hence the effects of lateral ground displacements should be properly considered in the design. Thus the key issue in the design of pile foundations in laterally spreading soils is to determine the forces developed due to ground displacement, defined as p-y relations.

Along with the above said dynamic forces, the pile carries the axial load of the super structure also during liquefaction, which is not taken into account in the current method of pile design under earthquake loading. The variation of axial load along the depth of the pile should also be considered for the safe and economic design of piles.

The offshore piles are subjected to combined loading and they are more to prone to the attack of liquefaction-induced lateral spreading. The analysis of the load-displacement behaviour of a pile is a soil-structure interaction problem. The analysis is complex for the piles subjected to both axial and lateral loads simultaneously. Again the non-availability of the correct information regarding the actual failure and deformation patterns of piles in liquefiable areas magnifies the complexity of the phenomenon. Analysis and design procedures for piles in liquefying grounds have large uncertainties due to a lack of physical data against which they can be evaluated and a lack of understanding of the physical mechanisms involved. The prediction of flexural behaviour of piles in liquefiable region is considered as a kinematic soil-structure interaction problem involving large permanent deformations of ground and piles. The deep foundation and the superstructure are assumed to be responding pseudostatically to the lateral permanent displacement of the ground.

A brief review of literature on the subject has been presented as follows for setting the over all objective and scope of the present thesis.

## 1.2 Review of literature

Importance of liquefaction related damage to the piles has been amply revealed during past earthquakes, from the 1964 Niigata earthquake to the 1995 Kobe earthquake. Permanent ground displacement induced by soil liquefaction is among the serious liquefaction hazards. Many civil engineering structures, especially lifeline facilities are mostly affected by the liquefaction induced permanent ground displacement. Hamada and O'Rourke(1992) investigated liquefaction induced permanent ground deformation and lifeline performance during past earthquakes in Japan and U.S.A. from the 1906 San Francisco earthquake to the 1989 Loma Prieta earthquake through the Japan-U.S. cooperative research program. Thereafter many studies have been performed in order to clarify the mechanisms of generation of liquefied ground flow and to estimate the value of permanent ground displacement. Analytical and experimental investigations were conducted to obtain the flexural response of pile foundations in liquefiable soils. The literature pertaining to theoretical and experimental studies are presented under different headings as follows.

### *1.2.1 Analytical investigations*

Mishra (1992) studied the response of laterally loaded piles under liquefied soil conditions and determined the ultimate lateral load capacity and the flexural behaviour of single piles under the condition of loss of support over the liquefied zone and lateral spreading. This study revealed the significant influence of liquefied zone on the lateral load capacity and the flexural behaviour. It has been shown that the top nonliquefied soil cover increases the load capacity and decreases the pile top deflection. The work was subsequently published by Basudhar et al (2002) with minor modifications.

O'Rourke et al (1994) made a comprehensive analytical study on the response of pile foundation to lateral spread. A computer code B-STRUCT had been developed and failure mechanisms on the basis of relative stiffness and applied axial load were determined. The results show quantitatively how the behaviour of deep foundation changes as the ground alters its force-displacement characteristics from a soil-like to a fluid-like medium. They have also developed dimensionless plots to determine surface soil displacement required to induce the formation of a plastic hinge under excessive bending conditions. The study consisted of three different models for liquefied soil-structure interaction, two subgrade reaction models with both drained and undrained strength parameters and a model to account for the viscosity of liquefied soil.

Bartlett and Youd (1995) presented an empirical model for predicting the amount of horizontal ground displacement resulting from liquefaction-induced lateral spread. The model was developed from multiple linear regression analysis of U.S. and Japanese case histories of lateral spread. The ground displacements has been correlated with the slope of ground conditions, earthquake magnitude, distance from the seismic energy source, thickness of the liquefiable sediments, and fine contents and particle size distribution.

Ishihara and Cubrinovsky (1998) investigated the effects of the lateral flow and softening of the soil due to liquefaction on the degradation of the spring constants to be considered in analyzing such problems. Back analyses were made for cases of damage to foundations for which field data such as soil properties and damage features were available. They made an extensive study on the geotechnical aspects of 1995 Kobe earthquake and found that degree of degradation in the spring constants depends on the relative displacement of pile and the surrounding soil. This study pointed out that the spring constant should be reduced to 1/1000 to 1/100 of the value used in normal soil conditions.

Tokimatsu et al (1998) investigated the causes of pile damage during the 1995 Hyogoken-Nambu earthquake. This study indicated the significant effects of ground movements on pile damage due to the occurrence of damages at the interface between

liquefied and nonliquefied layers. Based on the aerial photographic survey, the variations of lateral ground displacement with the distance from waterfront were formulated. They conducted p-y analysis in which pile foundations were subjected to cyclic or permanent ground displacements with or without the inertial force from the super structure.

Tokimatsu (1999) summarized the field performance of various pile foundations that experienced lateral ground spreading during past earthquakes and generalized the trends. A pseudo-static analysis were conducted for well-documented case histories of pile foundations to estimate the scaling factors for p-y springs of laterally spreading soils. It has been found that both the coefficient of the horizontal subgrade reaction of piles and the maximum reaction force of laterally spreading soils are 0.05-0.2 times those of nonliquefied soils.

Berril et al (2001) studied the effect of lateral spreading on the piled foundations. They have pointed out that the main threat to piled foundations in lateral spreading comes from loads imposed by the non-liquefied crust and not from the drag forces of the liquefied soil. They could find clear evidence of passive failure as the crust drove against the buried pier, piled through to buried ground.

Bhattacharya (2004) proposed a new theory of pile failure and it states that if piles are too slender they require lateral support from the surrounding soil so as to avoid buckling instability. The lateral support can fall to zero due to seismic liquefaction and hence a slender pile may then buckle. The study also points out that there is a fundamental omission in the seismic pile design in liquefiable areas and hence there is a need to reconsider the safety of existing piled foundations designed based on the current codes of practice. It suggests the need of having a minimum diameter of pile depending on the depth of liquefiable soil and discusses a way to identify the existing unsafe structures.

Klar et al (2004) conducted a numerical analysis of seismic soil-pile interaction in order to investigate the influence of flow mechanism. They employed two models-a simplified model, where pore pressure at any depth is that of the free field, and a more

complete model in which the pore pressure is associated with three dimensional flows. The soil behaviour was modeled by a non linear, quasi-hysteretic constitutive relation. The study concluded that there is a pore-pressure threshold below which both models yielded similar results.

Zhang et al (2004) proposed a semi empirical approach to estimate liquefaction-induced lateral displacements using standard penetration test or cone penetration test data. A lateral displacement index obtained by integrating the maximum cyclic shear strains with depth has been introduced. This study proposed empirical correlations between actual lateral displacement, the lateral displacement index, and geometric parameters of the ground.

### *1.2.2 Experimental investigations*

Hamada et al (1994) conducted laboratory tests on the fluid and solid characteristics of liquefied sand in order to understand the mechanical properties of liquefied sand. The mechanical properties of sand can be classified into the fluid characteristic of liquefied sand as viscous fluid and the solid characteristics of liquefied sand under large deformation. The study resulted in finding that viscosity of liquefied sand depends on relative density of sand and velocity of shear strain. Also it showed that the liquefied sand has a critical maximum shear strain which depend on relative density of sand.

Miyajima and Kitaura (1994) focused on the effects of force induced by liquefied ground flow on underground structures. Small scale tests were conducted and the viscosity coefficient was estimated using dropping ball method. The viscosity coefficient of completely liquefied sand was $10^5$ times greater than that of water and it has been concluded that this method can be used for the estimation of the force acting on underground structures in liquefied ground flow.

Ishihara et al (1999) conducted large-scale shaking table tests to examine the effects of lateral spreading on the performance of piles on a prototype scale. The soil behaviour in terms of pore water pressure, the effective stress paths, and ground displacements and the

pile behaviour in terms of bending moment, deflection, and crack development were evaluated.

Abdoun and Dobry (2002) presented results of physical modeling of deep foundations in the presence of liquefaction at the 100g-ton RPI centrifuge. The study signifies the importance of centrifuge modeling as an important tool to identify and quantify mechanisms involved during lateral spreading, calibrate analyses, and evaluate retrofitting strategies for pile foundations. They conducted experiments on single piles and pile groups. They also studied the effects of different soil profiles, mass and stiffening elements above ground to incorporate the effect of the super structure, and evaluated retrofitting strategies.

Tamari and Towhata (2003) studied the effect of liquefaction of backfill soil on the response of flexible underground structures. They conducted a series of shaking table tests on an aluminium fixed base structure model embedded in saturated cohesionless soil. They tried to develop stress-strain relationship as well as effective stress path of soil around the embedded structure. They observed that the natural period of the ground along with the structure and dilative nature of the soil significantly affects the type of soil-structure interaction.

From centrifuge model tests Ishihara (2004) found out the response of pile groups against seismically induced lateral spreading of soil. He examined the influence of number of piles and pile spacing on the total lateral force on piles. It was found that when the spacing between adjacent piles is more than 3 to 4 times the diameter of the pile, there is no interaction among piles and an individual pile in a group behaves as if it were an isolated single pile. As the spacing becomes smaller, group effects emerge. The total lateral force decreases if spacing decreases and if number of piles increases for the same spacing.

### *1.2.3 Summary of literature review*

The studies related to concerned problem conducted so far have given importance to the physical mechanisms of lateral flow and the prediction of ground displacement and the stiffness degradation parameter. Experimental studies made it possible to develop empirical

correlations for estimating the permanent ground movement, pressure exerted by the laterally spreading soil and degraded subgrade modulus arising out of softening of soils due to liquefaction. The effect of lateral spreading force on the flexural behaviour of piles and the analysis of laterally loaded piles under liquefied soil conditions have also been studied and relationships are available in the form of nondimensional charts. Significant effect of loss of support on the buckling of slender piles has also drawn the attention of researchers and a few works have been reported. But very few studies are conducted to find the response of piles under combined loadings and liquefied soil conditions. Also the effect of various soil parameters and pile characteristics on the flexural behaviour of piles in liquefiable areas has not been studied so far.

## 1.3 Objective of the present study

In view of the above literature review, an attempt is made in this thesis to analyze the flexural behaviour of the axially and laterally loaded piles under liquefied soil conditions. The external loads such as the axial load from the superstructure and the lateral loads due to the inertial effects, wind, waves etc are considered along with the kinematic effects of permanent ground displacement. The relative displacement of soil and pile and the degradation in the stiffness of soil due to liquefaction have been considered in the present analysis. Winkler's idealization of the soil to be made up of discrete springs is assumed to be valid in the study. The effect of various parameters like slenderness of the pile, flexural rigidity, location of the pile, end conditions of the pile, stiffness of the soil, slope of the surface topography, and depth of liquefaction on the flexural behaviour of the axially and laterally loaded piles under liquefied soil conditions have been considered in the present analysis.

## 1.4 Organization of the thesis

After describing the introduction, literature review, and the objective of the present study in this chapter, the remaining sections are covered as following.

The chapter two deals with the generalized procedure for finding the flexural response of pile foundations under liquefied soil conditions. The results obtained in the analysis and the discussions are presented in the Chapter 3. The conclusions obtained from the present study and the future studies of the concerned problem are described in Chapter 4. After these chapters, the references and the appendix are provided.

# Chapter 2

# GENERALIZED PROCEDURE FOR FINDING THE FLEXURAL RESPONSE OF PILES UNDER LIQUEFIED SOIL CONDITIONS

## 2.1 Introduction

In Chapter 1 the importance of considering the effects of pile-soil movement, degradation of subgrade modulus on the behavior of piles has been highlighted. In this chapter after introducing the problem undertaken, the development of a generalized procedure of analyzing the problem has been presented explaining the physical process of interaction of the soil spreading and its effect on the piles and taking these effects in the analysis.

## 2.2 Statement of the problem

The idealization of the pile and the soil profile surrounding the pile for the assessment of the soil-pile interaction is shown in Fig 2.1.A pile of length, L and diameter, D is embedded in a homogeneous saturated sand deposit. The water table is at the top of a liquefiable stratum of thickness, $L_2$, above which is the non-liquefiable soil cover of thickness, $L_1$. Below the liquefiable stratum there is a firm, non-liquefiable soil layer. The pile is further embedded by a distance $L_3$ into this non-liquefiable stratum. Over the depth $L_2$, the soil is in a liquefied state and the pile has lost the support of the soil either completely or partially. The pile is subjected to a lateral load, $H_T$ and a moment, $M_T$ along with an axial load, P at the top.

In this problem the possible movement of the liquefied soil in the liquefied zone has also been considered. The liquefied soil flows with a maximum velocity at the ground level and the maximum soil displacement, $g_x$ is at the ground surface and it varies to zero at the lower end of the liquefied zone. This flowing mass will cause a drag force on the pile. There

are various possible distributions of soil displacement. A trapezoidal distribution is applied in the figure.

Thus for given inputs of $L_1$ , $L_2$ , $L_3$ and soil and pile properties, the objective is to find the flexural behaviour of the pile when it has lost the supporting capacity of the soil to a great extent over the specified length of the pile due to soil liquefaction. The effect of different types of loading, end conditions and the various soil parameters on the deflection as well as bending moment distribution of the pile along the length has to be determined.

## 2.3 Analysis

### *2.3.1 Mechanism*

The main factor in the design of pile foundations in laterally spreading soils is to quantify the forces arising from ground displacement. The schematic illustration of the soil-pile-structure interaction in laterally spreading soils is shown in Fig.2.2. Prior to the development of pore water pressure; only the inertial force from the superstructure is dominant (Phase 1). During shaking, the pore pressure develops. As a result, the cyclic shear strain in the deposit increases, producing large cyclic ground displacements. In this phase (Phase 2) both the inertial force and the kinematic forces resulting from the cyclic ground displacements play important roles. Towards the end of the shaking, residual components of shear strain may accumulate, resulting in permanent horizontal ground displacements. The intensity of ground shaking may be negligibly small in this phase. As a result, the kinematic forces due to permanent ground displacements have an important effect on pile performance (Phase3). Hence it can be seen that piles in laterally spreading soils would experience most severe loading condition in either Phase 1, 2 or 3. But the final failure and deformation modes would be controlled by the loading condition in Phase3. Apart from these dynamic loads due to the inertia of the superstructure and the forces due to the slope movements, the pile foundation continues to experience the axial loads of the superstructure. In addition the piles are very often subjected to lateral loads especially in onshore and offshore structures.

Therefore structurally, piles are often considered to be slender beam-columns with lateral support from the surrounding soil.

### *2.3.2 Basic subgrade-reaction theory*

The mechanical behaviour of the liquefied soil is complex and imprecisely understood and, as such, a relatively simple procedure has been adopted in this analysis to account for soil strength and stiffness. The choice of a simple interaction mechanism helps in the evaluation of important parameters without introducing unnecessary complexity in the formulation of the problem. A simplified pseudo-static design method using Subgrade-Reaction theory based on Winkler soil model has been adopted for the determination of flexural behaviour of the pile foundations in laterally spreading soils. In the Winkler soil model the soil pressure, p and the lateral deflection, y at a point are assumed to be related through a modulus of subgrade reaction, $k_h$.Thus,

$$p=k_h y \tag{2.1}$$

where $k_h$ has the units of force/length$^3$.

### *2.3.3 Modulus of subgrade reaction ($k_h$)*

In the case of cohesionless soils the value of $k_h$ is not constant and generally varies with depth. For homogeneous cohesionless soil deposits $k_h$ generally increases linearly with depth. In order to take care of the arbitrary variation of the $k_h$ in the soil deposits it is convenient to correlate it with the SPT, N values. The modulus of subgrade reaction for nonliquefied soils, $k_{hn}$ proposed by Architecture Institute of Japan 2001, and Japan Road Association 1997 is,

$$k_{hn}=80E_0D^{(-0.75)} \tag{2.2}$$

$$E_0=0.7N \tag{2.3}$$

in which $E_0$ is the modulus of deformation in MN/m$^2$, N is the SPT N-value, and D is the diameter of the pile in centimeters. $k_{hn}$ is in MN/m$^3$

### 2.3.4 *Stiffness degradation*

As soil liquefies, the stiffness of soil degrades and from case studies it has been found that the modulus of subgrade reaction for the laterally spreading soils are reduced by a scaling factor termed as Stiffness degradation parameter, $S_f$ as compared to the normal soil condition where there is no liquefaction. The results of the back analyses of the case histories of pile deformations during the past earthquakes have shown that the stiffness degradation parameter varies from 0.001 to 0.01(Ishihara 1998). It was also shown that the degree of stiffness degradation in the laterally flowing soil deposits is related to the displacement of the pile relative to the surrounding soil. Hence these modifications are incorporated in the modulus of subgrade reaction for the laterally spreading soils. The degradation of $k_{hn}$ with increasing displacement is expressed as (Tokimatsu et al 2002)

$$k_h = (k_{hn} S_f) \frac{1}{1 + \left| y_r / y_1 \right|} \qquad (2.4))$$

where $y_r$ is the relative displacement between ground and pile and $y_1$ is the reference value of $y_r$, $S_f$ is the scaling factor for the liquefied soil.

### 2.3.5 *Modified subgrade-reaction theory*

In reality, equation (2.1) may not be effective for the Phases 2 and 3 where the ground displacements are large Hence the soil is assumed to be a Winkler-type material with lateral soil force proportional to the relative displacement between pile and soil. Thus the modified equation is

$$p = k_h (y - g(z, x)) \qquad (2.5)$$

Where, g (z, x) is the permanent ground displacement profile with depth, z, near the pile.

### 2.3.6 *Permanent ground displacement profile*

When lateral spreading occurs near the waterfront, the permanent horizontal ground displacement generally decreases towards inland with a maximum value at the waterfront. The affected distance of such lateral spreading from the waterfront, $L_s$ is given as (Tokimatsu et al 1998),

$$L_s/L_2=(25\sim100)\, g_0/L_2 \tag{2.6}$$

Where, $g_0$ is the permanent horizontal ground displacement at the waterfront and is defined as,

$$g_0= min\ (g_{max}, g_w) \tag{2.7}$$

in which $g_w$ is the displacement of the quay wall and $g_{max}$ is the maximum possible permanent ground surface displacement of the liquefied soil. $g_{max}$ is found out using the relation (Hamada 1986),

$$g_{max}=0.75\ (L_2)^{0.5}\ (sl)^{0.33} \tag{2.8}$$

where, $g_{max}$ and $L_2$ are in meters and sl is the slope of the base of the liquefied layer or the gradient of the surface topography whichever is maximum.

The horizontal ground displacement at a distance; x from the waterfront, $g_x$ is expressed in a normalized form as shown in Fig.2.3 and defined as (Shamato et al 1998)

$$g_x/g_0=(0.5)^{(5x/Ls)}+\{1-(0.5)^{(5x/Ls)}\}g_{rs}/g_0 \tag{2.9}$$

where $g_{rs}$ is the permanent horizontal displacement of the level ground far away from the waterfront and may be assumed to be zero.

The permanent horizontal ground displacement profile with depth, z at a distance, x of a laterally spreading deposit, g(z,x) may be approximated as (Tokimatsu 1999),

$$For\ z<L_1,\ g\ (z, x)= g_x$$

$$For\ z>L_1\ and\ z< (L_1+L_2),\ g\ (z, x) = g_x \left[\cos\left\{\frac{\pi(z-L_1)}{2L_2}\right\}\right]$$

$$For\ z> (L_1+L_2),\ g\ (z, x) =0 \tag{2.10}$$

### *2.3.7 Governing differential equation*

For solving the problem analytically, the axially and laterally loaded pile is considered as a special case of beam-column on elastic foundation with external load coming at the top boundary. For an elastic pile of constant stiffness $E_pI_p$ and diameter D embedded in a Winkler medium and subjected to an axial load, P at the pile head, the governing differential equation for the horizontal deflection, y along the pile is (Hetenyi 1946)

$$E_p I_p \frac{d^4 y}{dz^4} + \frac{d}{dz}\left[P_z \frac{dy}{dz}\right] = -pD \qquad (2.11)$$

in which $E_p$ and $I_p$ are Young's modulus and moment of inertia of pile respectively.

Substituting equation (2.5) in equation (2.11), we get

$$E_p I_p \frac{d^4 y}{dz^4} + \frac{d}{dz}\left[P_z \frac{dy}{dz}\right] + k_h D(y - g(z,x)) = 0 \qquad (2.12)$$

Solutions to the above equation can be obtained either analytically or numerically. Analytical solutions are available in convenient form for the case of constant $k_h$ along the pile. For other distributions of $k_h$, solutions are most conveniently obtained by using finite difference method. Analytical solutions can be obtained using variational methods also.

### *2.3.7 Finite difference form*

Referring to the Fig.2.4, the pile is divided into (n+ 1) elements of which (n-1) elements are of equal length and the other two, one at the top and the other at the bottom, are of half the length of these elements. The nodes of the elements are considered at their centers with one node at the head of the pile and the other at its tip. The soil is assumed to be an ideal, homogeneous, isotropic, and an elastic half space, having Young's modulus , $E_s$, which is unaffected by the presence of the pile. The axial load distribution depends on $E_s$ and hence this parameter is considered.

Using central difference technique, the governing differential equation can be expressed in finite difference form in terms of the nodal deflections. The development of

finite difference equation is shown in appendix. For a typical node i on the pile, equation (2.12) can be written as

$$\frac{E_p I_p n^4}{L^4}\left[y_{i-2} - 4y_{i-1} + 6y_i - 4y_{i+1} + y_{i+2}\right] +$$
$$\frac{Pn^2}{L^2}\left[\left\{\alpha_i - \frac{(\alpha_{i+1} - \alpha_{i-1})}{4}\right\}y_{i-1} - 2\alpha_i y_i + \left\{\alpha_i + \frac{(\alpha_{i+1} - \alpha_{i-1})}{4}\right\}y_{i+1}\right] \quad (2.13)$$
$$+ k_h D(y - g) = 0$$

where $\alpha_i = P_i/P$ and $P_i$ is the axial load acting at node i.

For nodes 2 and n, the equation consists of the displacements at the imaginary nodes considered at the top (node 0) and tip of the pile (node (n+2)). These imaginary displacements are to be evaluated by employing the relevant boundary conditions.

***2.3.9 Axial load distribution***

The data for load transfer or axial load distribution over the length of the pile can be obtained from the elastic solutions reported by Poulos and Mattes 1969.The variation of axial load with depth depends on stiffness factor, K and L/D.

***2.3.10 Equilibrium conditions***

The development of algebraic equations involves application of equilibrium conditions and appropriate boundary conditions. The equations so obtained are not sufficient to solve the problem as the number of equations are less than the number of unknowns and falls short by 2. Therefore we need to have two more equations that are obtained from the force and the moment equilibrium equations.

$\Sigma M$ *(about pile tip)* $=0$ gives,

$$(0.5n\text{-}0.125 \;\; n\text{-}1 \;\; n\text{-}2 \;\; \ldots\ldots\ldots \;\; n\text{-}i\text{+}1 \;\; \ldots\ldots \;\; 1 \;\; 0.125)\;\{p_i D\} = \frac{H_T n^2}{L} + \frac{M_T n^2}{L^2} \quad (2.14)$$

$\Sigma H = 0$ gives,

$$(0.5 \;\; 1 \;\; 1 \;\; \ldots\ldots\ldots \;\; 1 \;\; \ldots\ldots \;\; 1 \;\; 0.5)\;\{p_i D\} = \frac{H_T n}{L} \quad (2.15)$$

### *2.3.11 Boundary conditions*

The various boundary conditions considered in the present analysis are presented in Table 2.1. The end conditions are: Free-Free, Fixed-Free, Fixed-Pinned and Fixed-Fixed.

| End conditions | Relevant boundary values |
|---|---|
| Free-Free | $E_p I_p y'' = M_T$ ,at $z=0$<br>$E_p I_p y'' = 0$ ,at $z=L$ |
| Fixed-Free with sway | $E_p I_p y' = 0$ ,at $z=0$<br>$E_p I_p y'' = 0$ ,at $z=L$ |
| Fixed-Free with no sway | $E_p I_p y' = 0$ & $E_p I_p y = 0$ ,at $z=0$<br>$E_p I_p y'' = 0$ ,at $z=L$ |
| Fixed-Pinned | $E_p I_p y' = 0$ & $E_p I_p y = 0$ ,at $z=0$<br>$E_p I_p y'' = 0$ & $E_p I_p y = 0$ ,at $z=L$ |
| Fixed-Fixed | $E_p I_p y' = 0$ & $E_p I_p y = 0$ ,at $z=0$<br>$E_p I_p y' = 0$ & $E_p I_p y = 0$ ,at $z=L$ |

**Table.2.1** Boundary conditions

The respective finite difference equations for different end conditions are given in appendix.

Thus having (n+1) equations in (n+1) unknowns, the simultaneous equations can be solved using Gauss elimination technique. The equations can be nondimensionalised and expressed in the matrix form.

### *2.3.12 Matrix form of the simultaneous equations*

The matrix form of the equation is

$$AY=B \tag{2.16}$$

in which A is the stiffness matrix of size (n+1) , Y is the displacement column vector of size (n+1) and B is the force column vector of size (n+1).

The stiffness matrix, A is obtained by

$$A=C+J \tag{2.17}$$

where C is the modified displacement coefficient matrix of size (n+1) and J is a coefficient matrix of size (n+1).

C is defined as,

$$C=F+GN_a \tag{2.18}$$

in which F is the displacement coefficient matrix of size (n+1) .

$$F = \begin{bmatrix} 0 & 0 & 0 & 0 & 0 & 0 & 0 & 0 & 0 & 0 \\ a & b & c & d & 0 & 0 & 0 & 0 & 0 & 0 \\ 1 & -4 & 6 & -4 & 1 & 0 & 0 & 0 & 0 & 0 \\ 0 & 1 & -4 & 6 & -4 & 1 & 0 & 0 & 0 & 0 \\ . & . & . & . & . & . & . & . & . & . \\ . & . & . & . & . & . & . & . & . & . \\ 0 & 0 & 0 & 0 & 1 & -4 & 6 & -4 & 1 & 0 \\ 0 & 0 & 0 & 0 & 0 & 1 & -4 & 6 & -4 & 1 \\ 0 & 0 & 0 & 0 & 0 & 0 & e & f & g & h \\ 0 & 0 & 0 & 0 & 0 & 0 & 0 & 0 & 0 & 0 \end{bmatrix} \tag{2.19}$$

a,b,c,d,e,f,g,h are elements which depends on the boundary conditions and they are given in Table.2.2.

| End conditions | Elements of the F matrix | | | | | | | |
|---|---|---|---|---|---|---|---|---|
| | a | b | c | d | e | f | g | h |
| Free-Free | -2 | 5 | -4 | 1 | 1 | -4 | 5 | -2 |
| Fixed-Free(no sway) | [illegible] | 7 | -4 | 1 | 1 | -4 | 5 | -2 |
| Fixed-Free(with sway) | [illegible] | 7 | -4 | 1 | 1 | -4 | 5 | -2 |
| Fixed-Pinned | 0 | 7 | -4 | 1 | 1 | -4 | 5 | 0 |
| Fixed-Fixed | 0 | 7 | -4 | 1 | 1 | -4 | 7 | 0 |

**Table.2.2** Boundary condition coefficients

G is the modification factor expressed as

$$G=\frac{\pi}{4Rn^2\left(\frac{L}{D}\right)^2}\cdot\frac{P}{\frac{\pi D^2 E_s}{4}} \qquad (2.20)$$

where $R=E_pI_p/E_sL^4$ is the pile flexibility factor and $E_s$ is the modulus of elasticity of soil.

$N_a$ the axial load distribution matrix of size (n+1) is defined as,

for i=2 to n ,

$$N_a(i,i-1) = \left[\left\{\alpha_i - \frac{(\alpha_{i+1}-\alpha_{i-1})}{4}\right\}\right], N_a(i,i) = -2\alpha_I \qquad (2.21)$$

$$N_a(i,i+1) = \left[\left\{\alpha_i + \frac{(\alpha_{i+1}-\alpha_{i-1})}{4}\right\}\right], N_a(1,i) = \alpha_i^t - \alpha_i^b$$

$$N_a(1,1) = -\alpha_1^b, N_a(1,n+1) = \alpha_{n+t}^t \text{ \& } N_a(n+1,i)=0 \text{ for } i=1 \text{ to } n+1,$$

where $\alpha_i$, $\alpha_i^t$, $\alpha_i^b$ are the $P_i/P$ values at the centre, top and tip of a pile element respectively and they are shown in Fig.2.5.

The coefficient matrix of size (n+1), J accounts for the matrix for the horizontal load and moment equilibrium conditions, U and the matrix for the modulus of subgrade reaction, k.

J is expressed as

$$J=\left(\frac{[U]}{Rn^4}\right)*\frac{D[k]}{E_s} \qquad (2.22)$$

where $U =$

$$\begin{pmatrix} 0.5n-0.125 & n-1 & n-2 & - & - & n-i+1 & - & - & 1 & 0.125 \\ 0 & 1 & 0 & 0 & 0 & 0 & 0 & 0 & 0 & 0 \\ - & - & - & - & - & - & - & - & - & - \\ - & - & - & - & - & - & - & - & - & - \\ 0 & 0 & 0 & 0 & 0 & 0 & 0 & 0 & 1 & 0 \\ 0.5 & 1 & 1 & 1 & 1 & 1 & 1 & 1 & 1 & 0.5 \end{pmatrix} \tag{2.23}$$

The matrix for modulus of subgrade reaction k is a diagonal matrix of size (n+1) and is defined as

for i = 1 to n+1.

$$k\ (i,\ i)\ = k_h\ \ at\ node\ i. \tag{2.24}$$

The displacement column vector, Y is defined as

for i = 1 to n+1.

$$Y(i) = y_i/D \tag{2.25}$$

The force vector B can be found out using the relation

$$B = O + T \tag{2.26}$$

where O is the applied force vector .

For Free-Free end condition,

$$O = \left( \frac{1}{Rn^2 \left(\frac{L}{D}\right)\left(\frac{E_s}{S_u}\right)} \right) * \begin{Bmatrix} \frac{H_T}{S_u D^2} + \frac{M_T}{S_u D^3 \frac{L}{D}} \\ \frac{-M_T}{S_u D^3 \frac{L}{D}} \\ 0 \\ - \\ 0 \\ \frac{H_T}{S_u D^2 n} \end{Bmatrix} \tag{2.27}$$

For other end conditions,

$$O = \left( \frac{1}{Rn^2 \left(\frac{L}{D}\right)\left(\frac{E_s}{S_u}\right)} \right) * \begin{Bmatrix} \frac{H_T}{S_u D^2} + \frac{M_T}{S_u D^3 \frac{L}{D}} \\ 0 \\ 0 \\ - \\ 0 \\ \frac{H_T}{S_u D^2 n} \end{Bmatrix} \tag{2.28}$$

in which $S_u$ is the undrained strength of the soil.

T , the lateral soil force vector is ,

$$T = [\, J \,] \times \frac{\{ g \}}{D} \tag{2.29}$$

where g is the ground displacement vector obtained from the permanent horizontal ground displacement profile.

The developed bending moment is $M_D$ The nondimensional bending moment coefficient, M' can be found out using

$$M' = \frac{M_D}{S_u D^3} = \frac{E_p I_p}{S_u D^3} \left( \frac{d^2 y}{dz^2} \right) \tag{2.30}$$

Using Matlab, computer programs have been developed for the analysis.

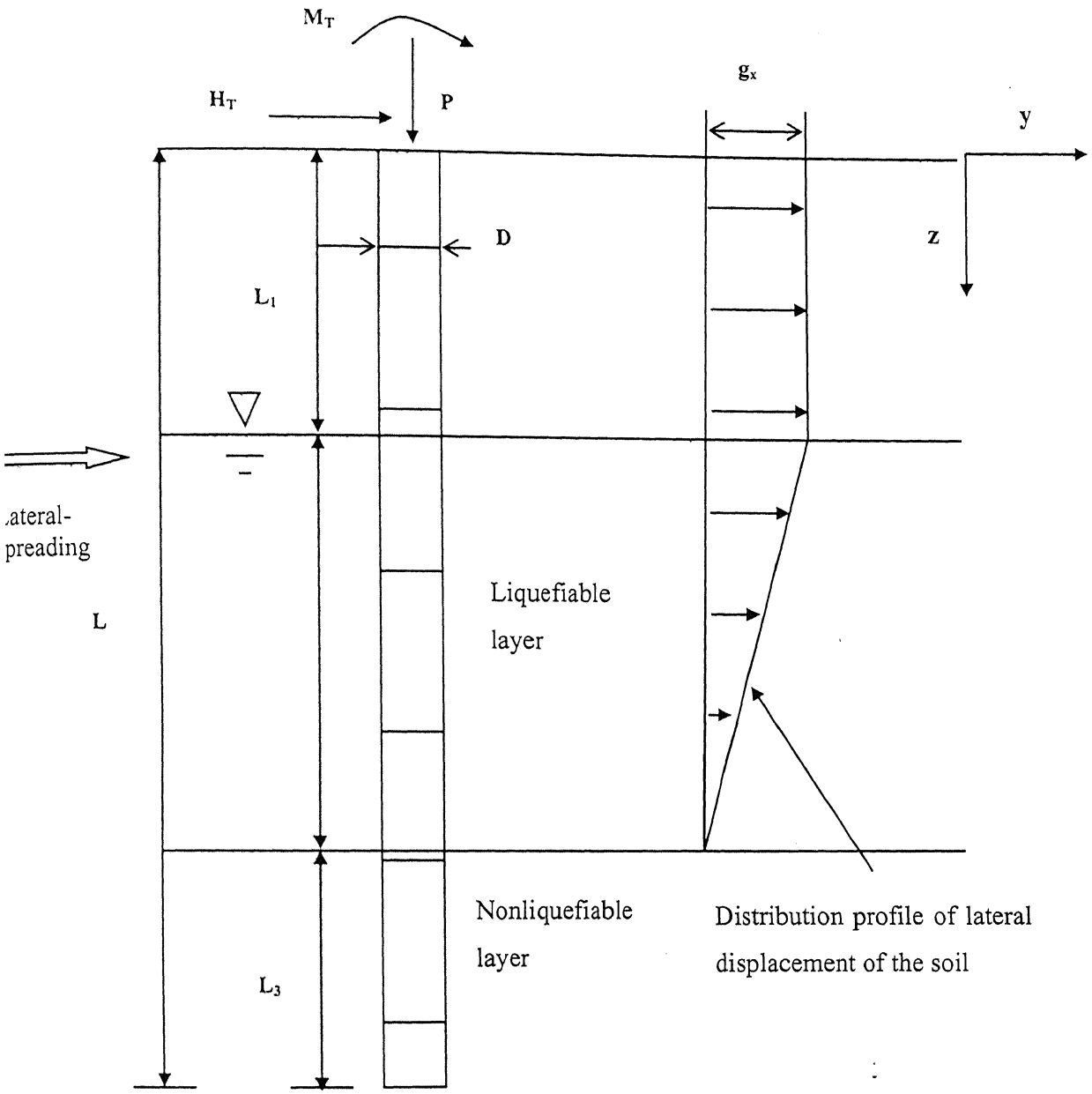


**Fig.2.1** Definition sketch

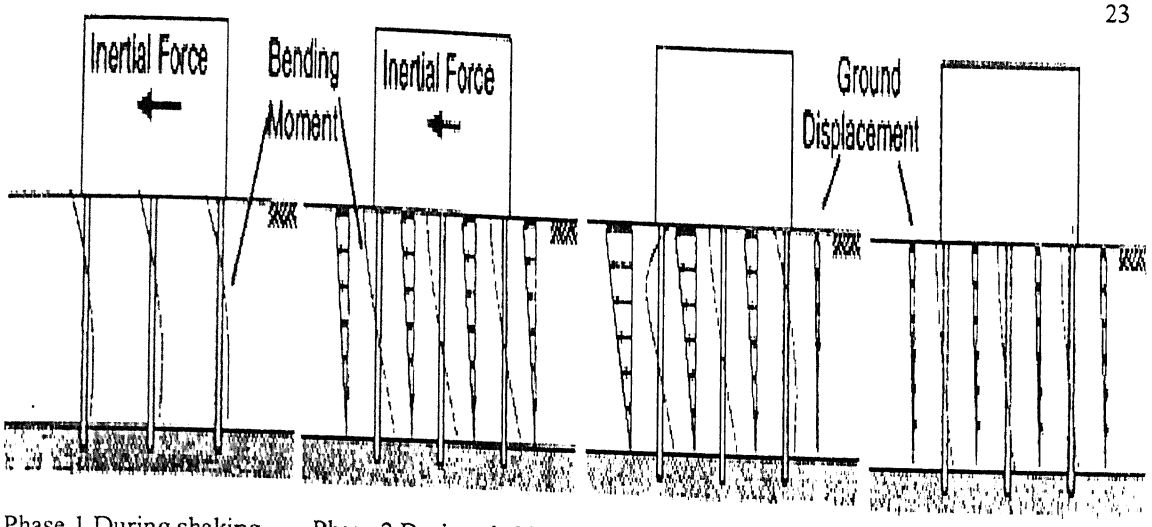


**Fig.2.2** Schematic representation of the soil-pile-structure interaction in laterally spreading soil (Tokimatsu 1999)

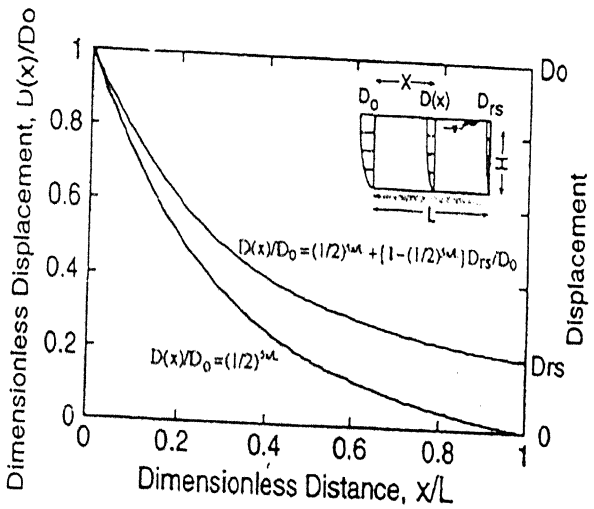


**Fig.2.3** Ground displacement profile (Tokimatsu 1999)
(Notations D,L and H in the figure corresponds to g,$L_s$,and $L_2$ respectively in the analysis)

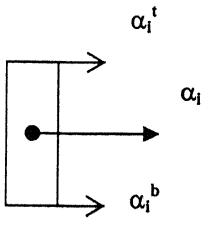


**Fig.2.5** Element View

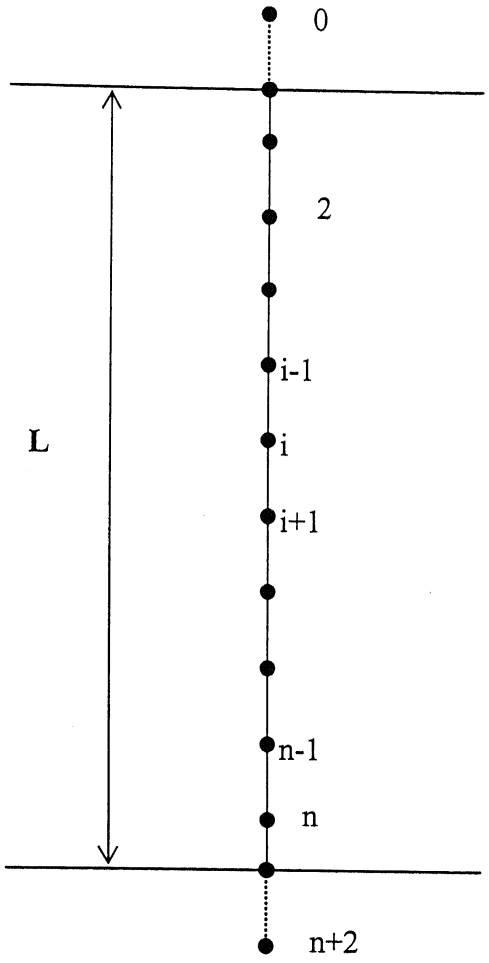


**Fig.2.4** Finite difference representation of the pile

# Chapter 3

# RESULTS AND DISCUSSIONS

## 3.1 Introduction

The analysis has been done by the taking the parameters as shown in Table.3.1 unless otherwise specified. The following values were chosen after taking into consideration a relatively broad range of values, which are recognized in geotechnical engineering practice to be consistent with the insitu conditions.

| | | |
|---|---|---|
| Number of elements, n+1=20 | Stiffness factor, $K=E/E_s=500$ | Moment factor, $M=\frac{M_T}{S_u D^3}=0$ |
| L/D ratio, L/D =25 | Pile flexibility factor, R=1E-4 | Scale factor for liquefied soil, $S_f$=1E-2 |
| Nonliquefied depth factor, $r=L_1/L=0.2$ | Soil modulus to soil strength ratio, $Q=E_s/S_u=200$ | N≤10(for liquefied soil) N≥60(for nonliquefied soil) |
| Liquefied depth factor, $s=L_2/L=0.6$ | Vertical load factor, $V=\frac{P}{\frac{\pi D^2 E_s}{4}}=0$ | Gradient of the surface topography, sl=1% |
| Embedded depth factor, $t=L_3/L=0.2$ | Horizontal load factor, $H=\frac{H_T}{S_u D^2}=0$ | Location factor, $L_x=x/L_s=0$ |

**Table.3.1** Values chosen for the analysis

The effect of these parameters are studied and the results are presented in the form of non-dimensional charts correlating nondimensional depth coefficient, Z=z/L

nondimensional deflection coefficient, Y=y/D, and nondimensional bending moment coefficient, M'=$\frac{M_D}{S_u D^3}$.

## 3.2 Convergence study

To find the optimum number of elements to be considered for the analysis, a convergence study has been carried out by varying the number of elements from 5 to 40 for different lengths of the pile. The results are shown in Fig.3.1 to Fig.3.8. The study has been conducted by evaluating the effect of number of elements on the nondimensional deflection and bending moment. It has been observed that, to obtain a fairly good convergence, the number of elements should be chosen in such a way that the nondimensional length of the elements other than that at the top and the tip of the pile should be more than 0.05 and it should be less than 0.07. Hence the nondimensional element size in the present study has been chosen as 0.053 (corresponding to a pile of length of 10m when divided into 20 elements).

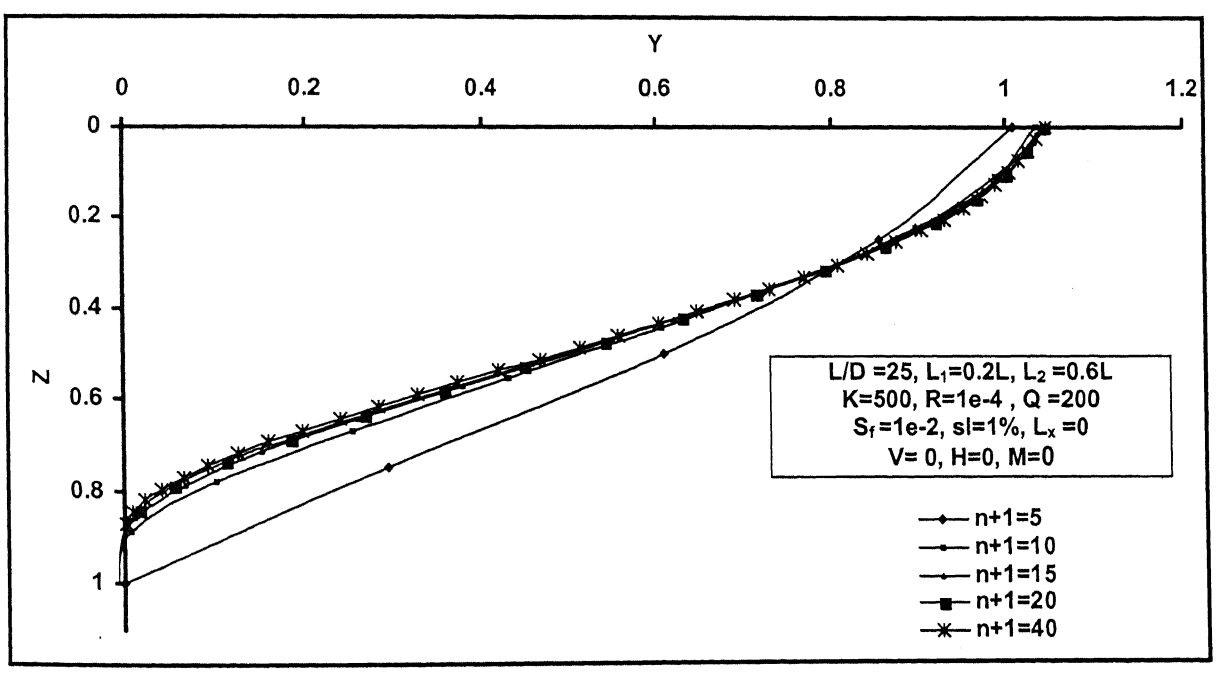


**Fig.3.1** Deflection pattern of a Free-Free pile for various numbers of elements. (L=10m)

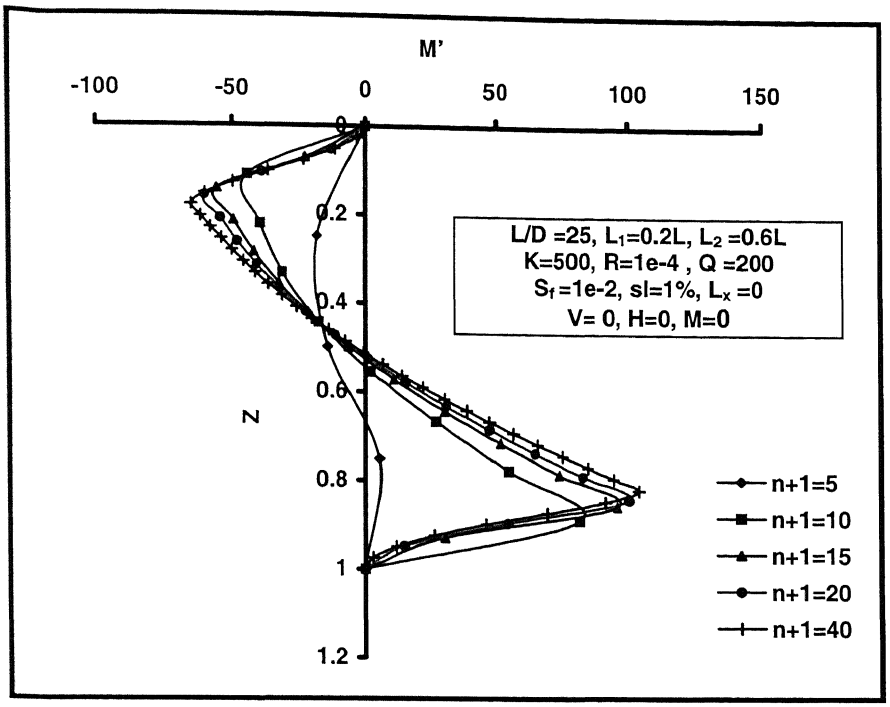


**Fig.3.2** Bending moment of a Free-Free pile for various number of elements. (L=10m)

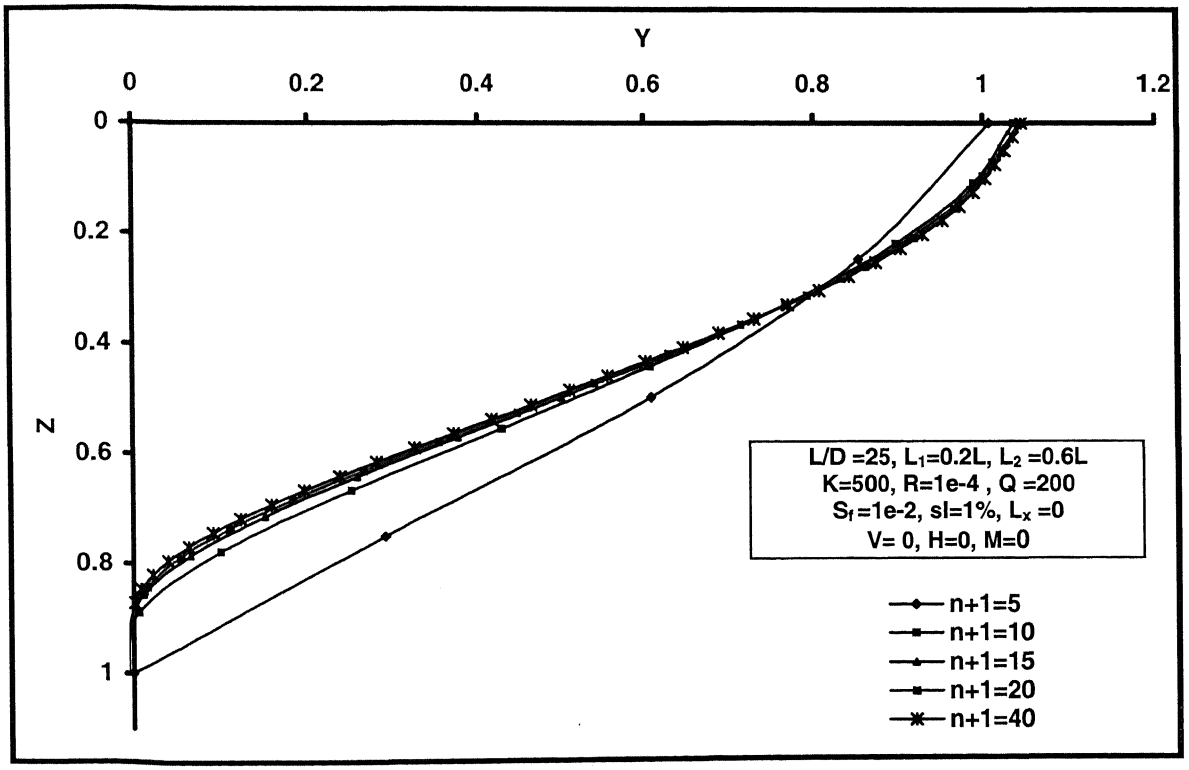


**Fig.3.3** Deflection pattern of a Free-Free pile for various number of elements (L=15m)

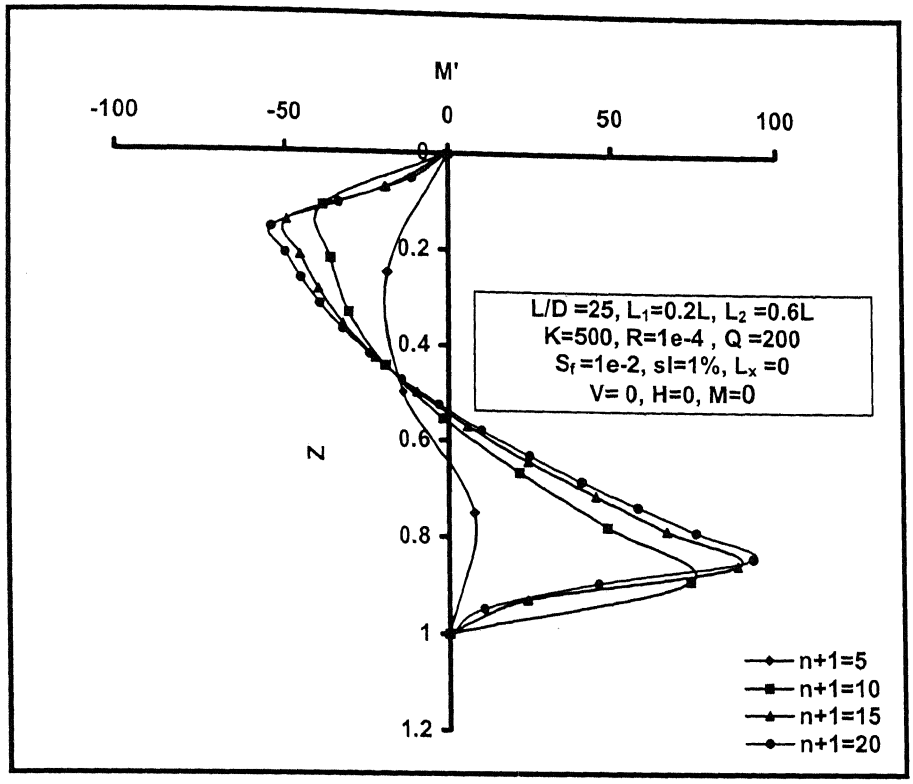


**Fig.3.4** Bending moment of a Free-Free pile for various number of elements (L=15m)

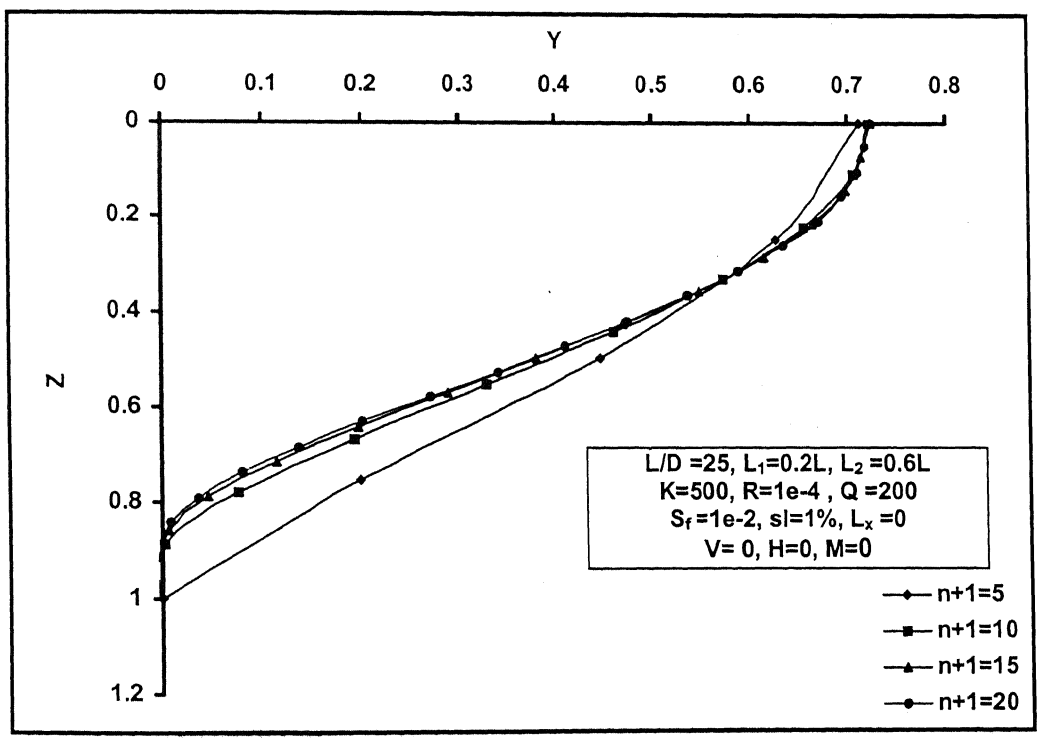


**Fig.3.5** Deflection pattern of a Free-Free pile for various number of elements (L=20m)

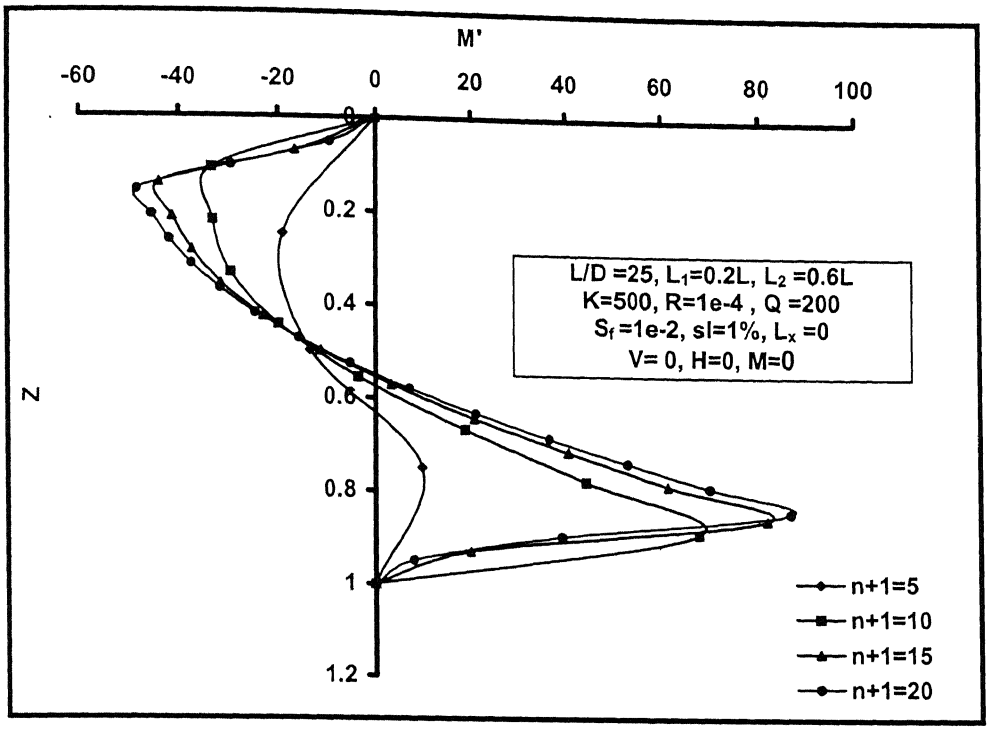


**Fig.3.6** Bending moment of a Free-Free pile for various number of elements (L=20m)

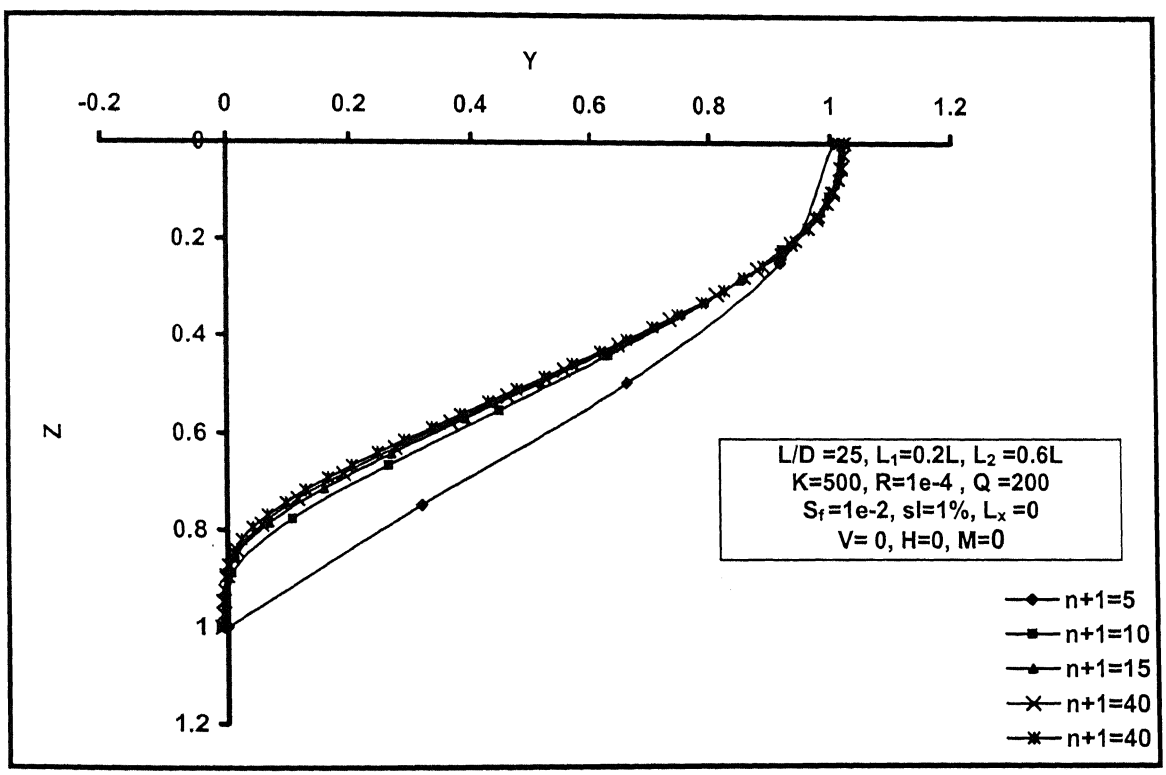


**Fig.3.7** Deflection pattern of a Fixed-Free pile for various number of elements (L=10m)

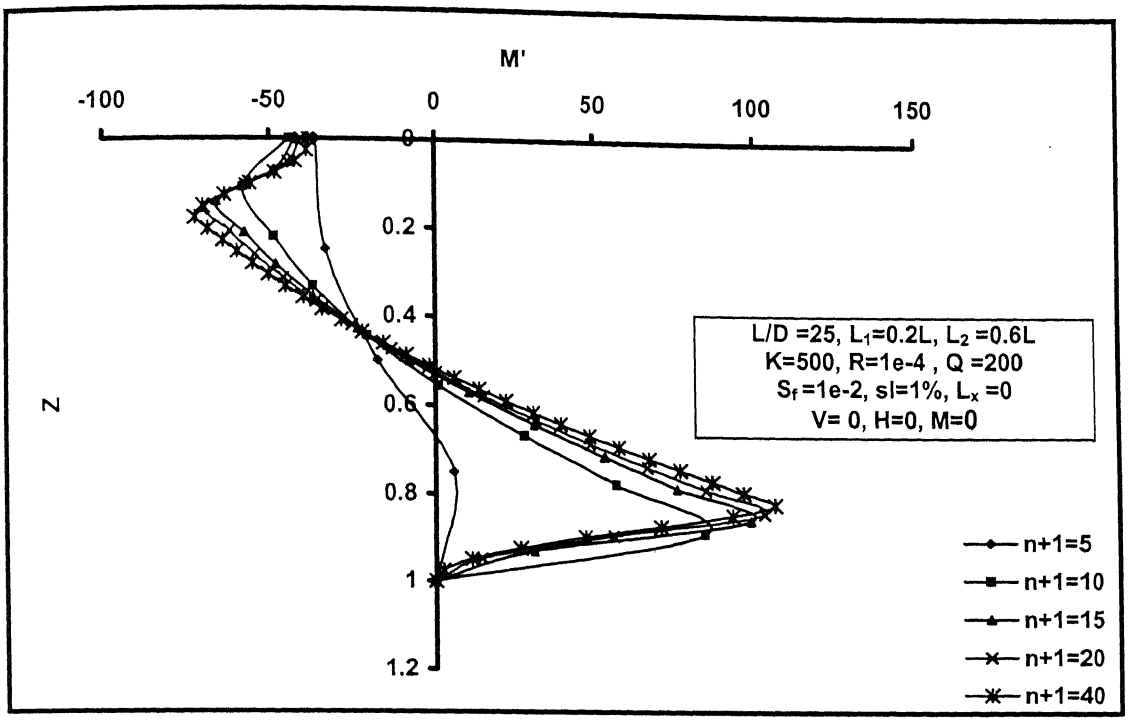


**Fig.3.8** Bending moment of a Fixed-Free pile for various number of elements (L=10m)

## 3.3 Validation of the model with field data

The validity of the program is checked by comparing the analytical results with the field observations. Detailed measurements of reinforced concrete pile deformation caused by the lateral spread at the Niigata Family Courthouse (NFCH) buildings in Niigata have been reported by Hamada (1992). The NFCH Building was a three-story reinforced concrete structure founded on reinforced concrete piles. As a result of the lateral spread during the 1964 Niigata earthquake in Japan, the building displaced horizontally approximately 0.5 to 1.5m, according to photogrametric studies performed by Yoshida and Hamada (1991). The 1964 Niigata earthquake had a magnitude of 7.5 and the epicenter was about 50 km from Niigata.

During site preparation for new construction, a 350mm diameter pile was excavated carefully and examined. It supported a small footing. Fig.3.9 shows the profile of the damaged pile and uncorrected standard penetration test (SPT) N values plotted with respect

to depth. In the upper 7-8 m of the soil profile, the SPT values are less than 10, indicating a loose liquefiable deposit. The water table, which is considered as the upper boundary of the liquefiable layer, was reported to be 1.5 to 2.0 m below the ground surface. The pile ended in the loose sand layer. The pile showed damage at a depth of about 2.0 m from the pile top, which is the interface between the liquefiable and nonliquefiable layer.

Deflection and bending moment values were obtained using the computer program for the pile along its length. The deformed shape of the pile, maximum moment, and location of maximum moment were used as the criteria for evaluating the compliance between field measurements and analytical results. The displacement and bending pattern for the pile at NFCH Building is presented in Fig.3.10. The analytical values are compared with the digitized measurements of transverse deflections obtained by Yoshida and Hamada (1991). The maximum deflection is at the top of the pile where the ground displacement is the maximum. The maximum bending moment is occurring at a depth of about 2m and in the field the pile has experienced cracks in that portion only. It can be seen from the Table.3.2 that good correlation exists between the predicted results and the observed measurements. The present study predicted a maximum deflection of 672.4 mm at the pile head and the maximum deflection reported in the field is 672 mm, the values being almost identical. The maximum bending moment obtained from analysis is 53.8kNm and that given by Yoshida and Hamada (1991) is 55.96kNm, the error being only 4% on the conservative side. Comparison of the deflection and bending moment along the length of the pile also shows that the analysis is giving conservative results in general and thus the acceptability of the model can be substantiated. It can be seen that at greater depths even though the predicted deflections are on the conservative side in comparison to the field measurements, the predicted values of bending moment shows the reverse trend; however, as the pile will be designed based on the maximum bending moment this discrepancy does not affect the predictions with regard to the safety of the design.

| Yoshida and Hamada (1991) | | | Present Study(2005) | | |
|---|---|---|---|---|---|
| Depth(m) | Deflection(m) | Bending moment(kNm) | Depth(m) | Deflection(m) | Bending moment(kNm) |
| 0 | 0.672 | 0 | 0 | 0.67239 | 0 |
| 0.035 | 0.6716 | -25.23 | 1.1669 | 0.65338 | -45.111 |
| 1.943 | 0.6517 | -55.96 | 2.3331 | 0.61544 | -53.779 |
| 3.322 | 0.5224 | -25.23 | 3.5 | 0.55489 | -51.223 |
| 4.346 | 0.4229 | -7.62 | 4.6669 | 0.47285 | -39.519 |
| 6.926 | 0.1741 | -0.49 | 5.8331 | 0.37422 | -21.716 |
| | | | 7 | 0.266455 | 0 |

**Table.3.2** Comparison of predicted data with the field observations

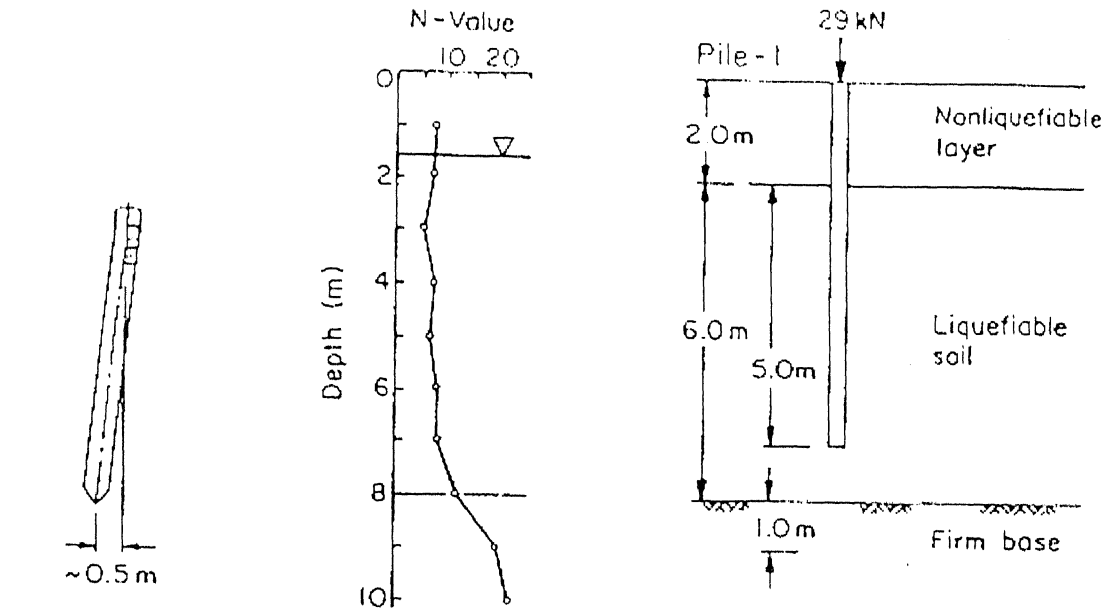


Broken Piles SPT values Simplified model

**Fig.3.9** Observed pile deformation and soil conditions at NFCH Building (O'Rourke1994)

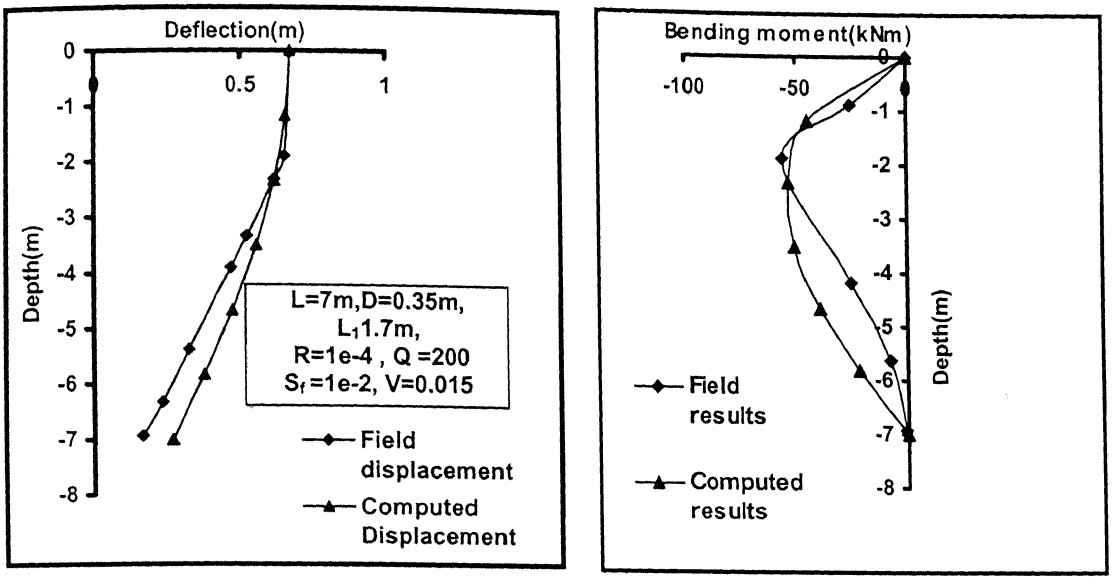


**Fig.3.10** Comparison of the pile behavior obtained from the present analysis and the field observations for the pile at the NFCH Building

## 3.4 Calibration of the program

The developed program is calibrated in the following way. Results were obtained for a Free-Free pile and Fixed-Free pile subjected to horizontal load and embedded in a homogeneous nonliquefied soil layer in which $k_h$ is constant with depth. The parameters chosen for Free-Free pile are Z=1, H=25, L/D=25, $k_hD/E_s$=0.3, Q=200 and R=0.1. The parameters chosen for Fixed-Free pile are Z=1, H=25, L/D=25, $k_hD/S$=0.3, Q=100 and R=0.01. The results were then compared with the closed form solution developed by Hetenyi (1946). The deflection coefficient at the ground line for the Free-Free pile is obtained as 0.067 and the corresponding solution for the horizontal displacement given by Hetenyi provided identical result. For the Fixed-Free pile the predicted deflection coefficient at the ground line is 0.0537 where as the corresponding analytical solution is 0.0535. Thus the correctness of the program is verified.

## 3.5 Parametric studies

The effect of various parameters on the deflection as well as the bending moment developed during the lateral spreading has been studied and it is discussed in the following sections. The analysis has been done for the two different end conditions of the pile i.e. Free-Free pile and the Fixed-Free pile and the effect of end conditions are also verified.

### *3.5.1 Effect of vertical load factor.*

The vertical load factor, V is varied from 0 to 9. When there is no load acting on the pile only the lateral spreading force comes into play. As the maximum velocity of the soil is at the ground surface, the pile top is likely to experience the maximum deflection.

The results of the analysis for Free-Free pile are shown in Fig.3.11 to Fig.3.13. The nondimensional deflection at the pile head increases with the increase in V and when V exceeds a critical range of vertical load factor, it starts decreasing with the increase in V (Fig.3.11). But the nondimensional deflection at the top interface between nonliquefied layer and the liquefied layer increases with increase in V and beyond the critical range, pile deflection at the interface becomes the maximum. The particular value of V beyond which the maximum deflection increases enormously can be termed as Critical load factor, which in the present analysis is 7.

The nondimensional bending moment is maximum at the bottom interface between liquefied layer and the firm base (i.e. at Z=0.8), which is a positive value. The maximum nondimensional negative moment, which is usually lesser than that of the maximum nondimensional positive bending moment, occurs at the top interface between nonliquefied layer and the liquefied layer (i.e. at Z=0.2). As V increases nondimensional bending moment also increases. Beyond the critical value of V the pile shows an abnormal increase in the bending moment (Fig3.12).

The maximum deflection coefficient and the maximum positive bending moment coefficient are referred as $Y^*$ and $M^*$ respectively. $Y^*$ shows a nonlinear increase with the increase in V (Fig3.13a). For V=0 to V=7, Y* =1.04. But beyond that $Y^*$ shows a sharp

increase to 2.5 at V=8.5 and then for V=9 it decreases to 1.6. M* decreases nonlinearly with increase in V (Fig3.13b) and beyond V=4 it increases gradually till V=8 beyond which the rate of increase in its value is very high; when V=8.5, the value of M* is around 2500 and then it decreases. The trend is shown in Table 3.3. Generally the piles may not be designed for such a high value of bending moment and is likely to fail for the given liquefaction depth and other soil data when V is equal to 8.5. For such conditions it may be more appropriate to take into account the inelastic/ plastic behavior of the pile-soil interaction. From the study it has been observed that till V=8.5, the developed methodology at least predicted values showing an expected trend of behavior i.e. increased deflection with increased values of the vertical load. However, it is seen from the obtained data that for V=9 the trend of behavior is different (maximum deflection decreases with the increase in V from 8.5 to 9) in contrast to the earlier one as discussed. Thus, the analysis is not reliable when the value of V exceeds 8.5.

This behavior can be explained as follows. Failure of the pile can be expected when the vertical load factor reaches the critical load factor. Also, the pile can fail before attaining the critical stage if the moment developed is greater than the yield moment of the section which can be obtained from the structural properties of the pile.

This indicates that if the vertical load factor exceeds a certain value, the pile failure will occur not only because of the lateral spreading but also due to the axial load. Hence while designing the piles, care should be given not only to the lateral loads developed during the liquefaction but also to the axial load transferred by the super structure.

The results of the analysis of Fixed-Free pile are shown in Fig.3.14 to Fig.3.16.The nondimensional deflections are less compared to the Free-Free pile. But the nondimensional bending moments are larger than that of the Free-Free pile. The behaviour of the pile is same in both the cases except that the maximum deflection in the Fixed-Free pile doesn't shift to the liquefied range. The critical range of vertical load factor is around 6.These changes can be inferred as the effect of fixity introduced at the pile head.

| Free-Free Pile | | | Fixed-Free Pile | | |
|---|---|---|---|---|---|
| V | Y* | M* | V | Y* | M* |
| 0 | 1.04 | 100.4245 | 0 | 1.0225 | 103.1691 |
| 2 | 1.05 | 89.8849 | 2 | 1.027 | 94.1907 |
| 4 | 1.05 | 87.0652 | 4 | 1.029 | 92.4229 |
| - | - | - | 4.5 | 1.0284 | 97.6508 |
| - | - | - | 5 | 1.0268 | 104.3115 |
| - | - | - | 5.5 | 1.0268 | 115.509 |
| 6 | 1.05 | 117.8432 | 6 | 1.1703 | 416.4851 |
| 6.5 | 1.0372 | 139.8965 | 6.5 | 1.0365 | 137.8858 |
| 7 | 1.0448 | 175.4362 | 7 | 1.0386 | 157.383 |
| 7.5 | 1.0805 | 238.6292 | - | - | - |
| 8 | 1.1881 | 422.6381 | - | - | - |
| 8.5 | 2.5331 | 2486.9 | - | - | - |
| 9 | 1.6269 | 614.171 | - | - | - |

**Table3.3** Variation of Y* and M* with V

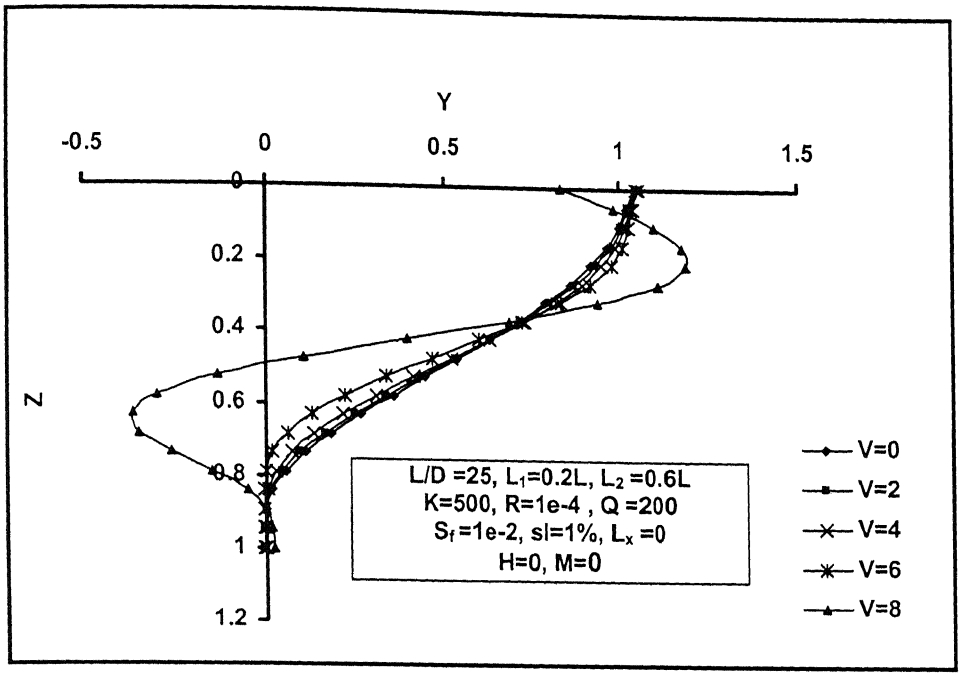


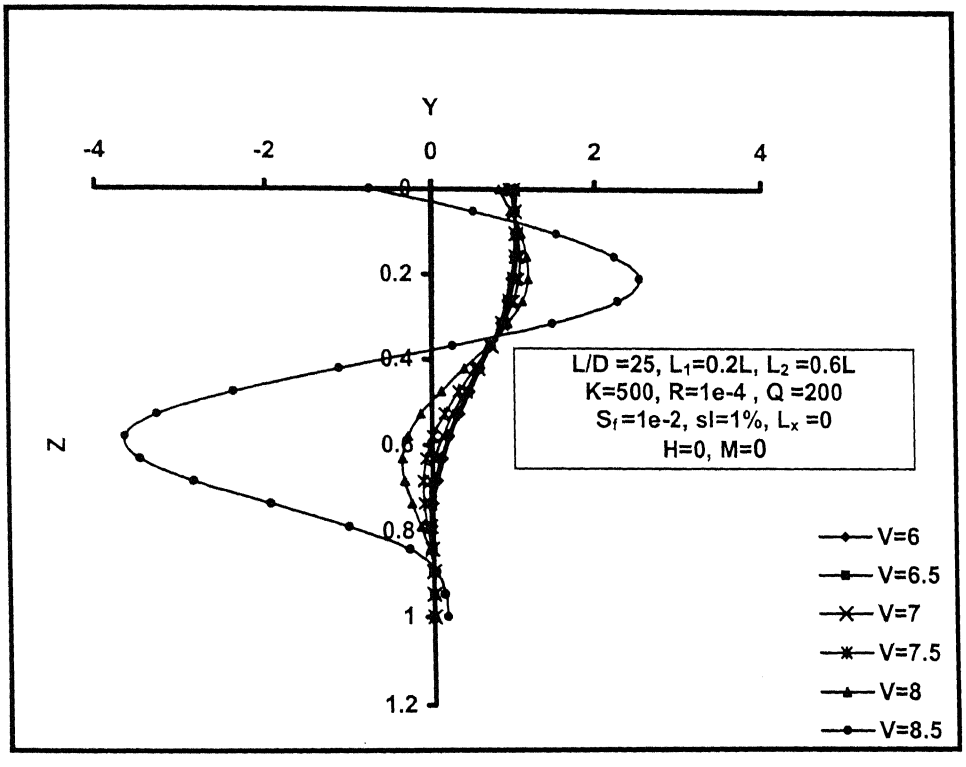


**Fig.3.11** Variation of Y of a Free-Free pile with Z for different V.

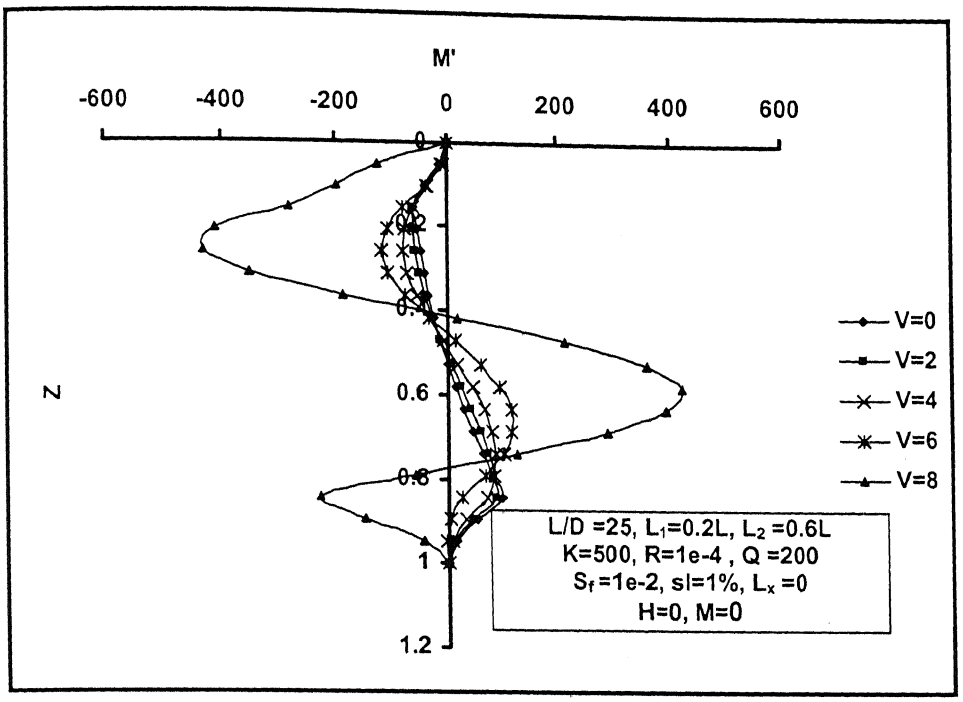


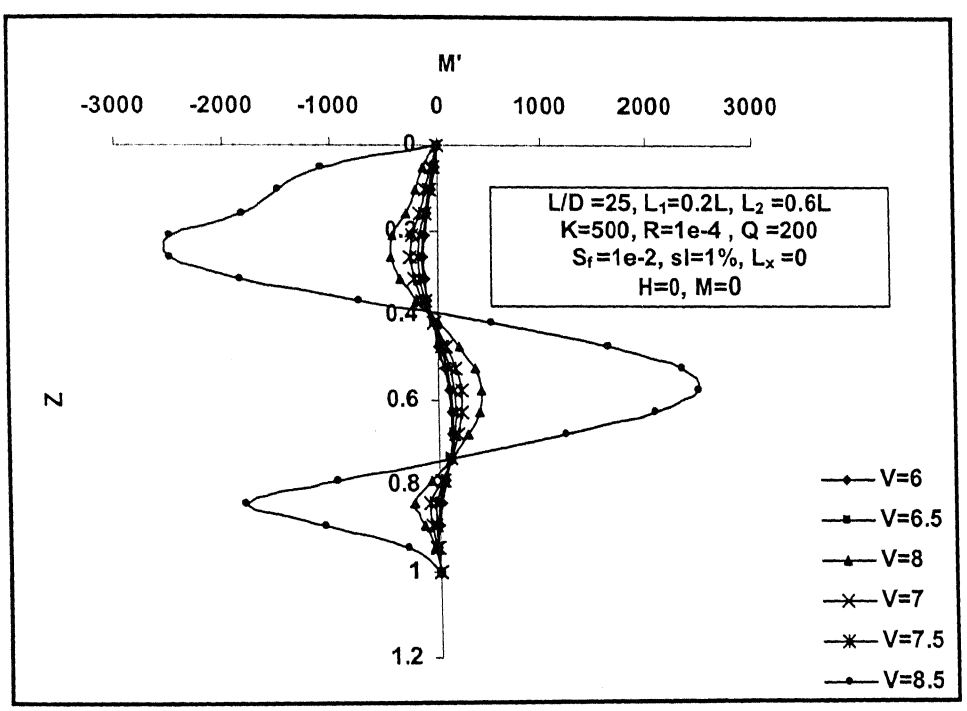


**Fig.3.12** Variation of M' of a Free-Free pile with Z for different V.

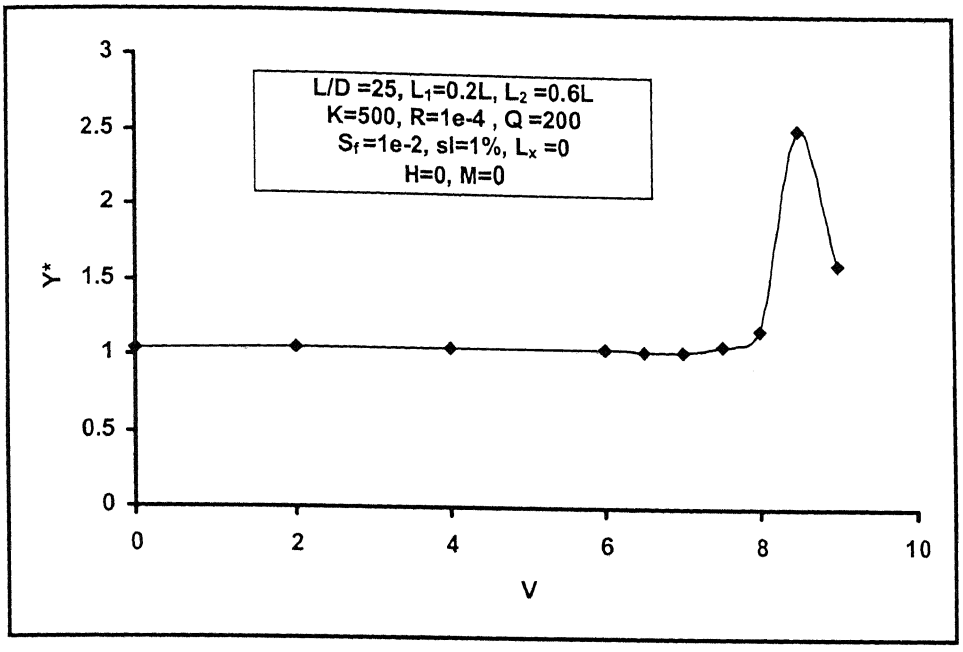


**Fig.3.13a** Effect of V on the Y* of a Free-Free pile

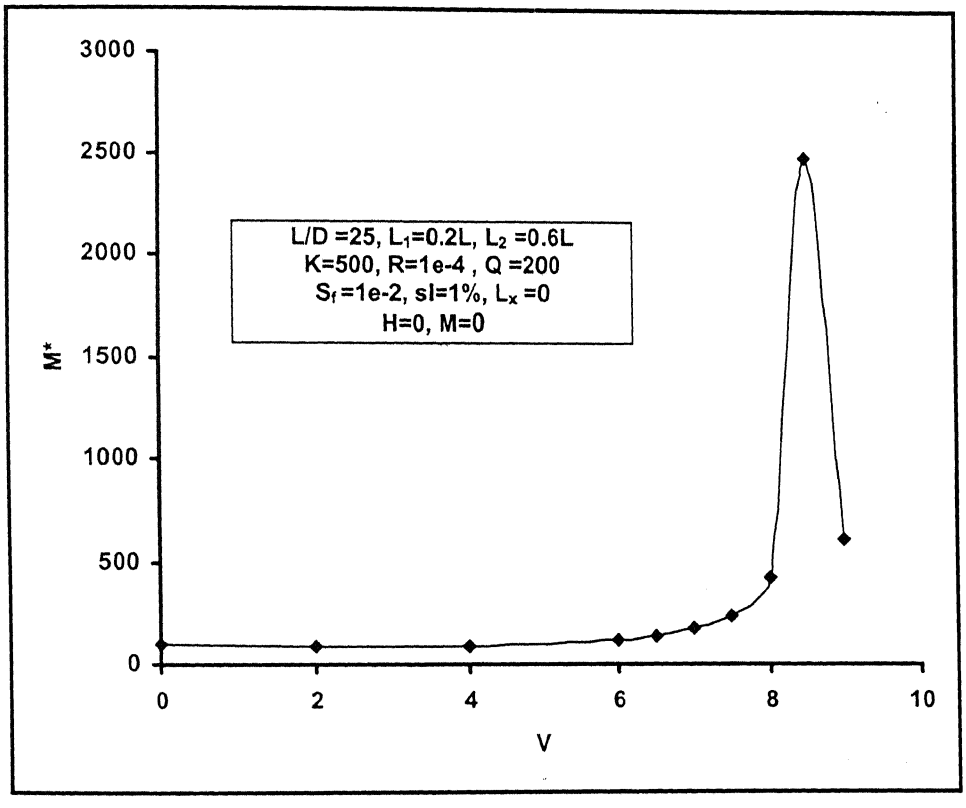


**Fig.3.13b** Effect of V on the M* of a Free-Free pile

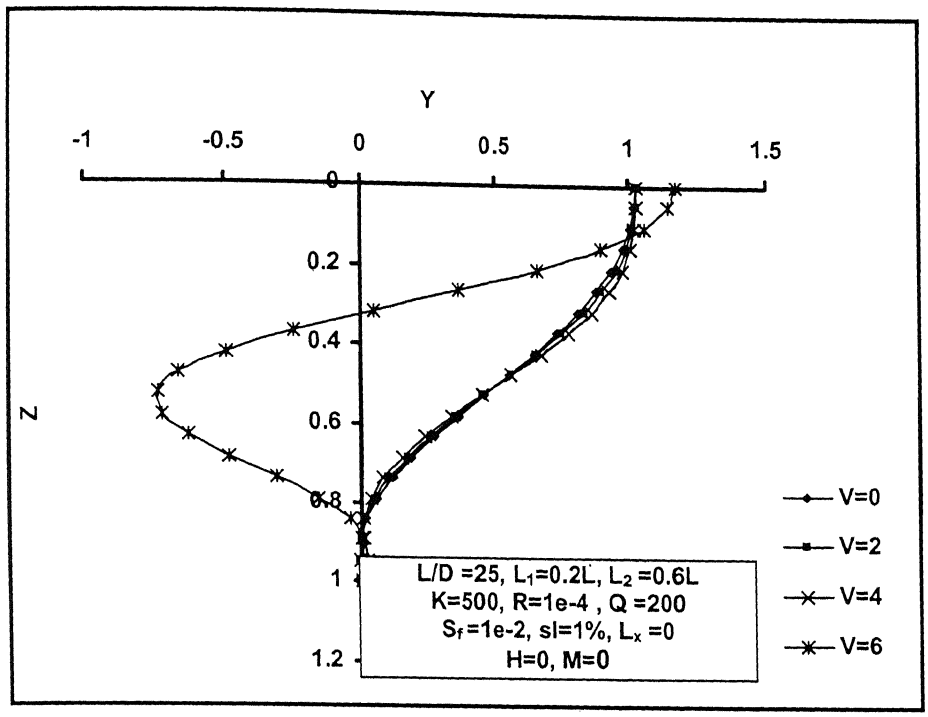


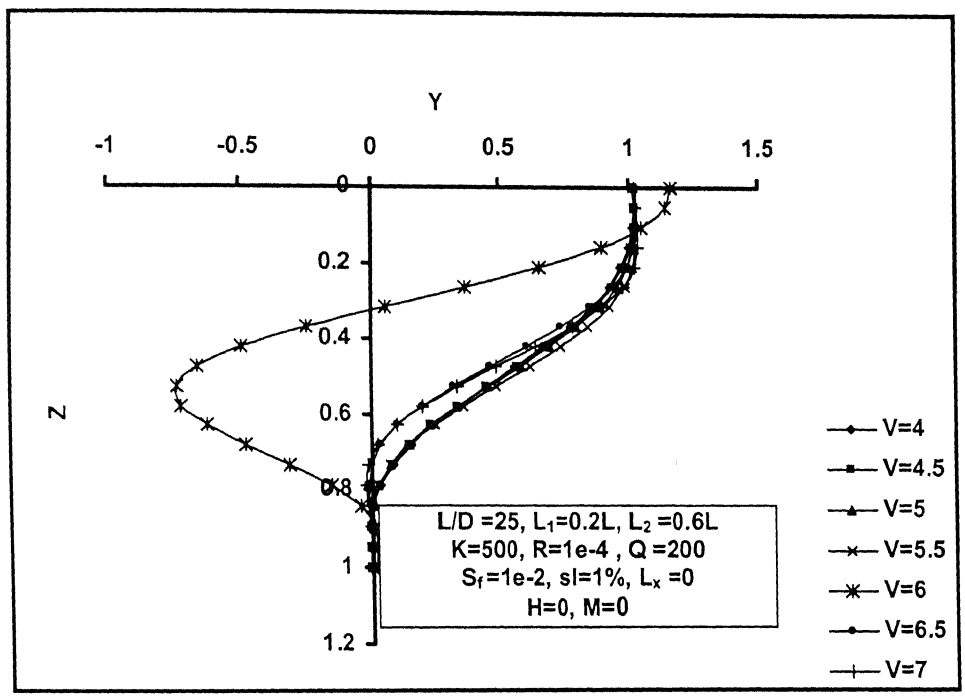


**Fig.3.14** Variation of Y of a Fixed-Free pile with Z for different V.

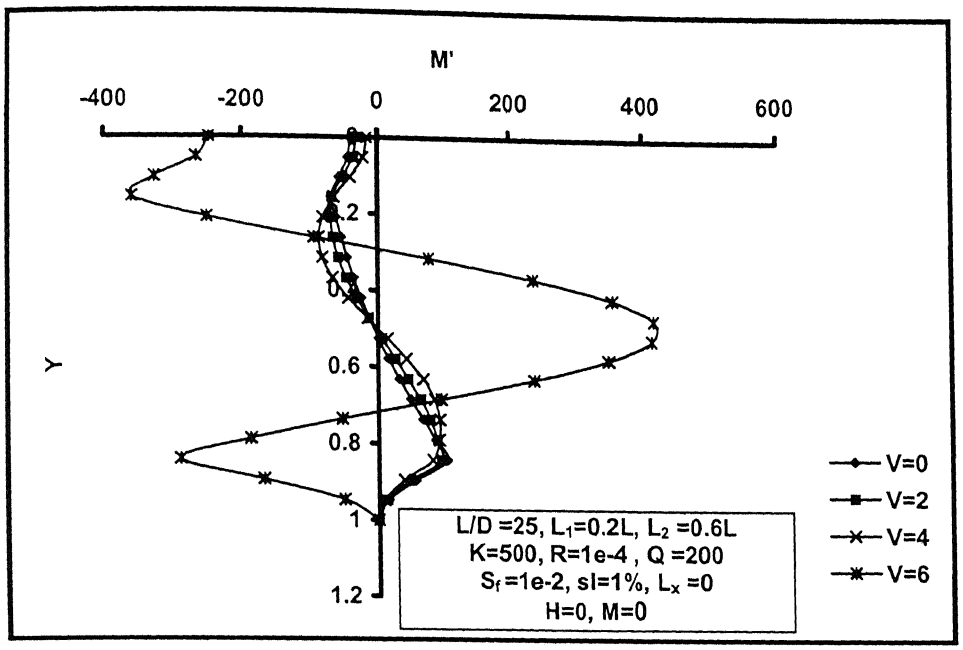


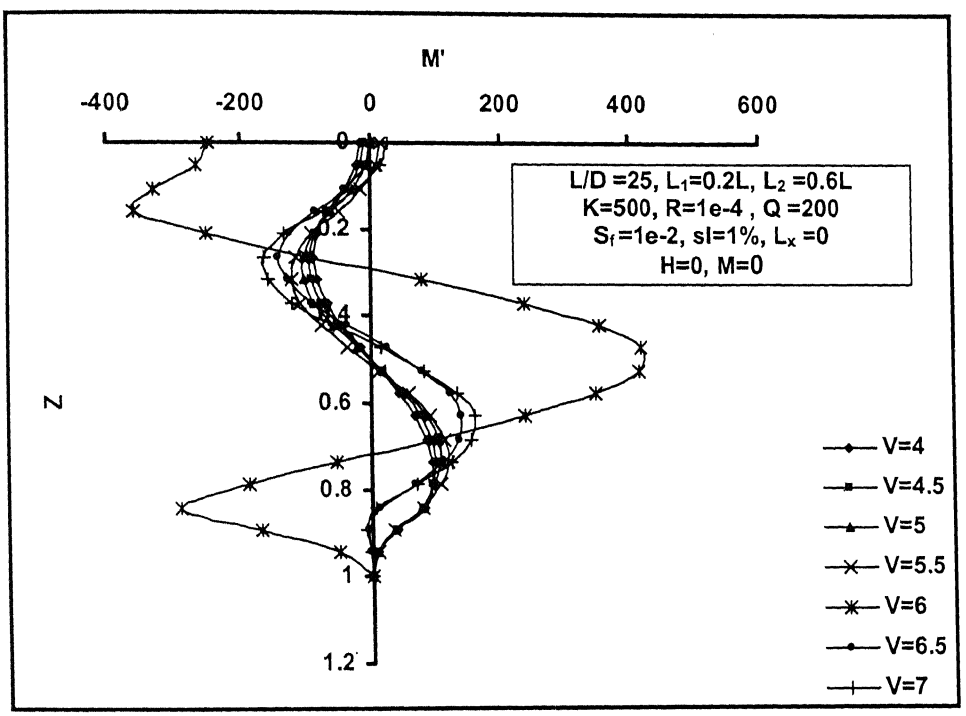


Fig.3.15 Variation of M' of a Fixed -Free pile with Z for different V.

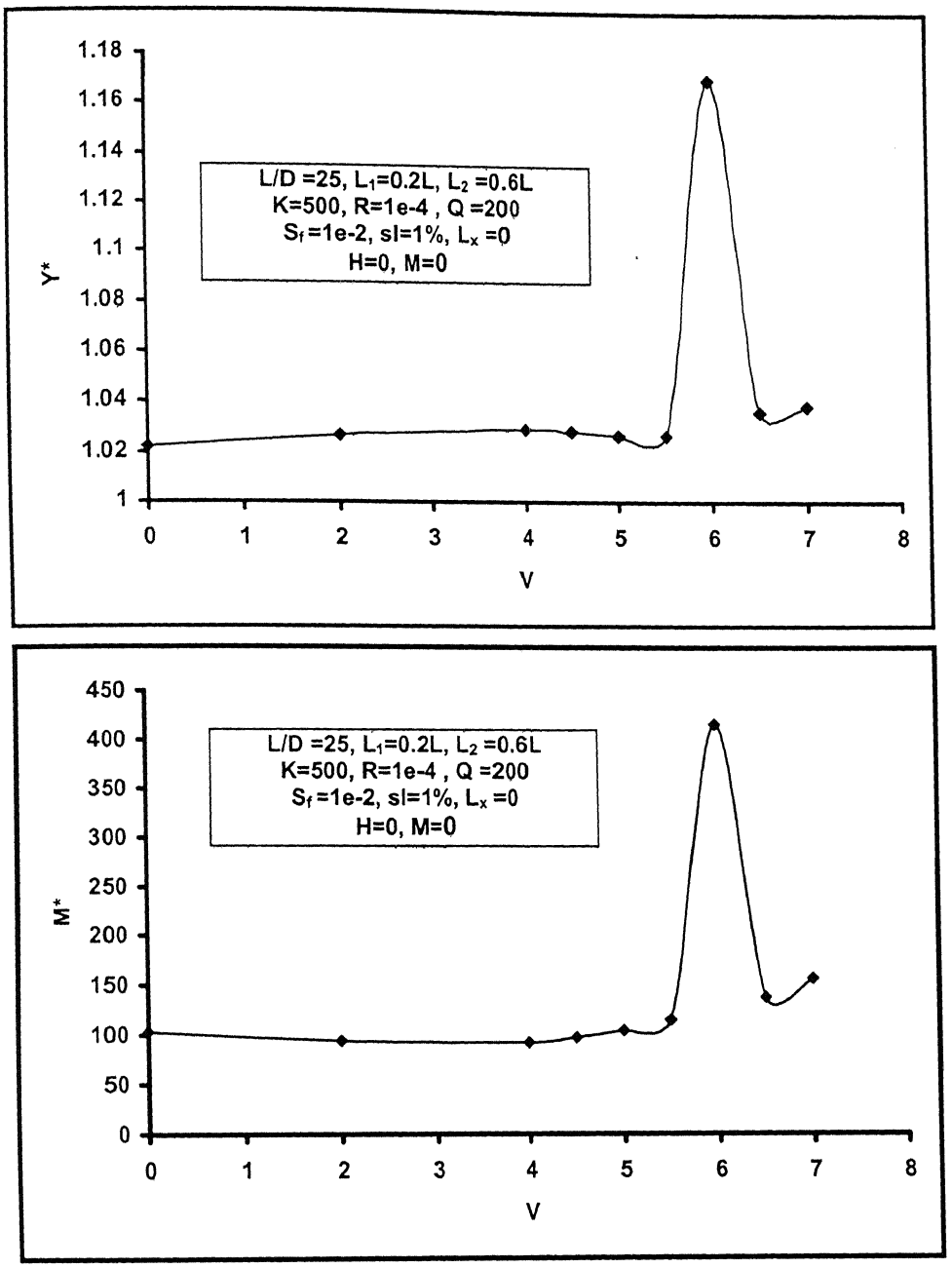


**Fig.3.16** Effect of V on the Y* and M* of a Fixed-Free pile

### 3.5.2 *Effect of horizontal load factor*

The Horizontal load factor, H is varied from 0 to 25.The results of Free-Free pile are shown in Fig.3.17 to Fig.3.19, which demonstrate that the variation of H negligibly affects the top deflection and the maximum deflection occurs at Z=0. The nondimensional maximum bending moment ($M^*$) decreases with increase in H. The maximum bending moments occur at the interfaces (of the liquefied and non-liquefied soil) and the positive maximum bending moment occurring at Z=0.8 (lower interface) is slightly more compared to the negative maximum bending moment (upper interface). The Y* shows a linear increase from 1.04 to 1.09 with H varying from 0 to 25 whereas the M* shows a linear decrease from 100 to 96 (Fig3.19).

The behavior is similar in the case of Fixed-Free pile as shown in Fig.3.20 to Fig.3.22.The deflections are less and the bending moments are more compared to that of Free-Free pile ( the difference in the values being of the order of 3 to 4%). The variation is shown in Table 3.4.

| Free-Free Pile | | | Fixed-Free Pile | | |
|---|---|---|---|---|---|
| H | Y* | M* | H | Y* | M* |
| 0 | 1.04 | 100.4245 | 0 | 1.0225 | 103.1691 |
| 5 | 1.05 | 99.5794 | 5 | 1.0273 | 102.8337 |
| 10 | 1.06 | 98.7343 | 10 | 1.032 | 102.4983 |
| 15 | 1.07 | 97.8892 | 15 | 1.0368 | 102.1629 |
| 20 | 1.079 | 97.0441 | 20 | 1.0416 | 101.8275 |
| 25 | 1.0878 | 96.199 | 25 | 1.0463 | 101.4921 |

**Table 3.4** Variation of Y* and M* with H

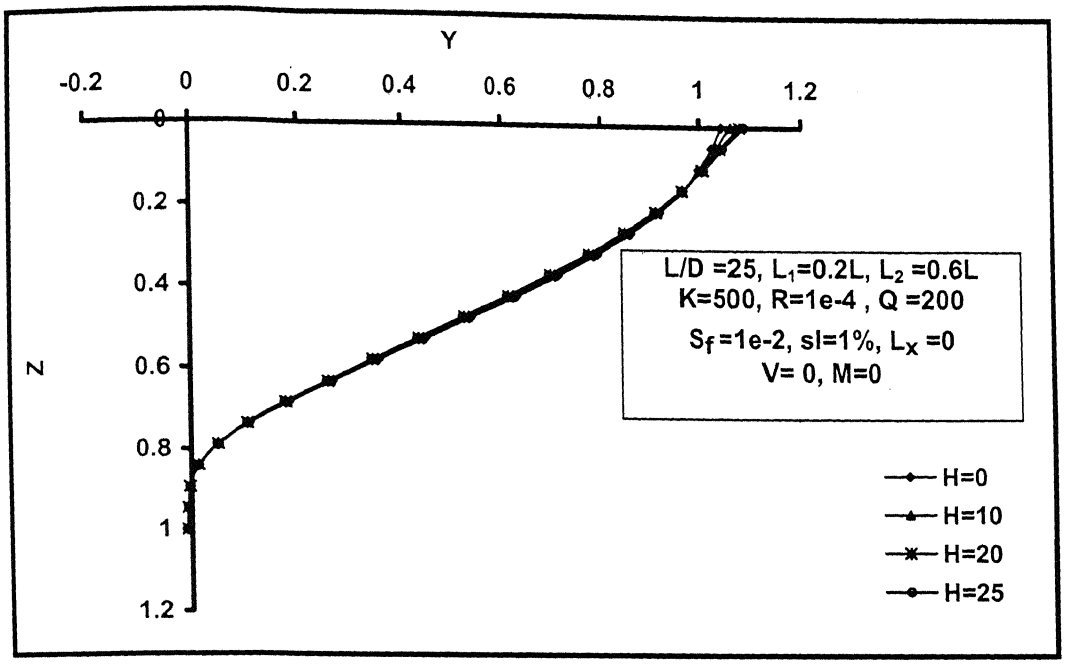


Fig.3.17 Variation of Y of a Free-Free pile with Z for different H.

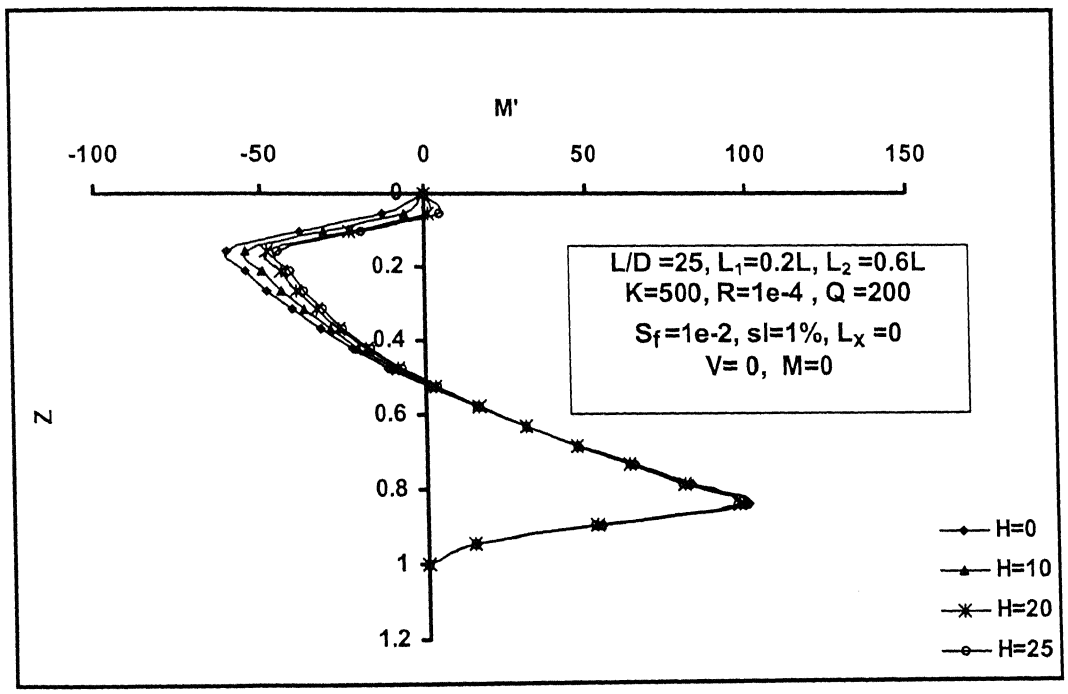


Fig.3.18 Variation of M' of a Free-Free pile with Z for different H

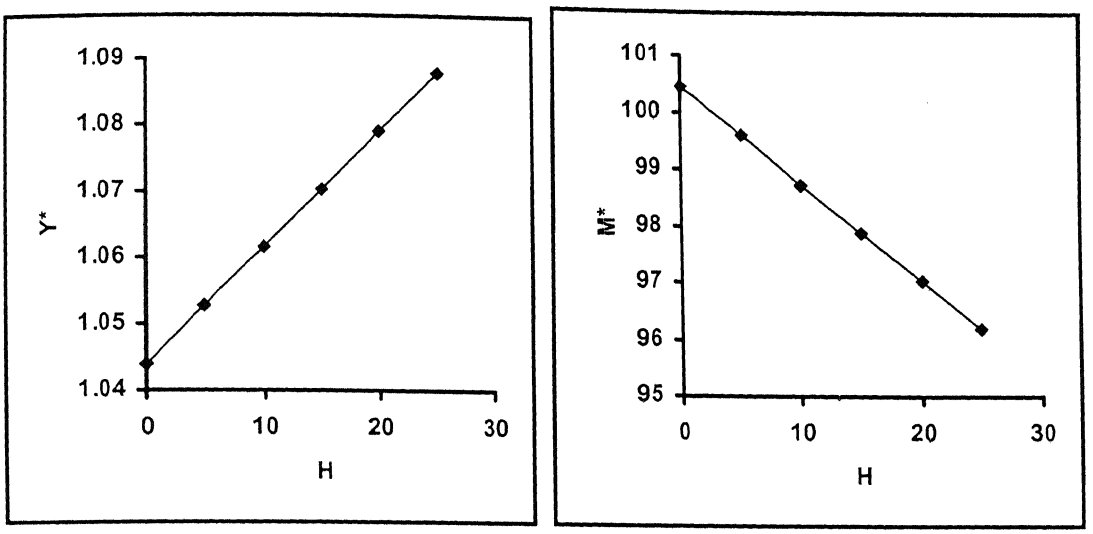


**Fig.3.19** Effect of H on the Y* and M* of a Free-Free pile

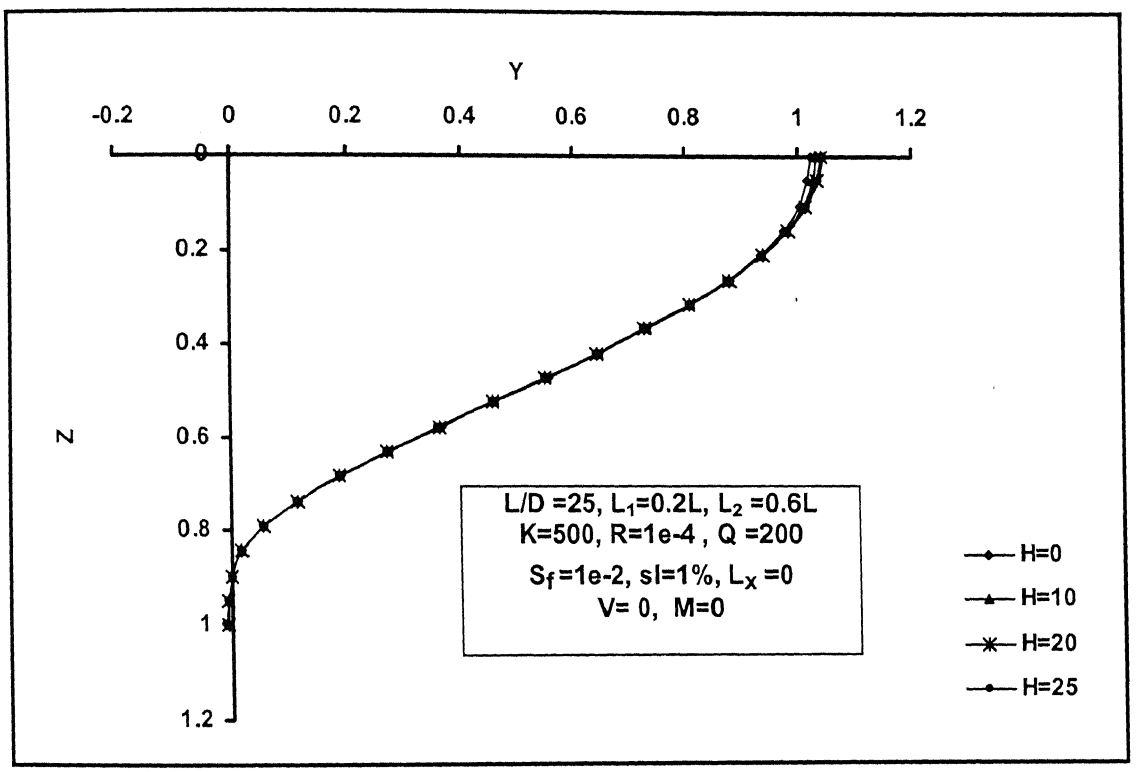


**Fig.3.20** Variation of Y of a Fixed-Free pile with Z for different H

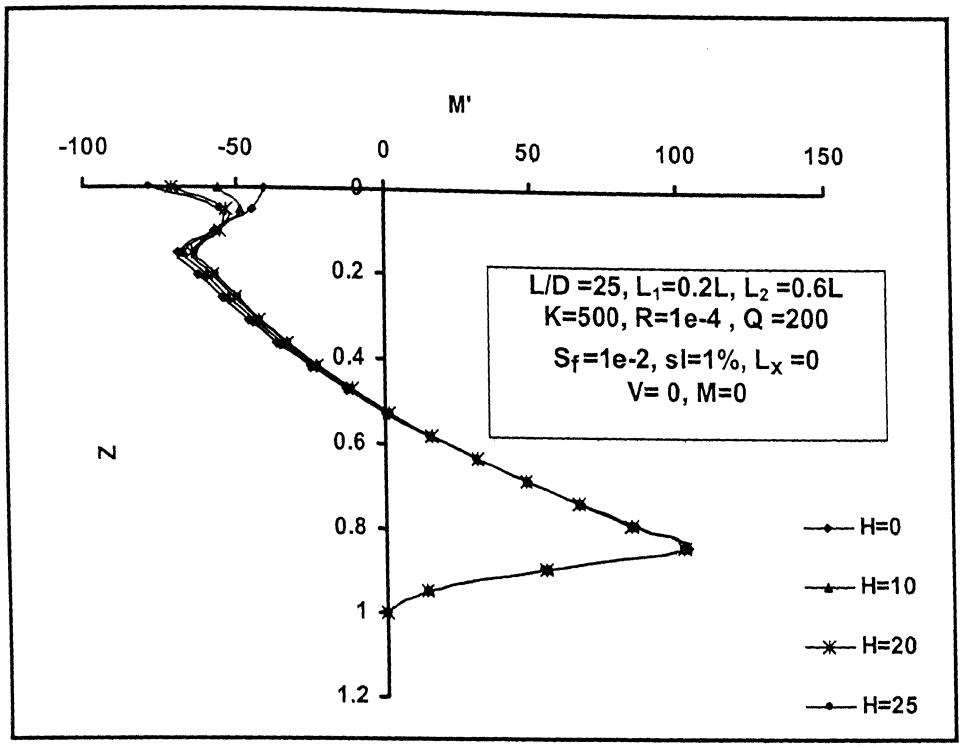


Fig.3.21 Variation of M' of a Fixed -Free pile with Z for different H

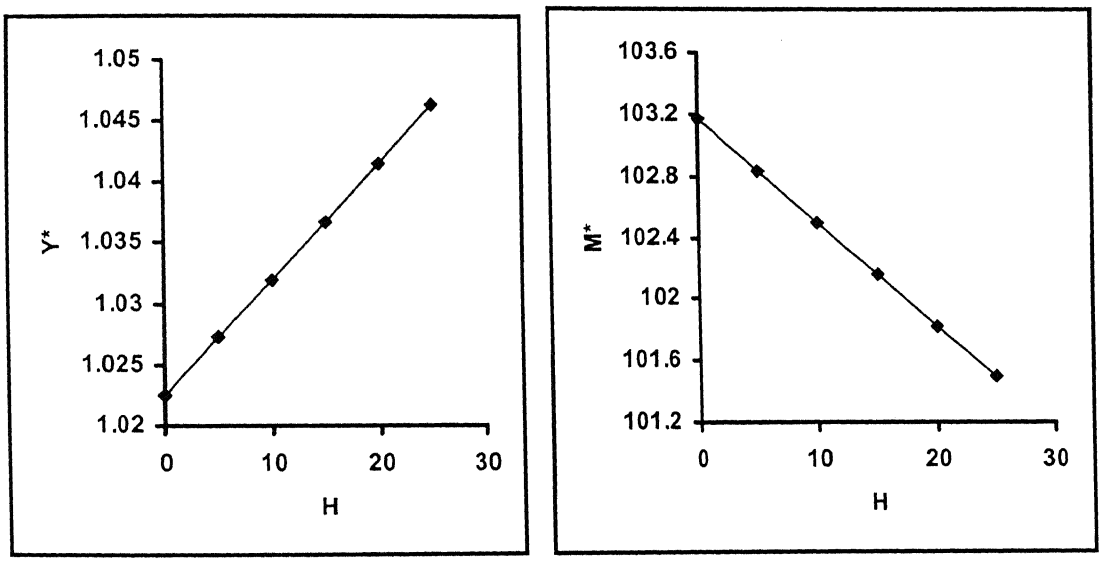


Fig.3.22 Effect of H on the Y* and M* of a Fixed-Free pile

### 3.5.3 *Effect of moment factor*

The effect of Moment factor, M is studied by varying it from 0 to 120; the results with Free-Free end conditions are shown in Fig.3.23 to Fig.3.25 It is seen from these figures that M has a very negligible effect on the flexural behavior (Fig.3.23 and Fig.3.24). The maximum deflection coefficient, Y*, occurs at the top and it increases linearly as M increases. The deflection in the liquefied region decreases as M increases. The maximum bending moment coefficient, M*, decreases linearly with increase in M up to M=100 and then linearly increases (Fig.3.25). This is because the applied moment exceeds the developed bending moment. The change in Y* and M* with moment factor M is shown in Table 3.5.

The Moment factor does not have an appreciable effect on the behavior of Fixed-Free pile. As shown in Fig.3.26 to Fig.3.28, the trends of the plots remain same as that of the Free-Free pile except that the M* shows a continuous decrease with increase in M (Fig.3.28). The superstructure itself can take care of these applied moments and hence they are not transferred to the foundations and also, a very large moment has to be applied so as to rotate the pile cap. Such large moments are very rare in field situations.

| | Free-Free Pile | | Fixed-Free Pile | |
|---|---|---|---|---|
| M | Y* | M* | Y* | M* |
| 0 | 1.04 | 100.425 | 1.0225 | 103.1691 |
| 30 | 1.06 | 98.0794 | 1.0237 | 102.9781 |
| 60 | 1.08 | 95.7343 | 1.0248 | 102.7871 |
| 90 | 1.10 | 93.3893 | 1.026 | 102.5961 |
| 120 | 1.1161 | 120 | 1.0271 | 102.4051 |

**Table 3.5** Variation of Y* and M* with M

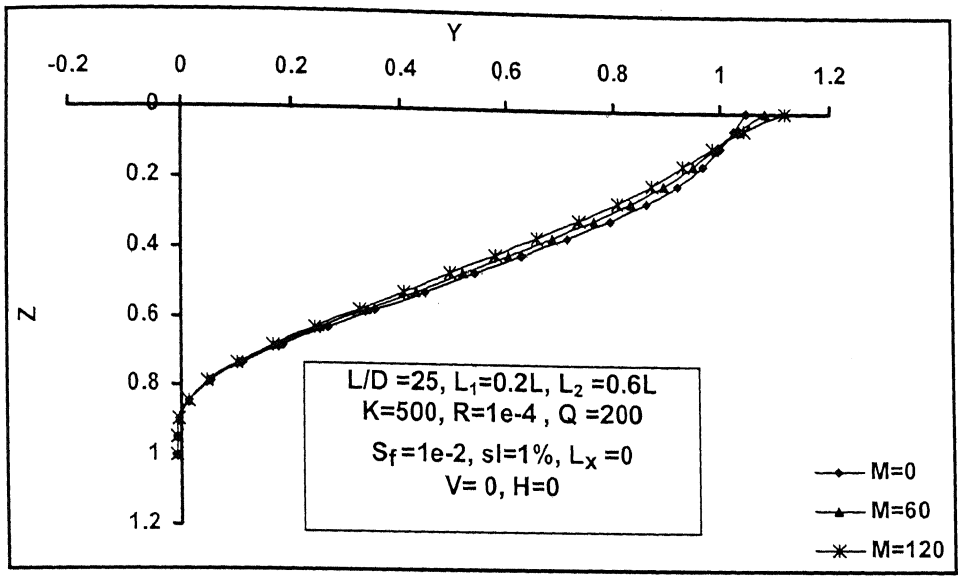


Fig.3.23 Variation of Y of a Free-Free pile with Z for different M

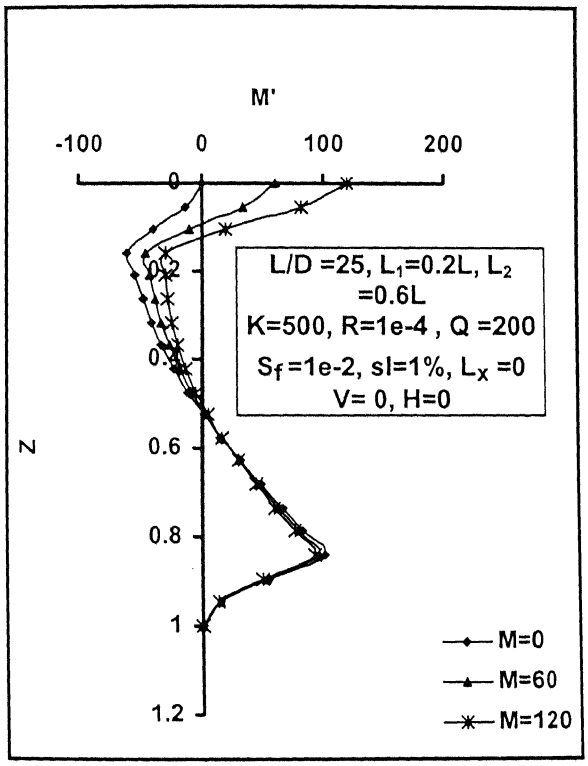


Fig.3.24 Variation of M' of a Free-Free pile with Z for different M.

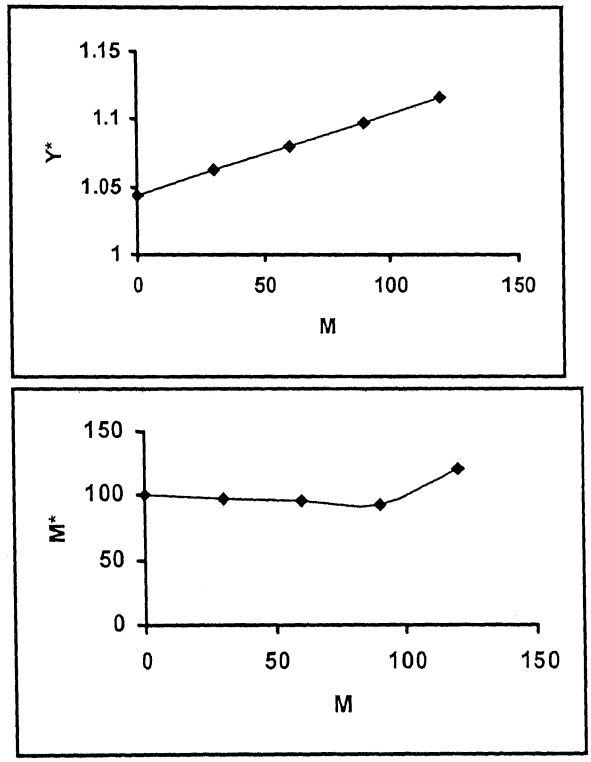


Fig.3.25 Effect of M on the Y* and M* of a Free-Free pile

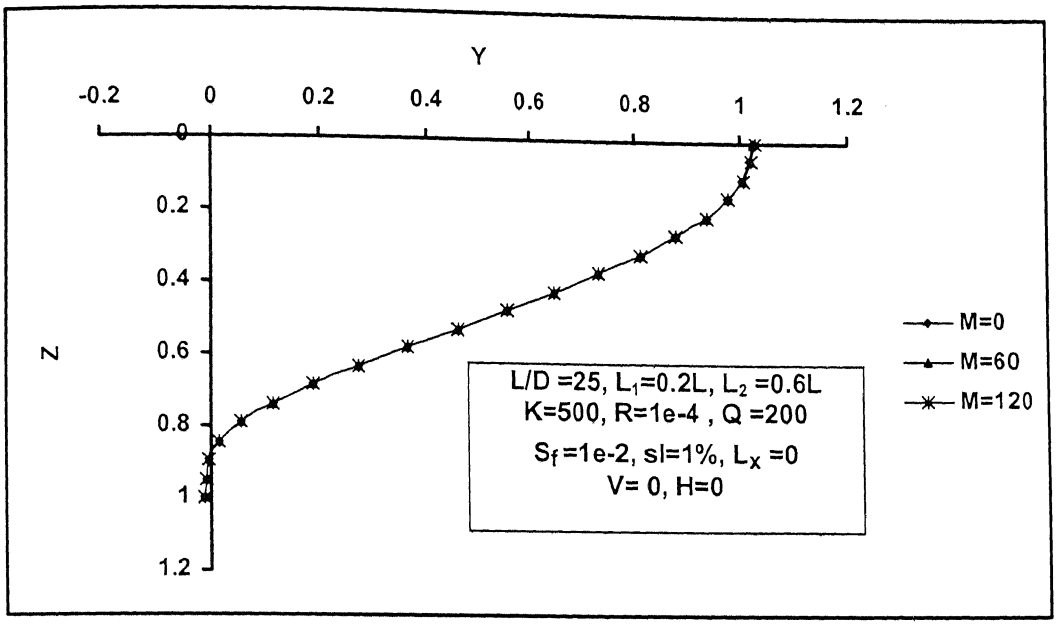


Fig.3.26 I Variation of Y of a Fixed-Free pile with Z for different M

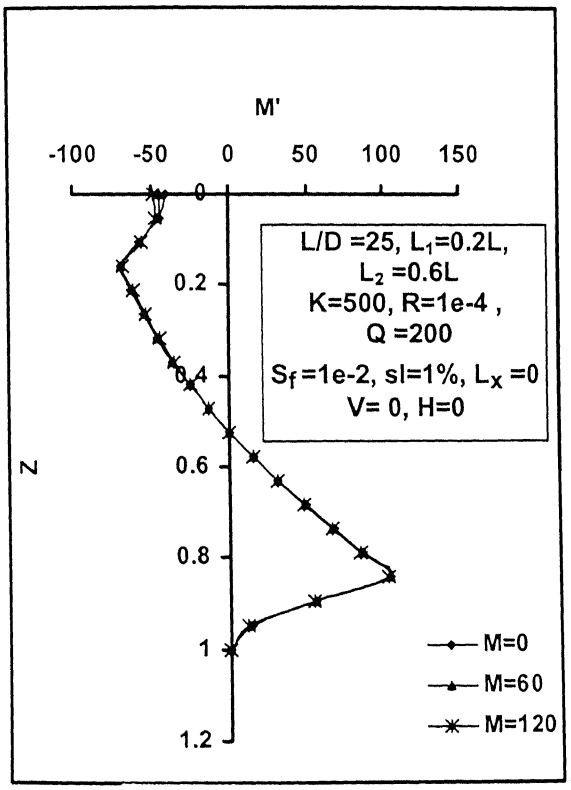


Fig.3.27 Variation of M' of a Fixed -Free pile with Z for different M

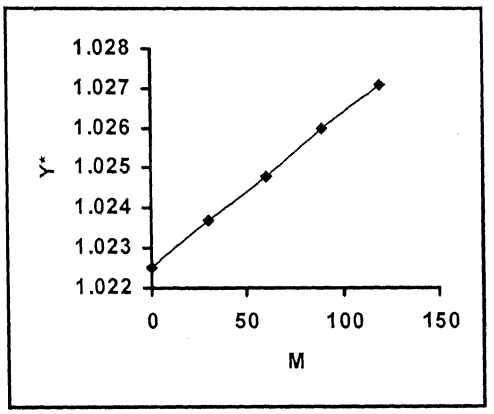


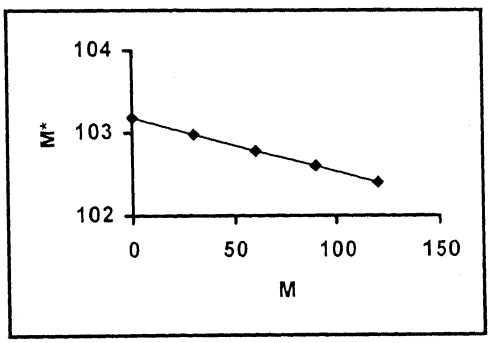


**Fig.3.28** Effect of M on the Y*and M* of a Fixed-Free pile

### *3.5.4 Effect of combined loading*

The effects of combined loading on the Free-Free pile are shown in Fig.3.29 to Fig.3.32. The effect of axial and lateral loads i.e. H and M is in such a way that one force contradicts the effect of the other. H and M increases the pile head deflection where as V reduces it. The deflection at the top interface is increased by the influence of V whereas H and M reduces it (Fig.3.29). Under normal range of V, Y* increases with H and M. But when V exceeds the critical value, Y* reduces with lateral loads (Fig3.31). In the presence of lateral loads, the influence of V also changes. It is seen that as V increases, Y* increases with the increase in the lateral loads but in contrast, when V exceeds the critical value, Y* decreases. Fig.3.32 reveals that for the same H as M increases $M^*$ decreases. This is because the axial load imposes an increase in the maximum bending moment but the lateral load reduces it. Beyond critical range, V has prominent effect on the flexural behavior of the pile. Therefore it can be implied that when V is higher than the critical value, the presence of lateral loads and moment is beneficial.

The Fixed-Free pile shows a different behavior under combined loading which can be seen in Fig.3.33 to Fig.3.35.In this case the effect of M is negligible and hence not included in the analysis. In the normal range of V, the deflection is not affected by the axial as well as lateral loads (Fig.3.35). But beyond the critical range of V, Y* shows a normal range of values when H is less than 10.When H also exceeds 10, Y* increases by 1.8 times that of the normal range of deflection. This is because due to combined action of lateral load, axial load and the fixity of head, the pile head deflection is restricted, but the deflection in the liquefied region increases at a higher rate at higher values of loads. The bending moment increases with vertical load and the lateral load is not able to reduce it to the same extent as that of Free-Free pile, as pile head fixity also contributes to the developed bending moment. Beyond the critical range of V, M* decreases with H upto H is equal to 10 and then increases by 4 times. This is due to the larger moments developed in the liquefied region.

When V and H are above the limiting values, negative moment becomes larger than the positive moment, due to the larger deflection in the top interface.

This again substantiates the importance of considering axial load in the design of piles in lateral spreading areas. This also proves that the lateral loads aid the stability of piles to some extent. The Y* and M* for both the end conditions and for various loading conditions are given in Table 3.6.

| Free-Free Pile | | | | | | | |
|---|---|---|---|---|---|---|---|
| Y* | | | | M* | | | |
| M=0 | | | | | | | |
| H | V=0,M=0 | V=4,M=0 | V=8,M=0 | H | V=0,M=0 | V=4,M=0 | V=8,M=0 |
| 0 | 1.044 | 1.05 | 1.1881 | 0 | 100.4245 | 87.0652 | 423 |
| 10 | 1.0615 | 1.10 | 1.1674 | 10 | 98.7343 | 78.4786 | 363.6048 |
| 20 | 1.079 | 1.14 | 1.1467 | 20 | 97.0441 | 73.0219 | 309.7687 |
| M=50 | | | | | | | |
| H | V=0,M=50 | V=4,M=50 | V=8,M=50 | H | V=0,M=50 | V=4,M=50 | V=8,M=50 |
| 0 | 1.070 | 1.140 | 1.110 | 0 | 96.5 | 71.4 | 281 |
| 10 | 1.090 | 1.180 | 1.090 | 10 | 94.8 | 69.1 | 237 |
| 20 | 1.110 | 1.220 | 1.070 | 20 | 93.1 | 75.2 | 197 |
| M=100 | | | | | | | |
| H | V=0,M=100 | V=4,M=100 | V=8,M=100 | H | V=0,M=100 | V=4,M=100 | V=8,M=100 |
| 0 | 1.100 | 1.220 | 1.080 | 0 | 100 | 105 | 181 |
| 10 | 1.120 | 1.260 | 1.130 | 10 | 100 | 118 | 167 |
| 20 | 1.140 | 1.310 | 1.180 | 20 | 100 | 130 | 200 |

| Fixed-Free Pile | | | | | | | | |
|---|---|---|---|---|---|---|---|---|
| Y* | | | | | M* | | | |
| M=0 | | | | | | | | |
| H | V=0 | V=2 | V=4 | V=6 | H | V=0 | V=2 | V=4 | V=6 |
| 0 | 1.0225 | 1.030 | 1.029 | 1.1663 | 0 | 103.1691 | 94.1907 | 92.4 | 403.2 |
| 10 | 1.032 | 1.040 | 1.0411 | 1.0465 | 10 | 102.4983 | 92.739 | 90.4424 | 119.1 |
| 20 | 1.0416 | 1.050 | 1.0528 | 1.7035 | 20 | 101.8275 | 91.3713 | 88.5633 | 341.9 |

**Table 3.6** Variation of Y* and M* under combined loading

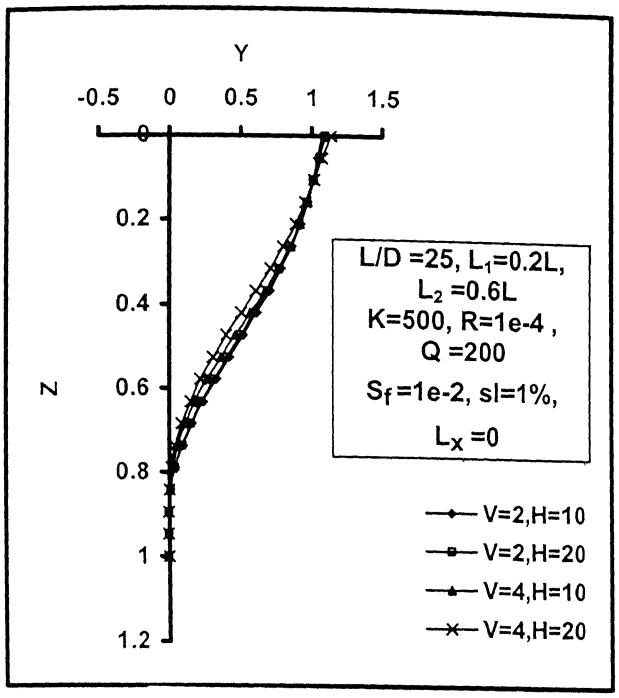


Fig.3.29 Variation of Y of a Free-Free pile with Z for different V and H

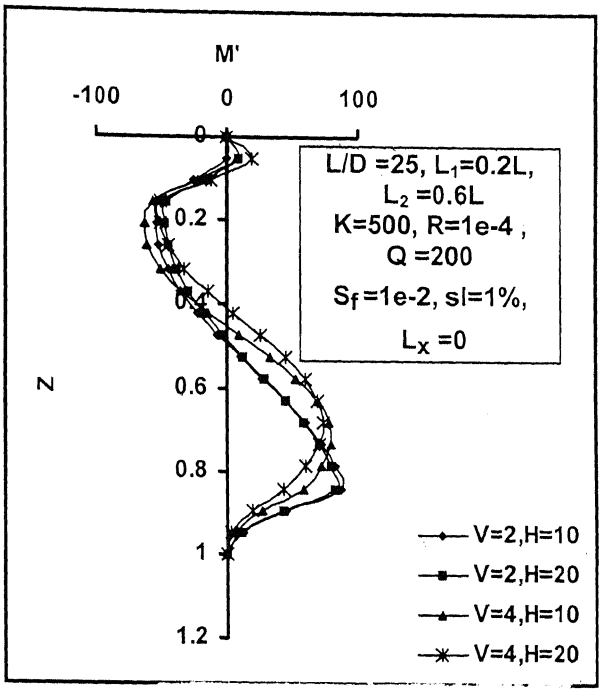


Fig.3.30 Variation of M' of a Free-Free pile with Z for different V and H.

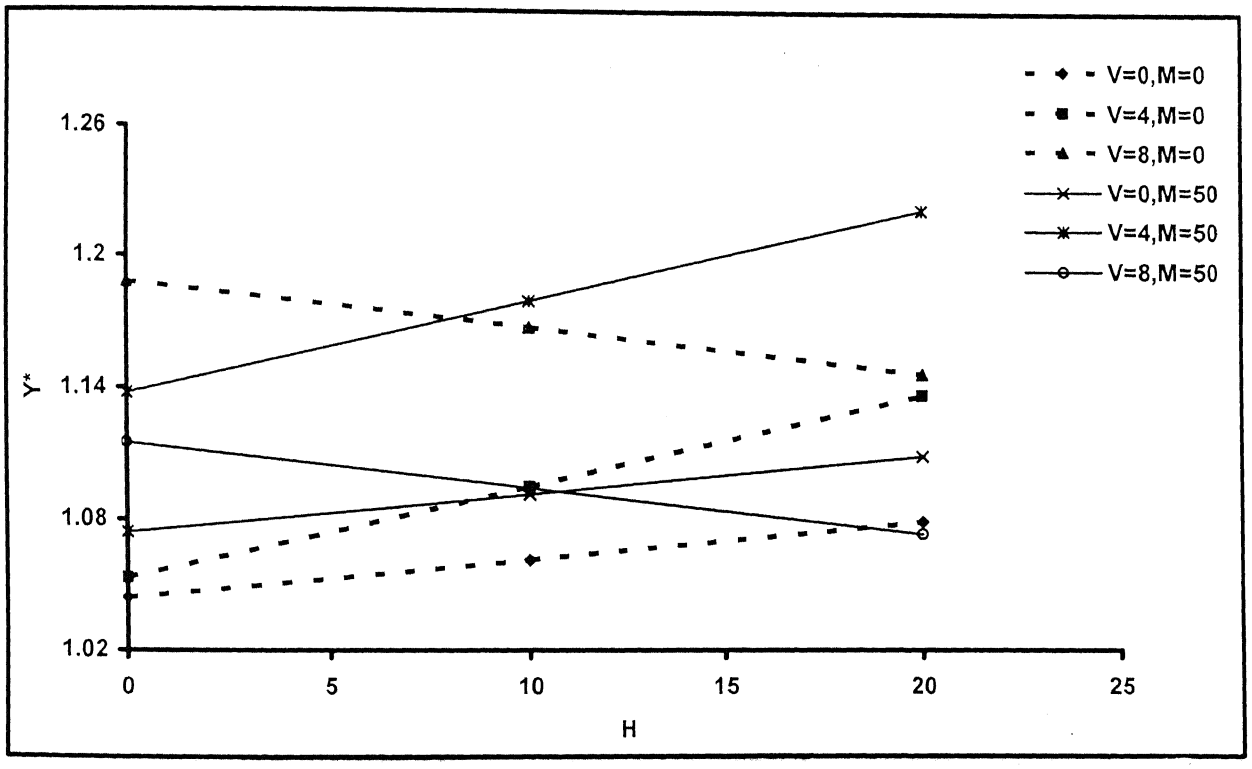


Fig.3.3 Effect of H on Y* of Free-Free pile for different V and M

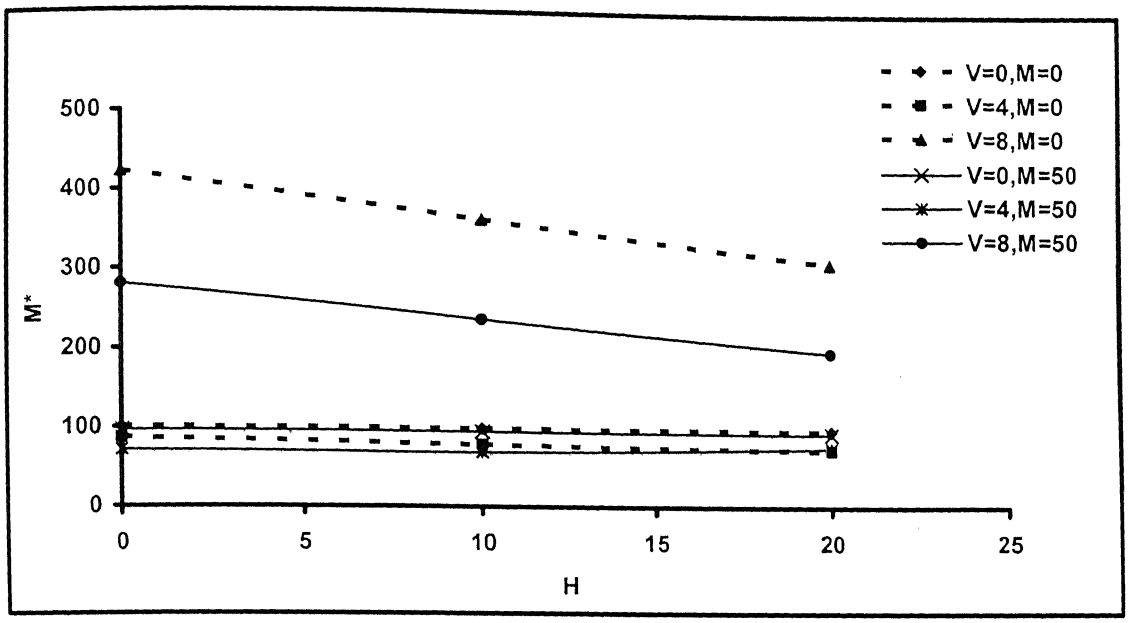


Fig.3.32 Effect of H on M* of Free-Free pile for different V and M

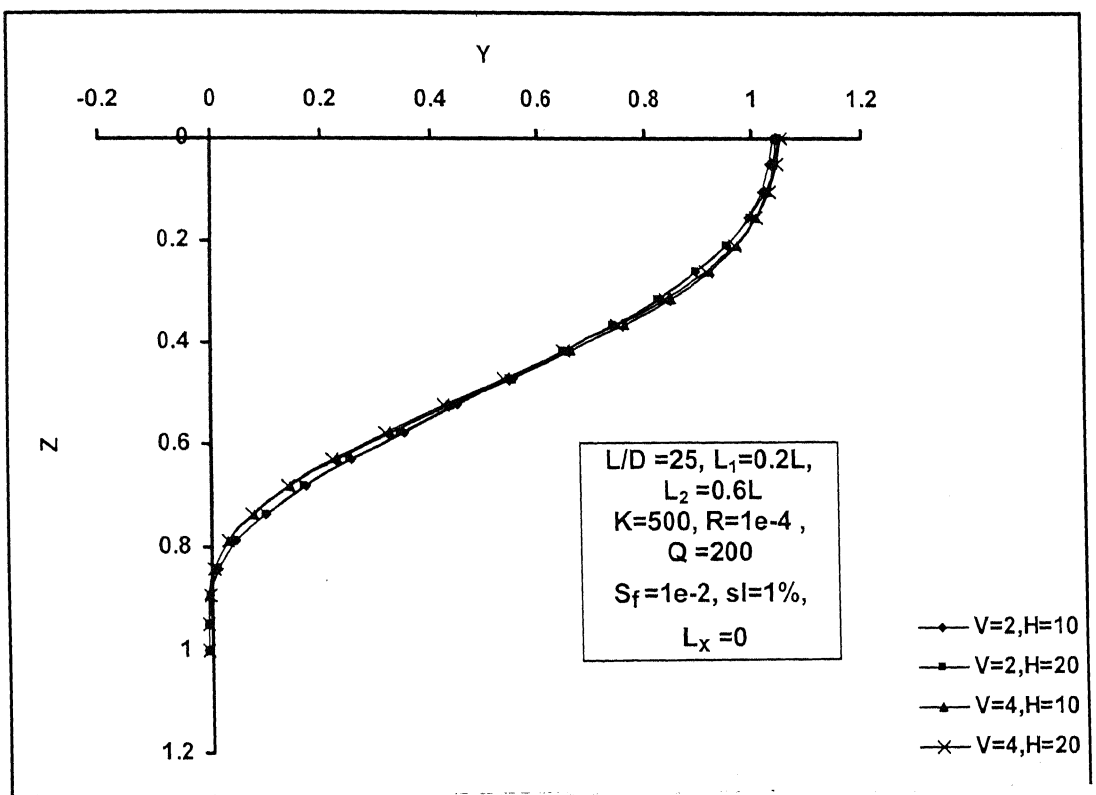


Fig.3.33 Variation of Y of a Fixed-Free pile with Z for different V and H

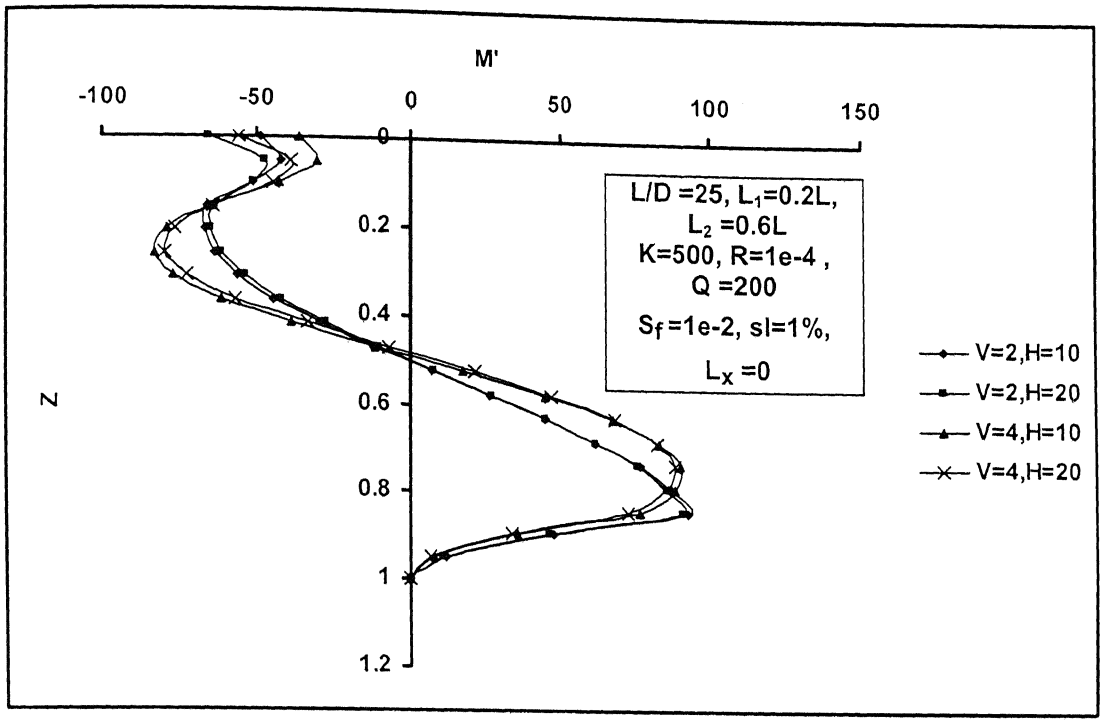


Fig.3.34 Variation of M' of a Fixed -Free pile with Z for different V and H

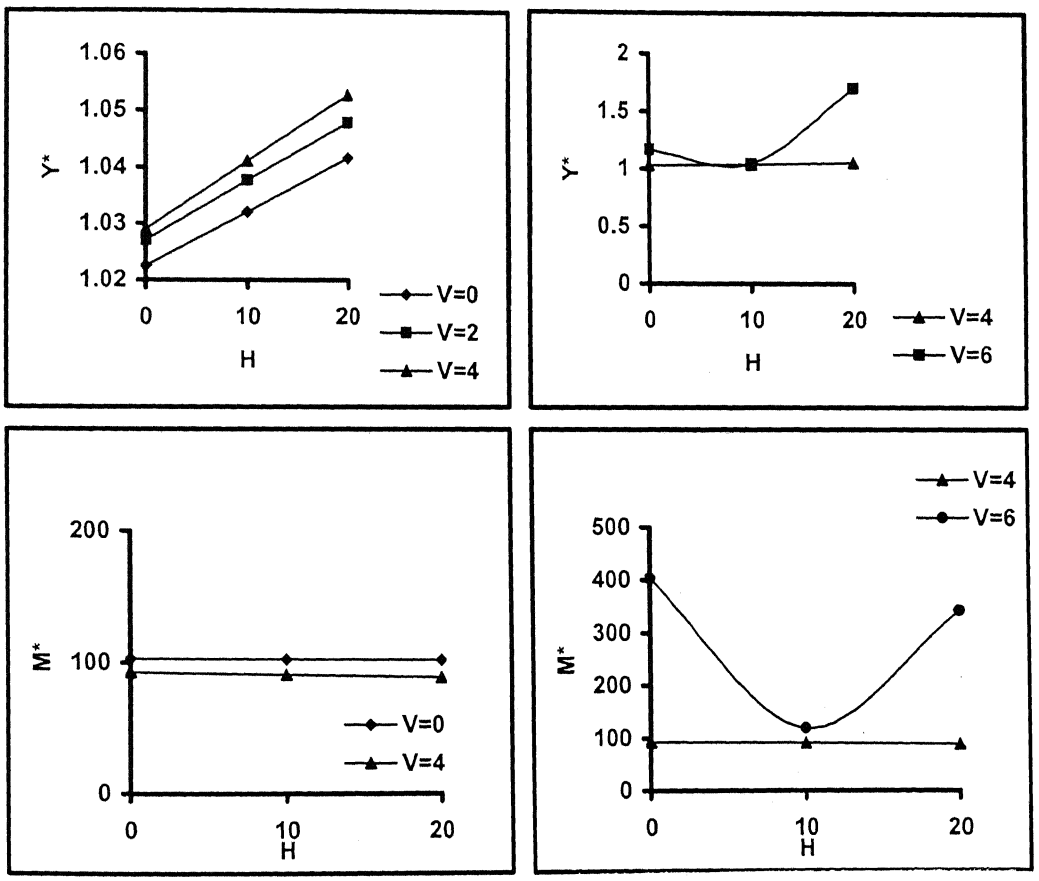


Fig.3.35 Effect of H on Y* and M* of Fixed-Free pile for different V

### 3.5.5 *Effect of stiffness factor*

The influence of stiffness factor, K on the flexural behavior of piles in liquefiable areas has been studied. The distribution of axial load depends on K. The axial load variation is assumed to be linear which can be expressed in the form

$$P(z) = P(1-\beta(z/L))$$

Where P (z) is the axial load at any depth z. P is the axial load at the pile head, L is the length of the pile and β is the variation coefficient. During liquefaction, the strength of the soil gets reduced and hence the load transfer to the firm embedded base increases. This effect is studied by two different values of K, K=500 and K=5000 for a vertical load factor V=2.The respective β values are 0.35 and 0.1.The results are plotted in Fig.3.36 and Fig.3.37. As K increases there is a negligible decrease in the deflection by 0.01D and the bending moment increases by 4%. The behavior is same in both the end conditions of pile.

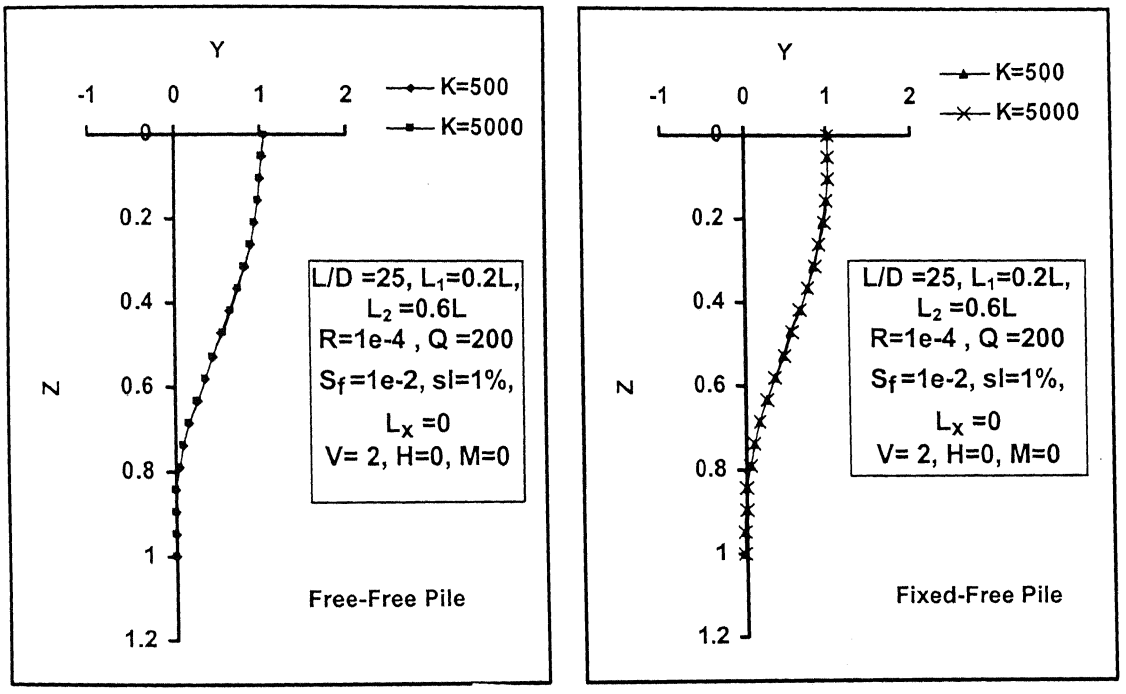


**Fig.3.36** Variation of Y with Z for different K

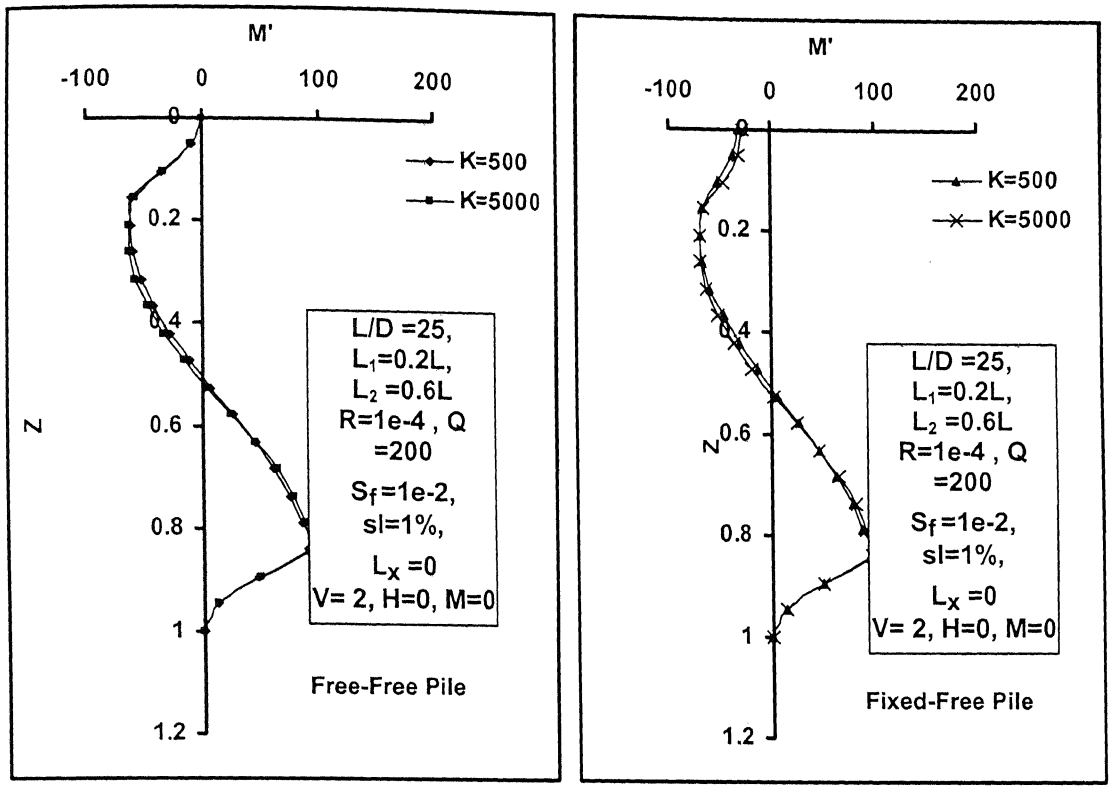


Fig.3.37 Variation of M' with Z for different K

### 3.5.6 *Effect of pile flexibility factor*

The influence of pile flexibility factor, R on the flexural behavior of piles in liquefiable areas has been studied. Under no external loading condition, the behavior of piles is shown in Fig.3.38 to Fig.3.42. The following observations are made from the above figures. The Y in the nonliquefied layer increases with increase in R (Fig.3.38 and Fig.3.40). Similar behavior is observed for M' (Fig.3.39 and Fig.3.41). The nondimensional deflection in the liquefied region decreases with increase in R. Y* occurs at the pile top and it varies nonlinearly with R (Fig3.42). M* in Free-Free pile occurs at the lower interface and it varies nonlinearly with R. At higher values of R indicating stiffer piles, the pile is able to resist the additional drag force exerted by liquefied soil and therefore the deformed shape does not exactly follow the soil deformation pattern. The developed moments will be larger as the

pile flexibility is less. The bending moment in the Fixed-Free piles is around 4 times that of the Free-Free pile when R is 0.007 and also the M* occurs at the pile head. The M* of Fixed-Free pile varies linearly with R.

| Free-Free Pile | | | Fixed-Free Pile | | |
|---|---|---|---|---|---|
| R | Y* | M* | Y* | M* (at bottom interface) | -M* (at the pile head) |
| 0.0001 | 1.04 | 100.425 | 1.0225 | 103.1691 | 69.2376 |
| 0.001 | 1.11 | 390.902 | 1.0166 | 468.5667 | 625.4676 |
| 0.007 | 1.10 | 717.611 | 0.9967 | 523.1 | 3421.5 |

**Table 3.7** Variation of Y* and M* with R under lateral spreading force

For a Free-Free pile subjected to lateral loading, Y* and M* increases if R increases. Also, the rate of increase in Y* with increase in H and M reduces. The results are shown in Fig 3.43 and Fig.3.44.

The charts for combined loading are shown in Fig 3.45 to Fig.3.50. Higher value of R causes increase in deflection and bending moment. The Fixed–Free pile has M* at the pile head at higher value of R. The trend of the graphs of R=1E-3 is same as that of R=1E-4 in normal range of V. This indicates that piles with high flexural rigidity can take care of greater axial loads. But the developed moment should be limited within the yield moment of the section. The values of Y* and M* under various loading are given in Table 3.8

| Free-Free Pile | | | | | | |
|---|---|---|---|---|---|---|
| Y* | | | | M* | | |
| **R=1E-4** | | | | | | |
| H | V=0,R=1E-4 | V=4,R=1E-4 | V=8,R=1E-4 | V=0,R=1E-4 | V=4,R=1E-4 | V=8,R=1E-4 |
| 0 | 1.044 | 1.050 | 1.1881 | 100.4245 | 87.0652 | 423 |
| 10 | 1.0615 | 1.100 | 1.1674 | 98.7343 | 78.4786 | 363.6048 |
| 20 | 1.079 | 1.140 | 1.1467 | 97.0441 | 73.0219 | 309.7687 |
| M | V=0,R=1E-4 | V=4,R=1E-4 | V=8,R=1E-4 | V=0,R=1E-4 | V=4,R=1E-4 | V=8,R=1E-4 |
| 0 | 1.044 | 1.050 | 1.1881 | 100.4245 | 87.0652 | 423 |
| 50 | 1.074 | 1.140 | 1.110 | 96.516 | 71.4 | 281 |
| 100 | 1.104 | 1.220 | 1.080 | 100 | 105 | 181 |
| M | H=0,R=1E-4 | H=10,R=1E-4 | H=20,R=1E-4 | H=0,R=1E-4 | H=10,R=1E-4 | H=20,R=1E-4 |
| 0 | 1.044 | 1.0615 | 1.079 | 100.4245 | 98.7343 | 97.0441 |
| 50 | 1.074 | 1.0915 | 1.109 | 96.516 | 94.8258 | 93.1356 |
| 100 | 1.104 | 1.1215 | 1.1391 | 100 | 100 | 100 |
| **R=1E-3** | | | | | | |
| H | V=0,R=1E-3 | V=4,R=1E-3 | V=8,R=1E-3 | V=0,R=1E-3 | V=4,R=1E-3 | V=8,R=1E-3 |
| 0 | 1.110 | 1.140 | 1.200 | 391 | 360 | 330 |
| 10 | 1.120 | 1.150 | 1.210 | 389 | 357 | 334 |
| 20 | 1.130 | 1.170 | 1.220 | 387 | 354 | 339 |
| M | V=0,R=1E-3 | V=4,R=1E-3 | V=8,R=1E-3 | V=0,R=1E-3 | V=4,R=1E-3 | V=8,R=1E-3 |
| 0 | 1.110 | 1.140 | 1.200 | 391 | 360 | 330 |
| 50 | 1.120 | 1.150 | 1.210 | 383 | 350 | 336 |
| 100 | 1.120 | 1.170 | 1.230 | 375 | 339 | 349 |
| M | H=0,R=1E-3 | H=10,R=1E-3 | H=20,R=1E-3 | H=0,R=1E-3 | H=10,R=1E-3 | H=20,R=1E-3 |
| 0 | 1.110 | 1.120 | 1.130 | 391 | 389 | 387 |
| 50 | 1.120 | 1.1249 | 1.130 | 383 | 381 | 379 |
| 100 | 1.120 | 1.130 | 1.140 | 375 | 373 | 371 |

| Fixed-Free Pile | | | | | | | |
|---|---|---|---|---|---|---|---|
| Y* | | | | M* | | | |
| R=1E-4 | | | | | | | |
| H | V=0,R=1E-4 | V=4,R=1E-4 | V=6,R=1E-4 | H | V=0,R=1E-4 | V=4,R=1E-4 | V=6,R=1E-4 |
| 0 | 1.0225 | 1.029 | 1.1663 | 0 | 103.1691 | 92.4 | 403.2474 |
| 10 | 1.032 | 1.0411 | 1.0465 | 10 | 102.4983 | 90.4424 | 119.1688 |
| 20 | 1.0416 | 1.0528 | 1.7035 | 20 | 101.8275 | 88.5633 | 341.9241 |
| R=1E-3 | | | | | | | |
| H | V=0,R=1E-3 | V=4,R=1E-3 | V=6,R=1E-3 | H | V=0,R=1E-3 | V=4,R=1E-3 | V=8,R=1E-3 |
| 0 | 1.020 | 1.030 | 1.040 | 0 | 468 | 469 | 469 |
| 10 | 1.020 | 1.040 | 1.050 | 10 | 469 | 470 | 470 |
| 20 | 1.030 | 1.040 | 1.050 | 20 | 470 | 471 | 471 |

**Table 3.8** Variation of Y* and M* with R under combined loading

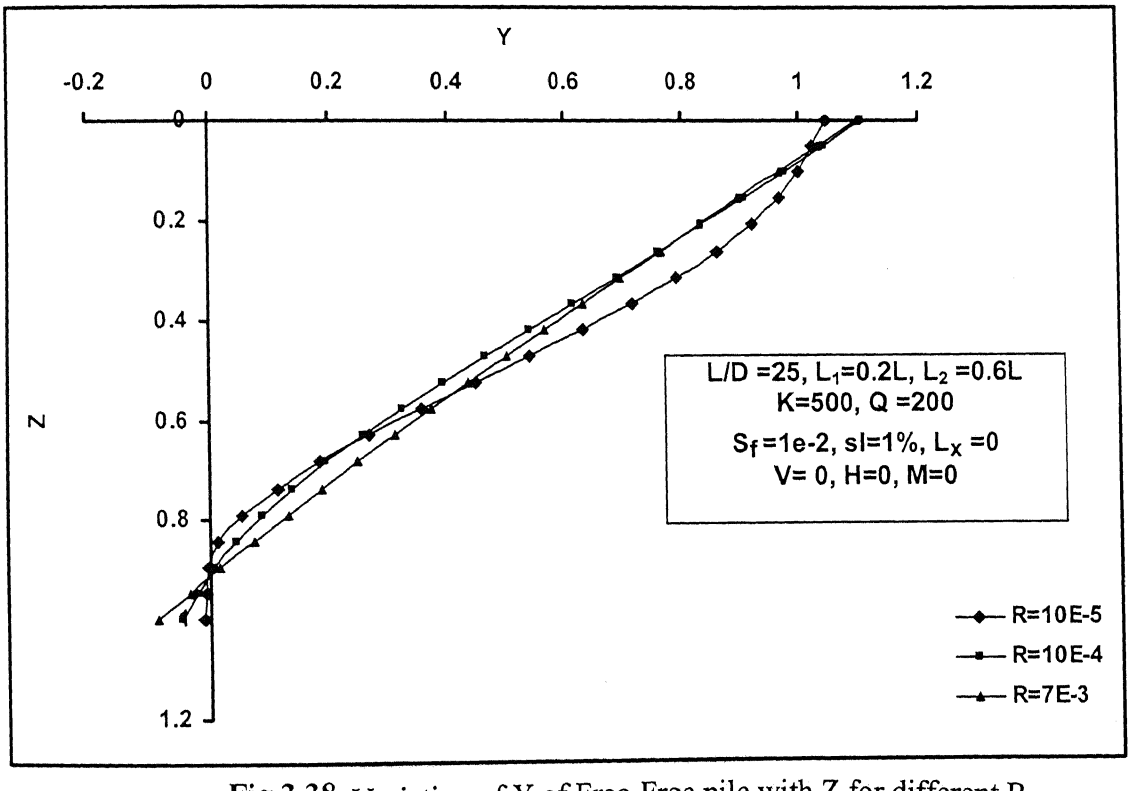


**Fig.3.38** Variation of Y of Free-Free pile with Z for different R

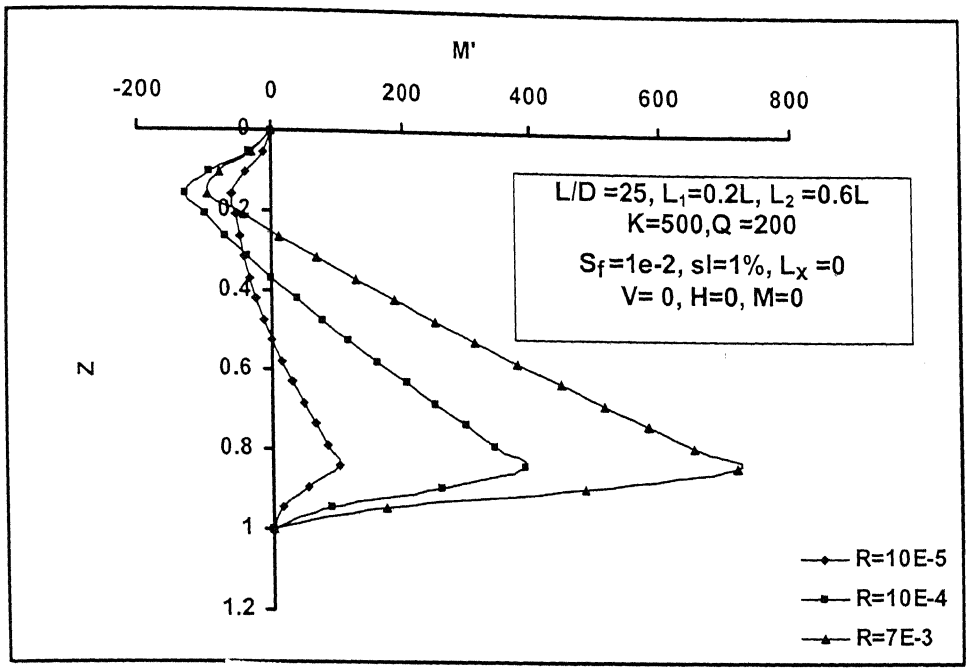


Fig.3.39 Variation of M' of Free-Free pile with Z for different R

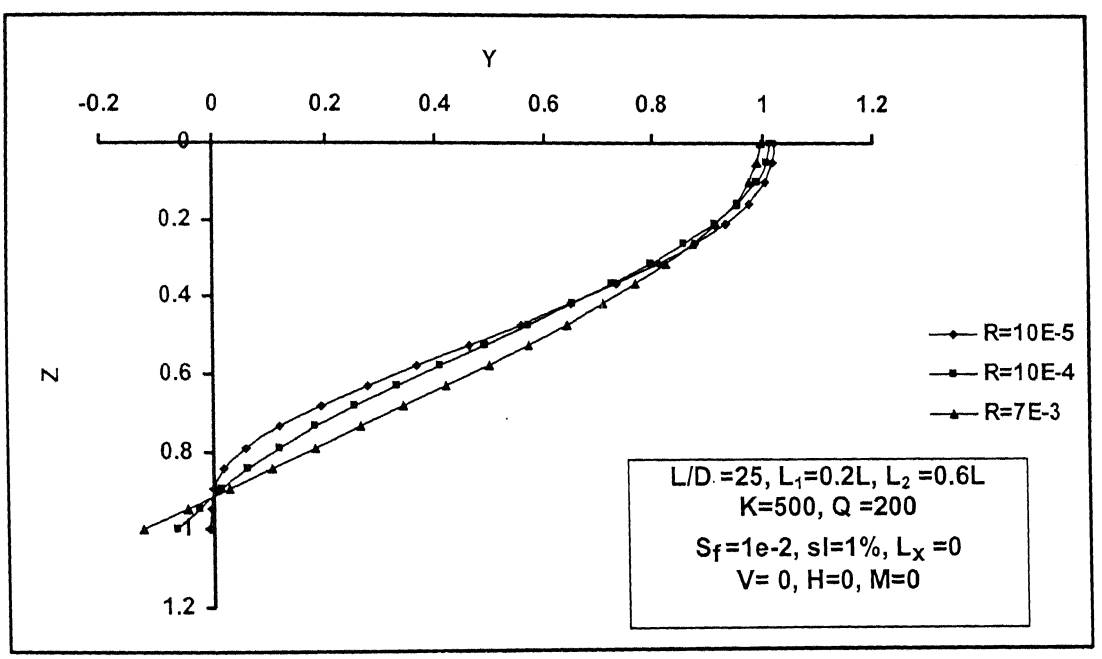


Fig.3.40 Variation of Y of Fixed-Free pile with Z for different R

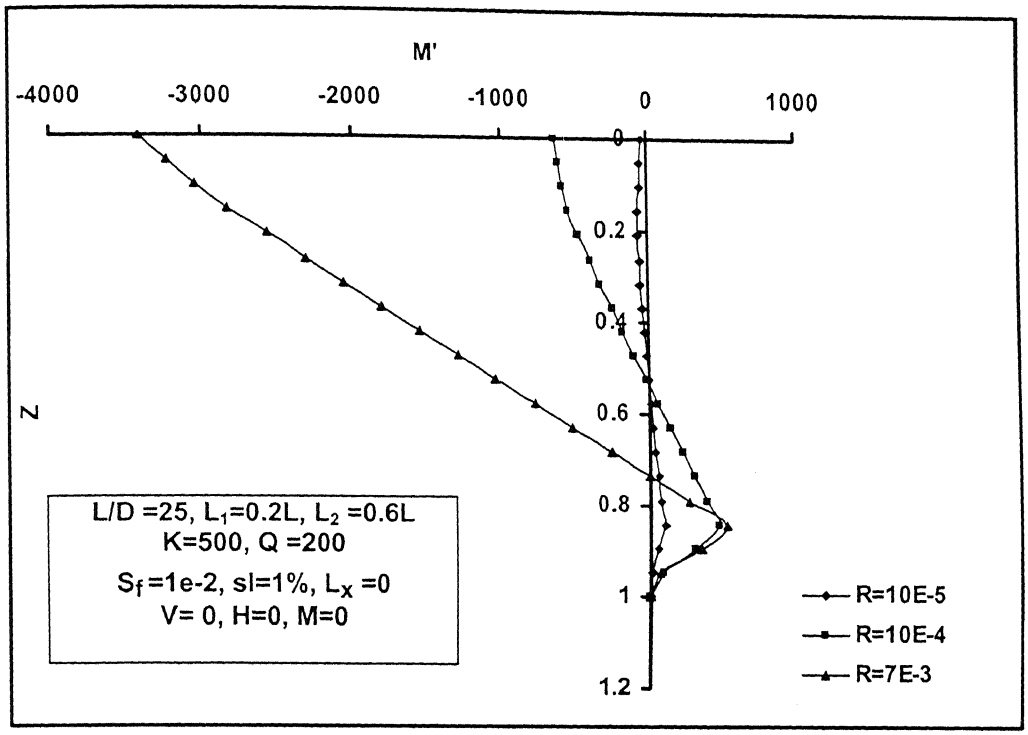


**Fig.3.41** Effect of R on the bending moment of Fixed-Free pile

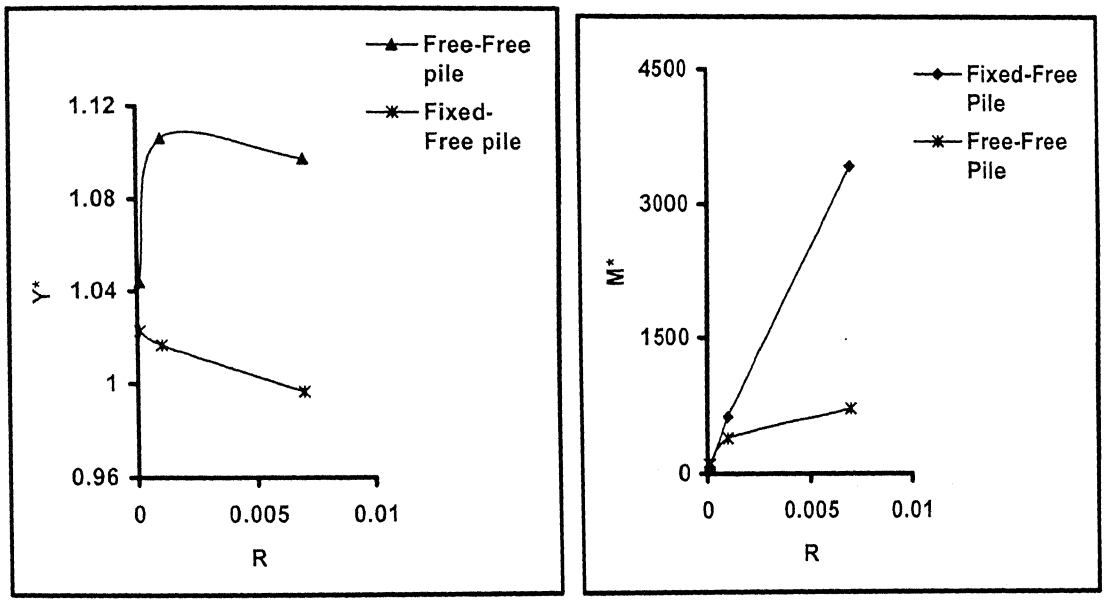


**Fig.3.42** Effect of R on Y* and M*

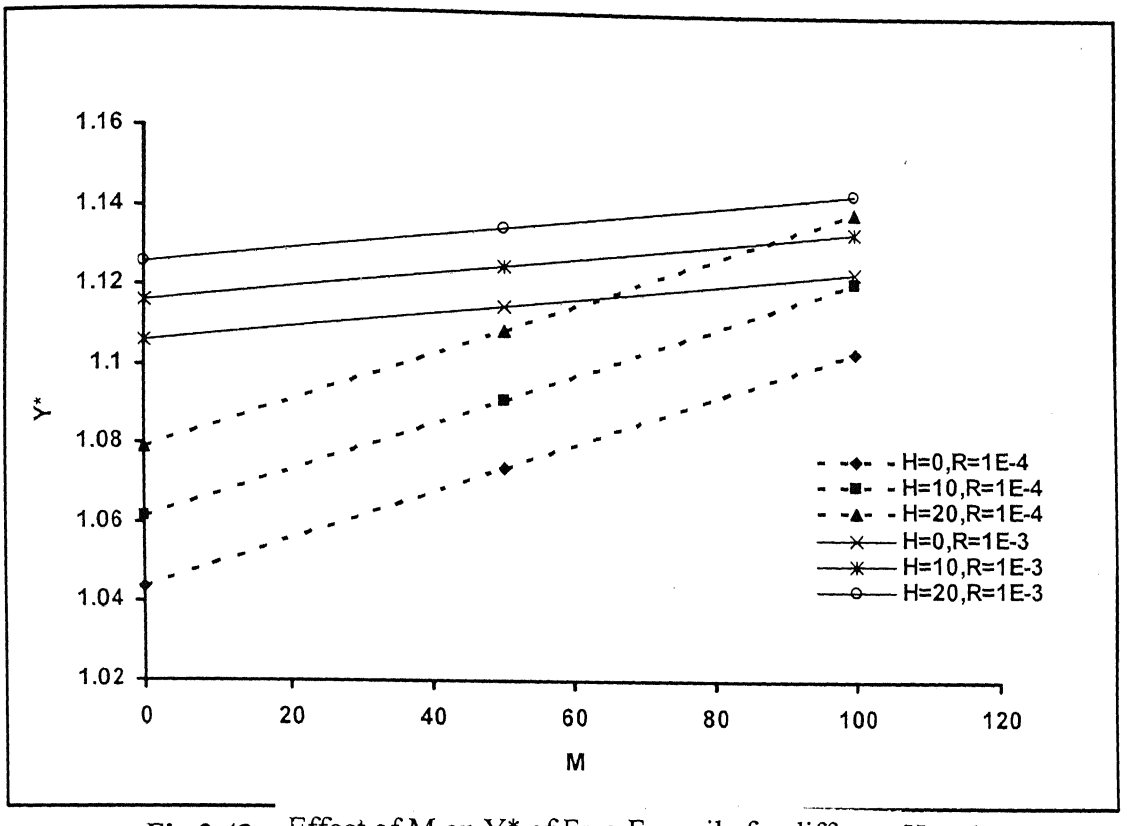


Fig.3.43 Effect of M on Y* of Free-Free pile for different H and R

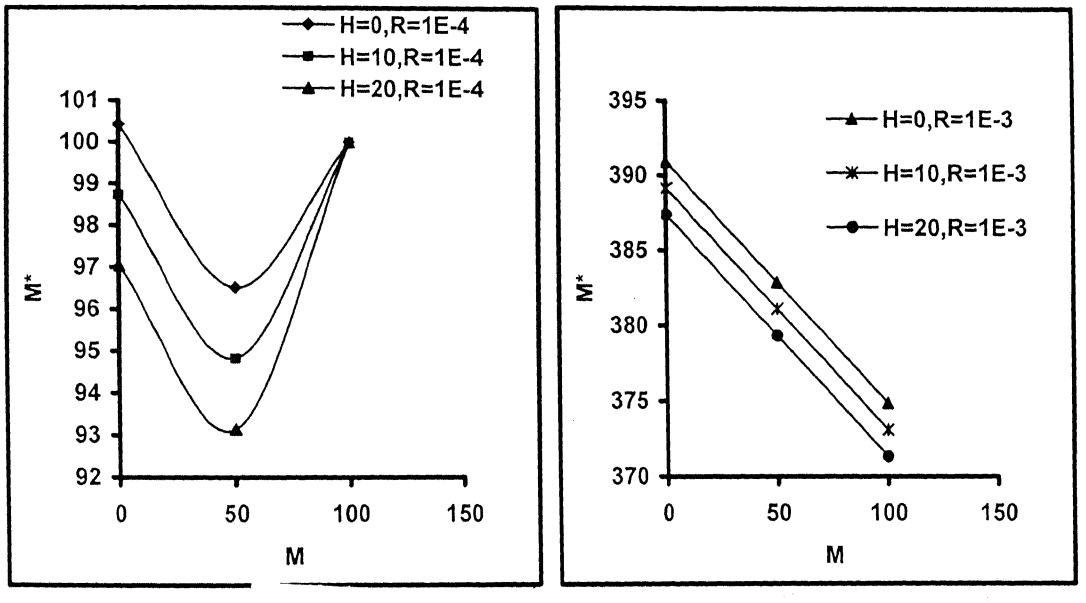


Fig.3.44 Effect of M on M* of Free-Free pile for different H and R

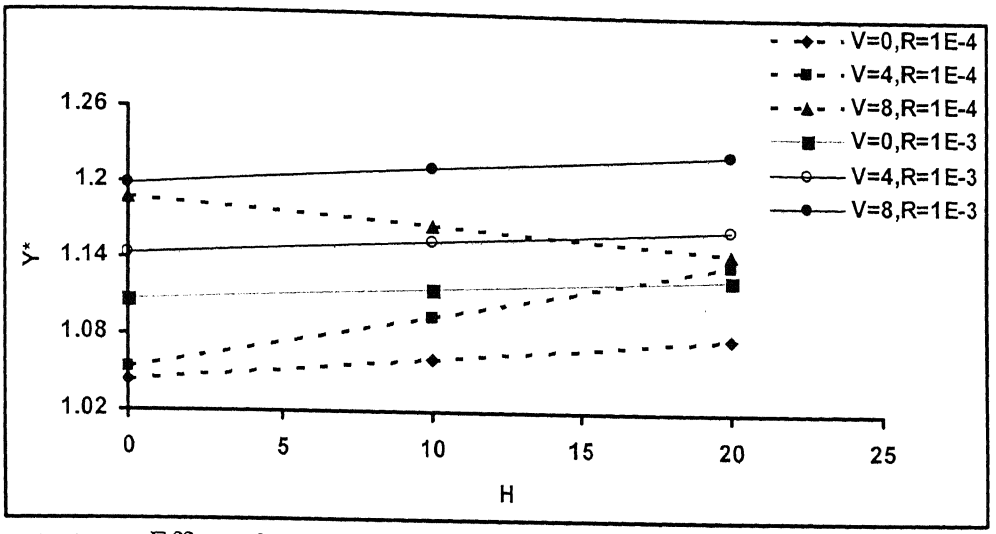


Fig.3.45] Effect of H on Y* of Free-Free pile for different V and R

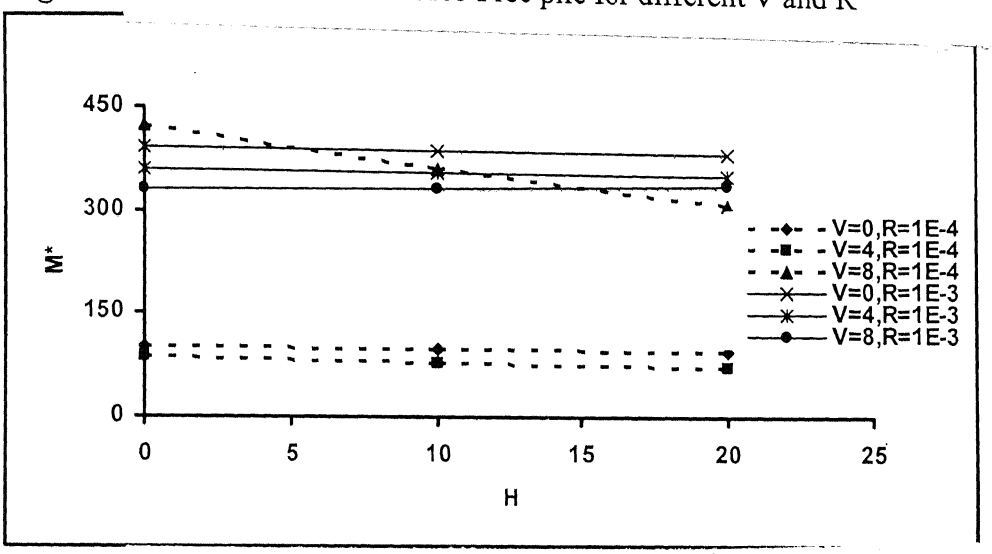


Fig.3.46] Effect of H on M* of Free-Free pile for different V and R

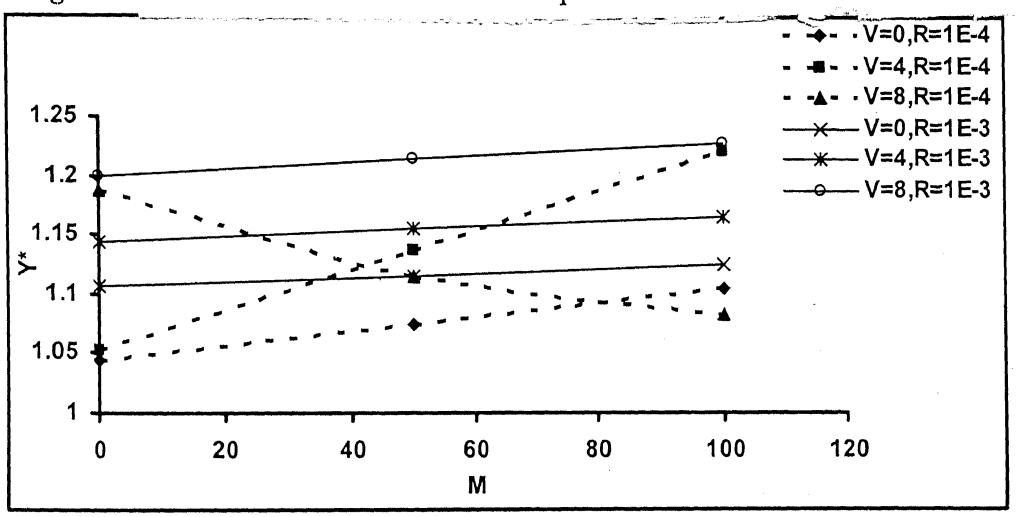


Fig.3.47[ Effect of M on Y* of Free-Free pile for different V and R

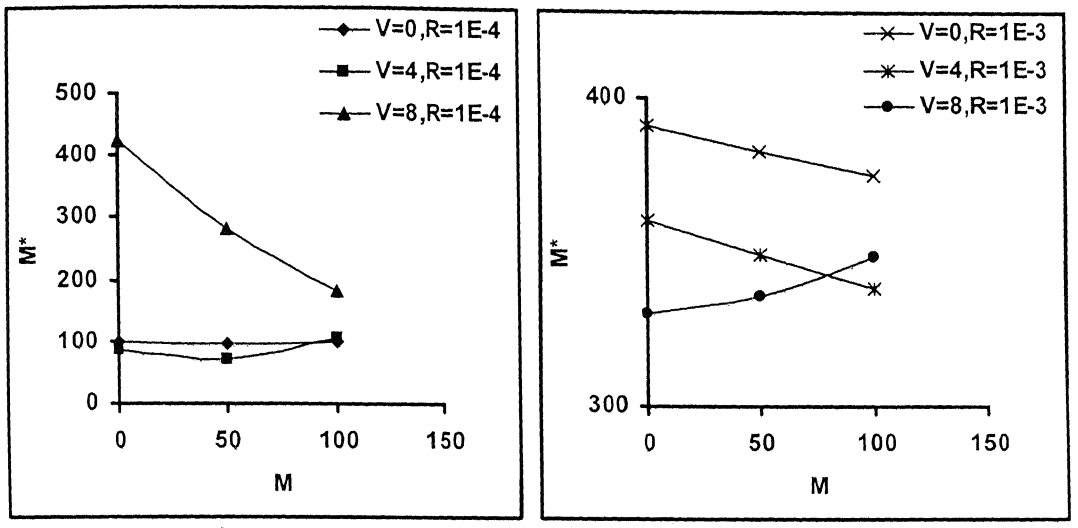


Fig.3.48 Effect of M on M* of Free-Free pile for different V and R (

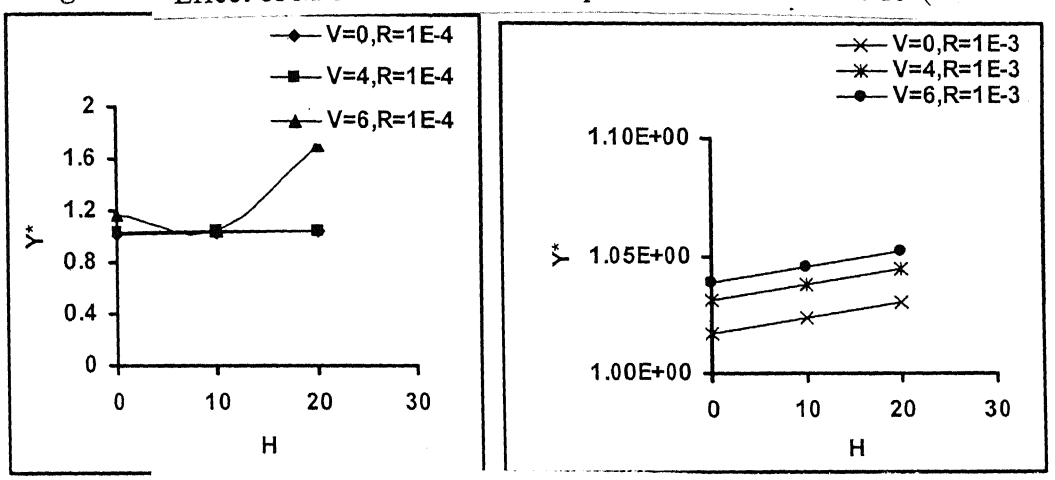


Fig.3.49 Effect of H on Y* of Fixed-Free pile for different V and R

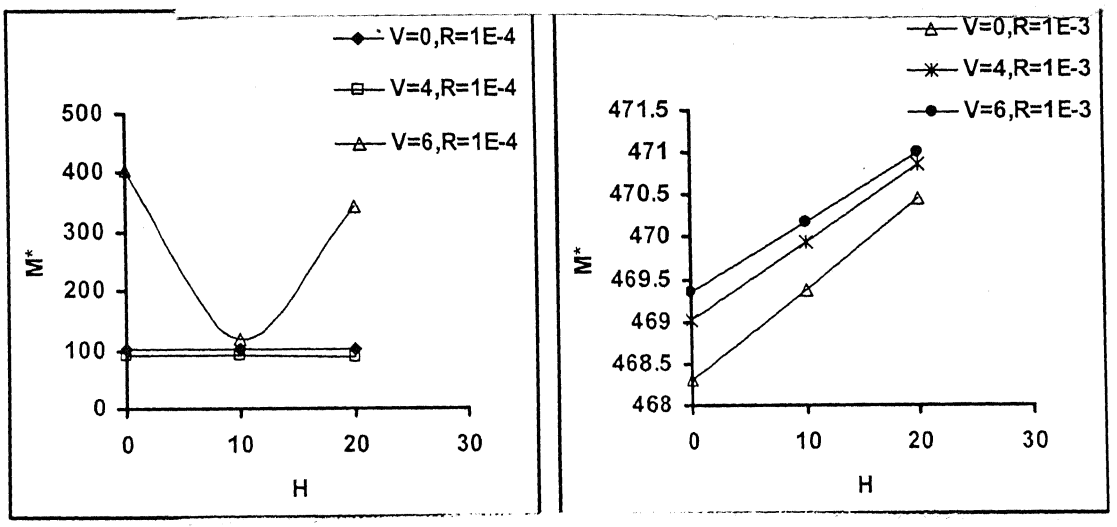


Fig.3.50 Effect of H on M* of Fixed-Free pile for different V and R

### *3.5.7 Effect of soil modulus to soil strength ratio*

The effect of the ratio (Q) of the soil modulus ($E_s$) to its un-drained shear strength ($S_u$) is studied and the results with no external loading are presented in Fig.3.51 to Fig.3.53. The Q does not have any influence on Y. But M' is directly proportional to Q. The maximum value of the deflection coefficient i.e. Y* has been found to be 1.04 (Table 3.9).

| | Free-Free Pile | | Fixed-Free Pile | |
|---|---|---|---|---|
| Q | Y* | M* | Y* | M* |
| 100 | 1.04 | 50.2122 | 1.0225 | 51.5845 |
| 200 | 1.04 | 100.4245 | 1.0225 | 103.1691 |
| 300 | 1.04 | 150.6367 | 1.0225 | 154.7536 |
| 400 | 1.04 | 200.849 | 1.0225 | 206.3382 |
| 500 | 1.044 | 251.0612 | 1.0225 | 257.9227 |

**Table 3.9** Variation of Y* and M* with Q

Under lateral loading, the influence of Q on the behavior of Free-Free pile is shown in Fig.3.54 and Fig.3.55. Y* decreases as Q increases. The rate of increase of Y* with M and H gets slightly reduced with the increment in Q. M* increases as Q increases. The increase in Q implies a reduction in $S_u$. This causes a reduction in the magnitude of real load and that is the reason for the apparent decrease in the magnitude of Y*.

The effect of Q on deformation and bending moment under combined loading is shown in Fig.3.56 to Fig.3.61. Y* and M* are found to decrease with the increase in Q. But if V exceeds the critical range then Y* and M* increases with Q. The variation of Q does not affect the trend of curves, except that in the Fixed-Free pile for Q=400, Y* and M* go on decreasing even if H exceeds 10.Table 3.10 shows the effect of Q on Y* and M* under combined loading conditions.

| Free-Free Pile | | | | | | |
|---|---|---|---|---|---|---|
| | Y* | | | M* | | |
| H | V=0,Q=200 | V=4,Q=200 | V=8,Q=200 | V=0,Q=200 | V=4,Q=200 | V=8,Q=200 |
| 0 | 1.044 | 1.050 | 1.1881 | 100.4245 | 87.0652 | 423 |
| 10 | 1.0615 | 1.100 | 1.1674 | 98.7343 | 78.4786 | 363.6048 |
| 20 | 1.079 | 1.140 | 1.1467 | 97.0441 | 73.0219 | 309.7687 |
| M | V=0,Q=200 | V=4,Q=200 | V=8,Q=200 | V=0,Q=200 | V=4,Q=200 | V=8,Q=200 |
| 0 | 1.044 | 1.050 | 1.1881 | 100.4245 | 87.0652 | 423 |
| 50 | 1.074 | 1.140 | 1.110 | 96.516 | 71.4 | 281 |
| 100 | 1.104 | 1.220 | 1.080 | 100 | 105 | 181 |
| M | H=0,Q=200 | H=10,Q=200 | H=20,Q=200 | H=0,Q=200 | H=10,Q=200 | H=20,Q=200 |
| 0 | 1.044 | 1.0615 | 1.079 | 100.4245 | 98.7343 | 97.0441 |
| 50 | 1.074 | 1.0915 | 1.109 | 96.516 | 94.8258 | 93.1356 |
| 100 | 1.104 | 1.1215 | 1.1391 | 100 | 100 | 100 |
| H | V=0,Q=400 | V=4,Q=400 | V=8,Q=400 | V=0,Q=400 | V=4,Q=400 | V=8,Q=400 |
| 0 | 1.044 | 1.050 | 1.190 | 200.849 | 174 | 845 |
| 10 | 1.050 | 1.070 | 1.180 | 199 | 166 | 786 |
| 20 | 1.060 | 1.100 | 1.170 | 197 | 157 | 727 |
| M | V=0,Q=400 | V=4,Q=400 | V=8,Q=400 | V=0,Q=400 | V=4,Q=400 | V=8,Q=400 |
| 0 | 1.044 | 1.050 | 1.190 | 200.849 | 174 | 845 |
| 50 | 1.059 | 1.0954 | 1.1515 | 196.9405 | 155.3873 | 690 |
| 100 | 1.074 | 1.1376 | 1.1148 | 193.0321 | 142.8802 | 561 |
| M | H=0,Q=400 | H=10,Q=400 | H=20,Q=200 | H=0,Q=400 | H=10,Q=400 | H=20,Q=400 |
| 0 | 1.044 | 1.0528 | 1.0615 | 200.849 | 199.1588 | 197.4685 |
| 50 | 1.059 | 1.0678 | 1.0765 | 196.9405 | 195.2503 | 193.5601 |
| 100 | 1.074 | 1.0828 | 1.0915 | 193.0321 | 191.3419 | 189.6516 |

**Table 3.10** Variation of Y* and M* with Q under combined loading

| Fixed-Free Pile | | | | | | |
|---|---|---|---|---|---|---|
| | Y* | | | M* | | |
| H | V=0,Q=200 | V=4,Q=200 | V=6,Q=200 | V=0,Q=200 | V=4,Q=200 | V=6,Q=200 |
| 0 | 1.0225 | 1.029 | 1.1663 | 103.1691 | 92.4 | 403.2474 |
| 10 | 1.032 | 1.0411 | 1.0465 | 102.4983 | 90.4424 | 119.1688 |
| 20 | 1.0416 | 1.0528 | 1.7035 | 101.8275 | 88.5633 | 341.9241 |
| H | V=0,Q=400 | V=4,Q=400 | V=6,Q=400 | V=0,Q=400 | V=4,Q=400 | V=6,Q=400 |
| 0 | 1.0225 | 1.030 | 1.170 | 206.3382 | 185 | 820 |
| 10 | 1.030 | 1.040 | 1.110 | 206 | 183 | 471 |
| 20 | 1.030 | 1.040 | 1.050 | 205 | 181 | 238 |

**Table 3.10** Variation of Y* and M* with Q under combined loading (contd)

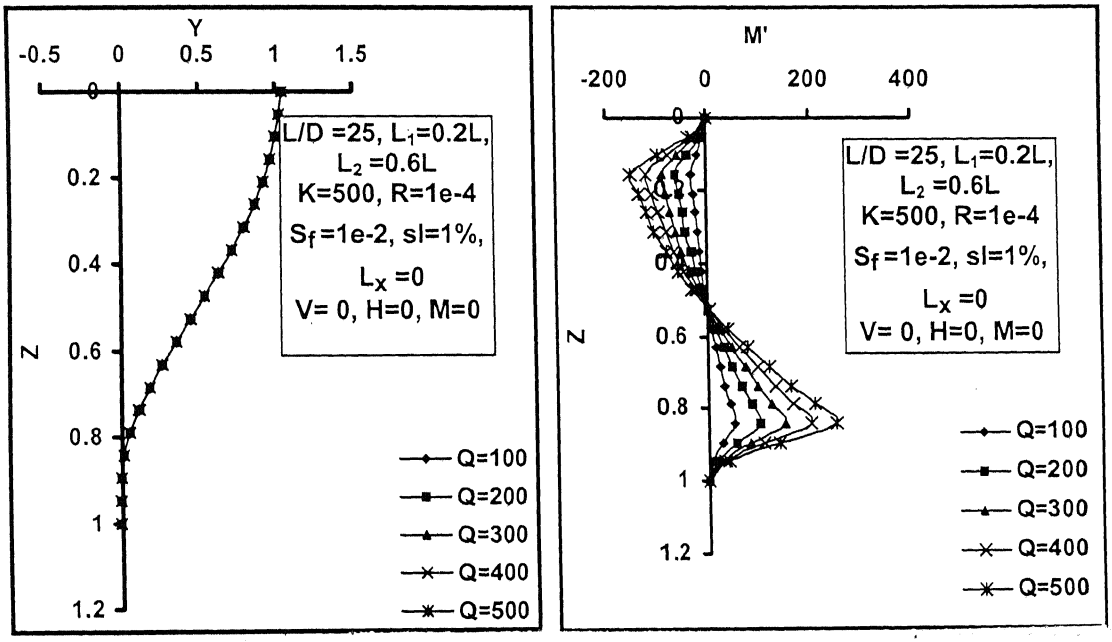


**Fig.3.51** Variation of Y and M' of Free-Free pile with Z for different Q

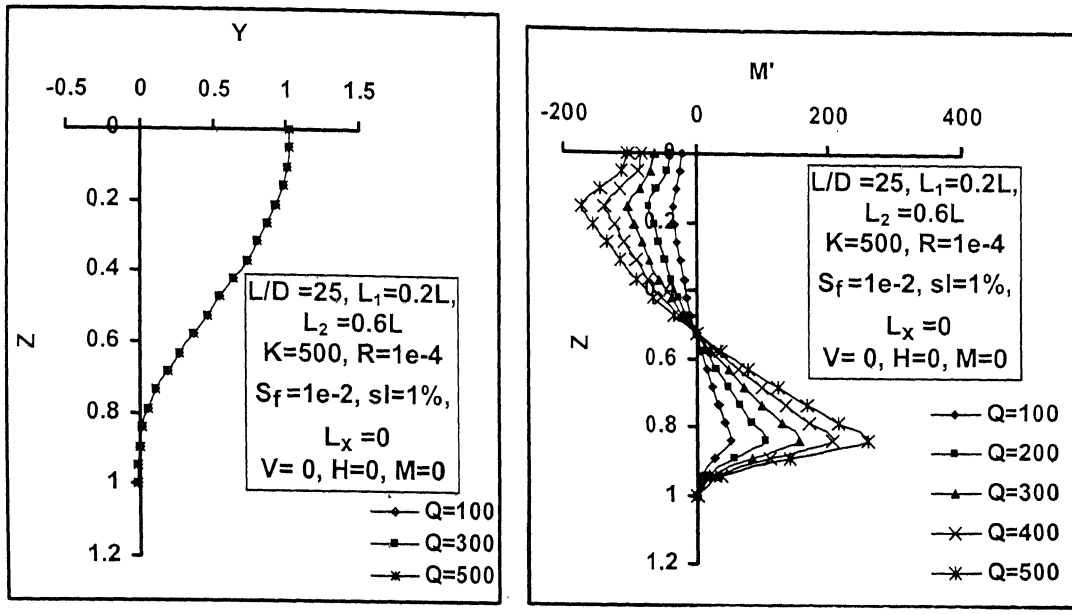


**Fig.3.52** Variation of Y and M' of Fixed-Free pile with Z for different Q

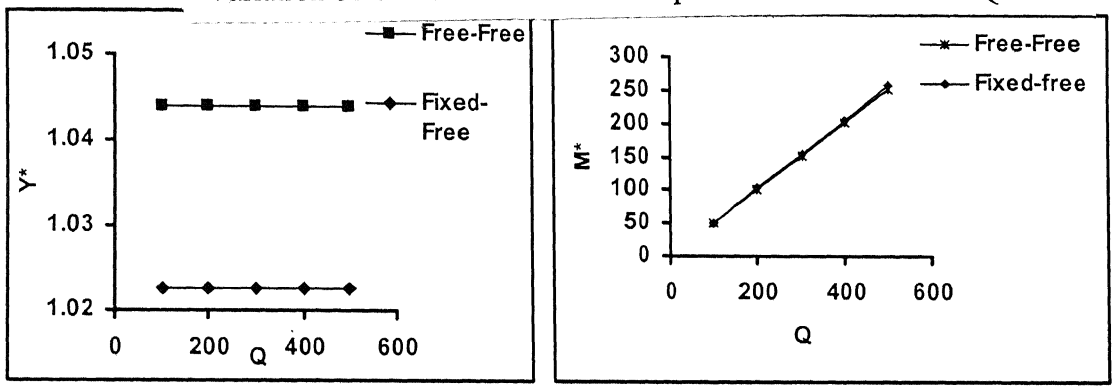


**Fig.3.53** Effect of Q on Y* and M*

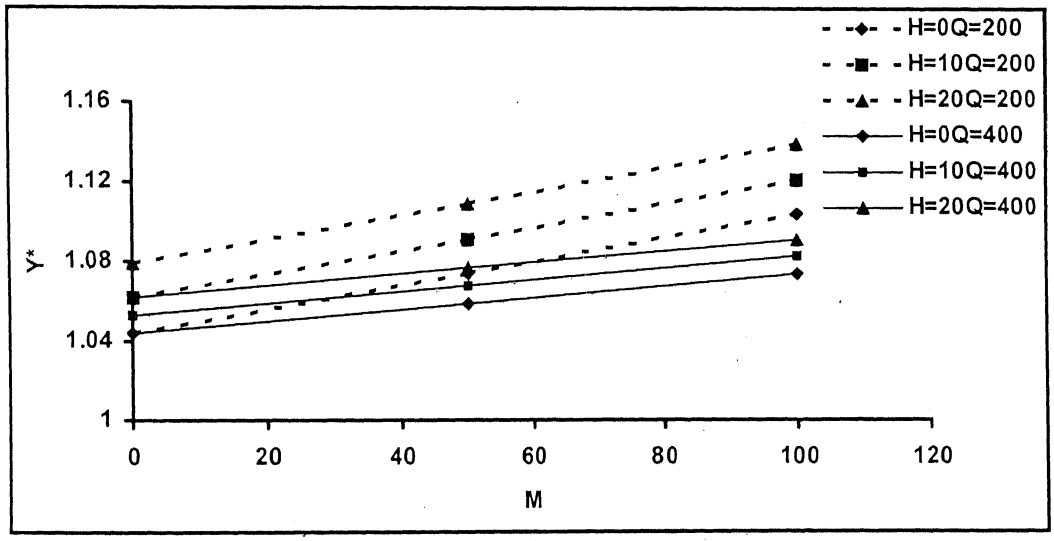


**Fig.3.54** Effect of M on Y* of Free-Free pile for different H and Q

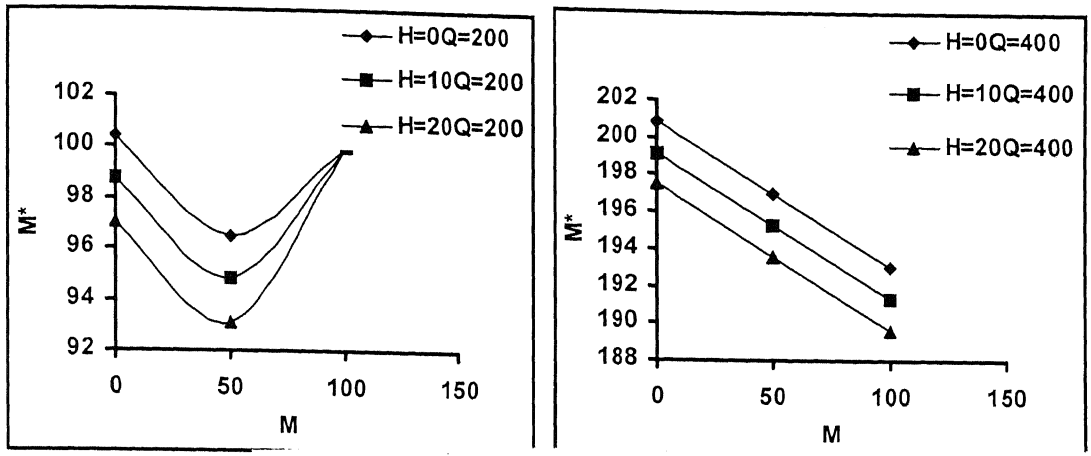


Fig.3.55 : Effect of M on M* of Free-Free pile for different H and Q

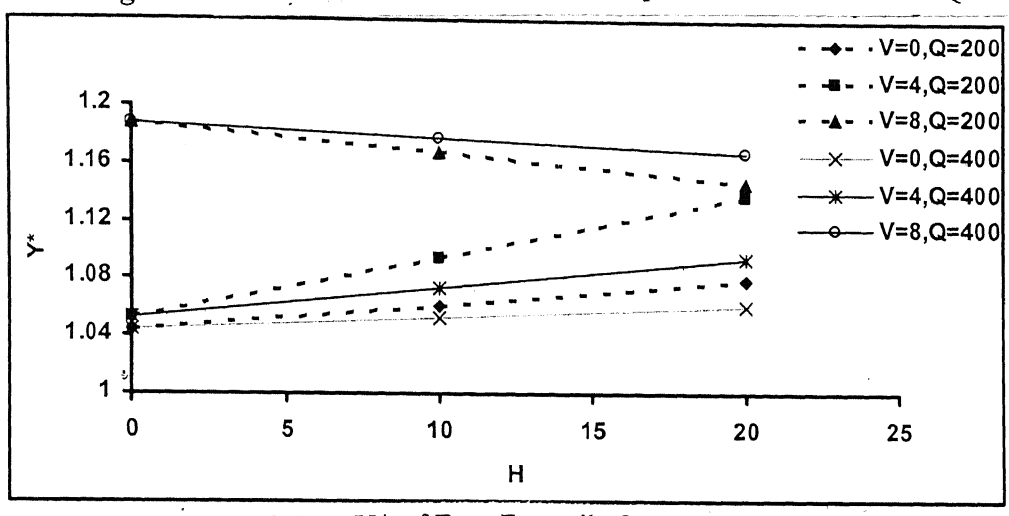


Fig.3.56 Effect of H on Y* of Free-Free pile for different V and Q

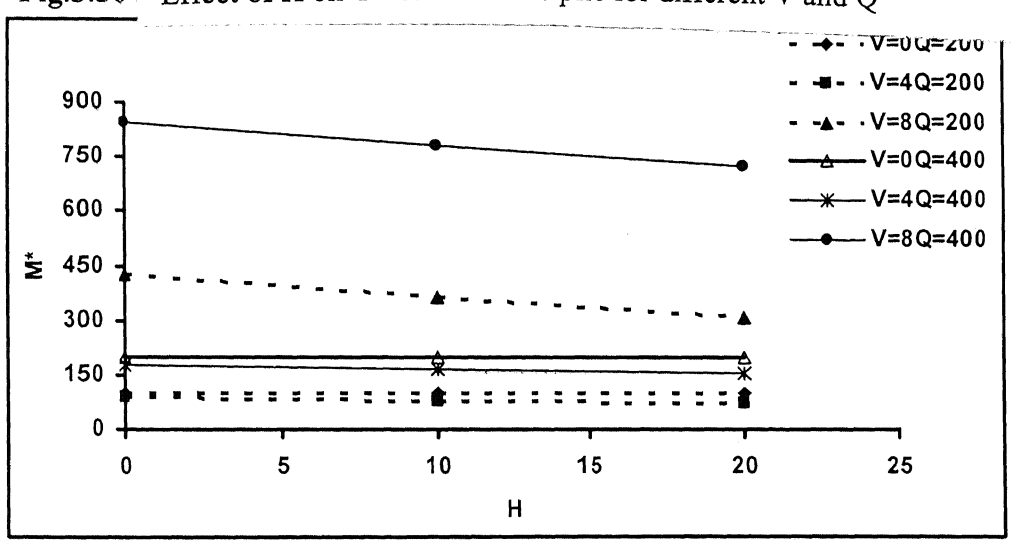


Fig.3.57 Effect of H on M* of Free-Free pile for different V and Q

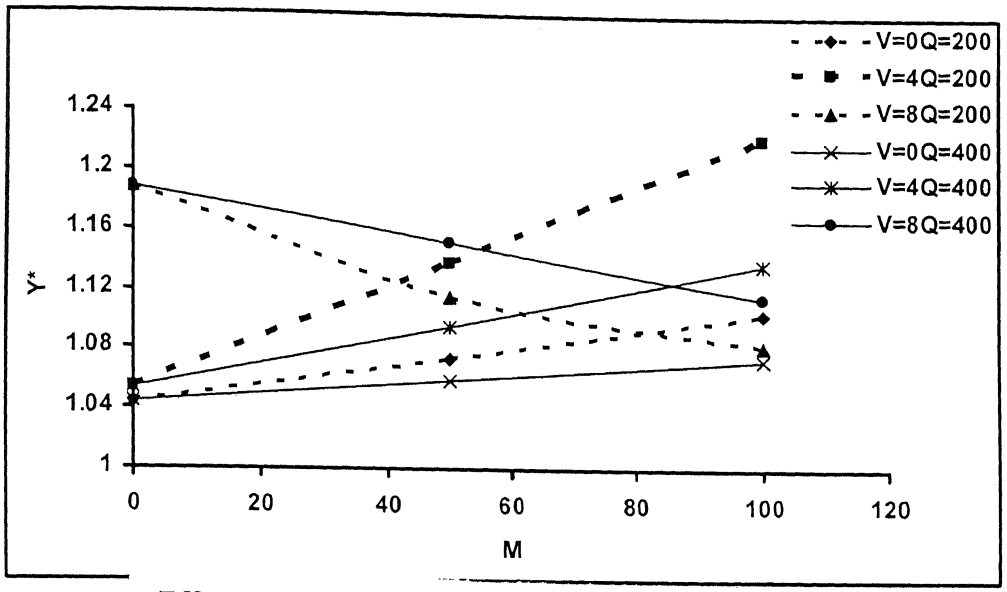


Fig.3.58 Effect of M on Y* of Free-Free pile for different V and Q

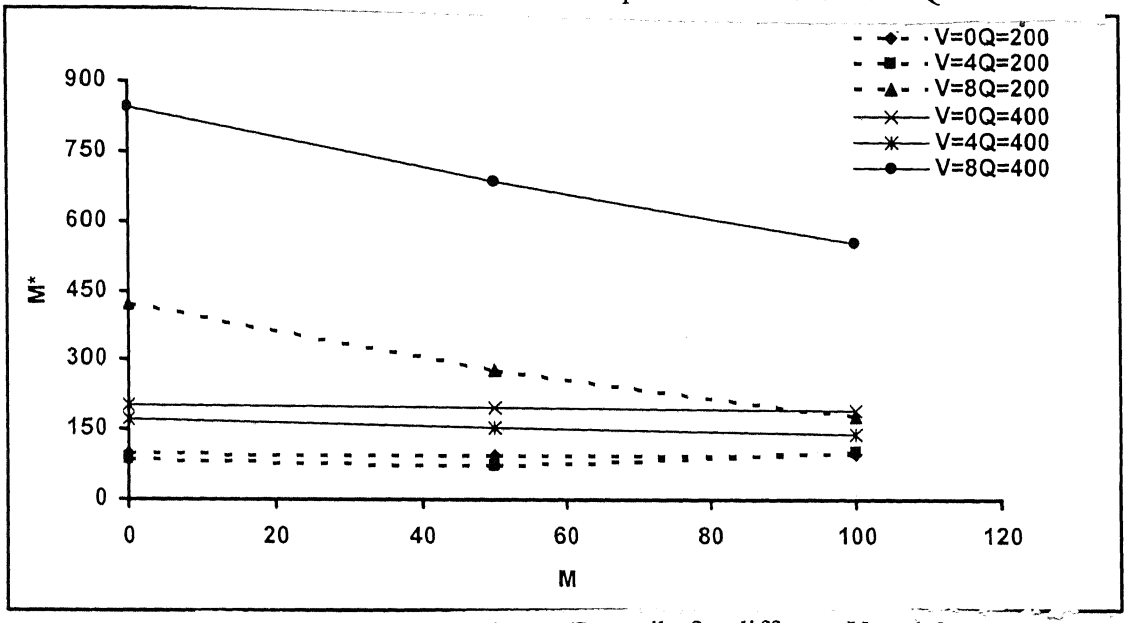


Fig.3.59 Effect of M on M* of Free-Free pile for different V and Q

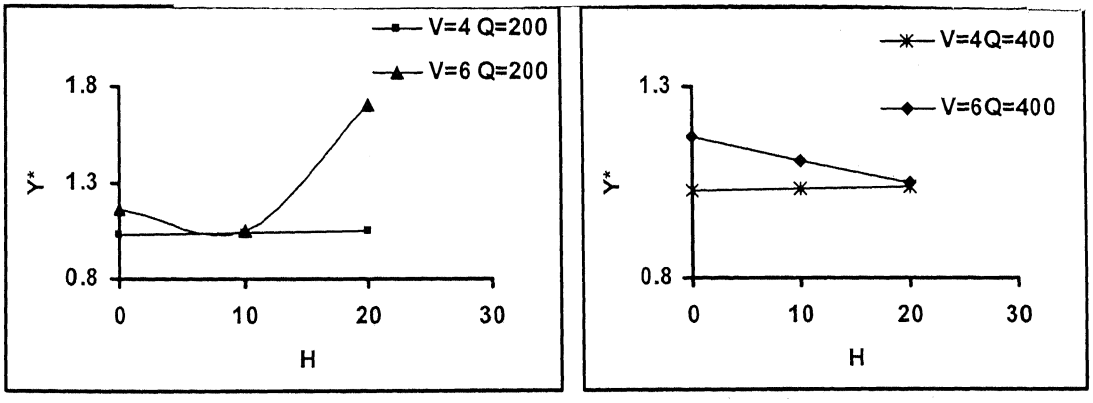


Fig.3.60 Effect of H on Y* of Fixed-Free pile for different V and Q

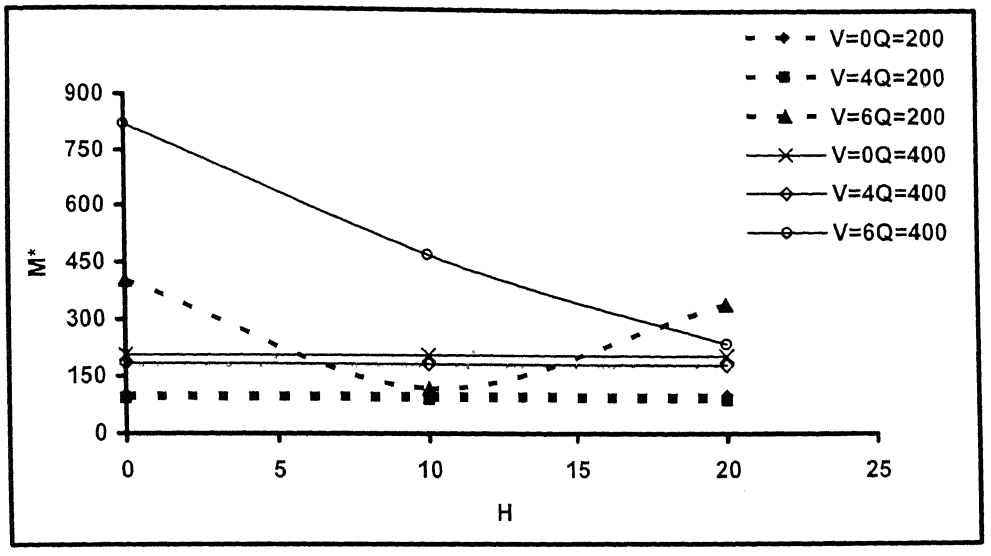


**Fig.3.61** Effect of H on M* of Fixed-Free pile for different V and Q

### *3.5.8 Effect of L/D*

The influence of L/D on the flexural behavior of the pile subjected only to lateral spreading is studied and it is presented in Fig.3.61 to Fig.3.65. The Y increases with increase in L/D. The Y* occurring at the pile top shows a linear increase with increase in L/D. When L/D =50, the maximum deflection is more than twice the diameter. The M' also increases with increase in L/D and the rate of increase in M* (occurring at Z=0.8) increases at an increasing rate and beyond L/D equal to 25 the rate of increase is constant with a sharp change in gradient from the earlier one; it indicates that L/D= 25 is the critical slenderness ratio (for the given set of data shown Fig.3.61) beyond which the piles are not suitable in liquefying areas. Slenderness should be below a particular limit depending on the lateral spreading forces in order to have allowable values of deflection and bending moment.

When lateral loading is also there along with lateral spreading forces, the influence of L/D is shown in Fig.3.66 and Fig.3.67. As L/D varies from 25 to 50, the Y* doubles and the M* increases by 6 times. As L/D increases the rate of decrease of Y* and M* with increase in H decreases from 3% to 1%.The rate of increase of Y* and the rate of decrease of M* with M also decreases from 5% to1%.

The effect of L/D on deformation and bending moment under combined loading is shown in Fig.3.68 to Fig.3.70.Whether it is V and H or V and M acting, the graphs show the same trend in variations. Y* increases by twice and M* increases by six times when L/D is increased from 25 to50.The variations in Y* and M* with loadings remain same for both L/D's except that in critical vertical loading. The variation of Y* and M* with L/D under lateral spreading force and combined loading conditions are shown in Table3.11 and Table 3.12 respectively.

| | Free-Free Pile | | Fixed-Free Pile | |
|---|---|---|---|---|
| L/D | Y* | M* | Y* | M* |
| 10 | 0.408 | 8.3145 | 0.406 | 8.3335 |
| 15 | 0.617 | 25.1594 | 0.6111 | 25.3708 |
| 20 | 0.83 | 54.9589 | 0.8167 | 55.9018 |
| 25 | 1.040 | 100.425 | 1.0225 | 103.1691 |
| 50 | 2.1366 | 637.795 | 2.051 | 688.8324 |

**Table 3.11**Variation of Y* and M* with L/D under lateral spreading force

| Free-Free Pile | | | | | | |
|---|---|---|---|---|---|---|
| | Y* | | | M* | | |
| H | V=0,L/D=25 | V=4,L/D=25 | V=8,L/D=25 | V=0,L/D=25 | V=4,L/D=25 | V=8,L/D=25 |
| 0 | 1.044 | 1.050 | 1.1881 | 100.4245 | 87.0652 | 423 |
| 10 | 1.0615 | 1.100 | 1.1674 | 98.7343 | 78.4786 | 363.6048 |
| 20 | 1.079 | 1.140 | 1.1467 | 97.0441 | 73.0219 | 309.7687 |
| M | V=0,L/D=25 | V=4,L/D=25 | V=8,L/D=25 | V=0,L/D=25 | V=4,L/D=25 | V=8,L/D=25 |
| 0 | 1.044 | 1.050 | 1.1881 | 100.4245 | 87.0652 | 423 |
| 50 | 1.074 | 1.140 | 1.110 | 96.516 | 71.4 | 281 |
| 100 | 1.104 | 1.220 | 1.080 | 100 | 105 | 180 |
| M | H=0,L/D=25 | H=10,L/D=25 | H=20,L/D=25 | H=0,L/D=25 | H=10,L/D=25 | H=20,L/D=25 |
| 0 | 1.044 | 1.0615 | 1.079 | 100.4245 | 98.7343 | 97.0441 |
| 50 | 1.074 | 1.0915 | 1.109 | 96.516 | 94.8258 | 93.1356 |
| 100 | 1.104 | 1.1215 | 1.1391 | 100 | 100 | 100 |
| H | V=0,L/D=50 | V=4,L/D=50 | V=8,L/D=50 | V=0,L/D=50 | V=4,L/D=50 | V=8,L/D=50 |
| 0 | 2.140 | 2.170 | 2.230 | 638 | 582 | 487 |
| 10 | 2.150 | 2.190 | 2.250 | 633 | 574 | 473 |
| 20 | 2.170 | 2.210 | 2.280 | 627 | 565 | 459 |
| M | V=0,L/D=50 | V=4,L/D=50 | V=8,L/D=50 | V=0,L/D=50 | V=4,L/D=50 | V=8,L/D=50 |
| 0 | 2.140 | 2.170 | 2.230 | 638 | 582 | 487 |
| 50 | 2.150 | 2.190 | 2.250 | 631 | 572 | 471 |
| 100 | 2.160 | 2.200 | 2.270 | 624 | 562 | 455 |
| M | H=0,L/D=50 | H=10,L/D=50 | H=20,L/D=50 | H=0,L/D=50 | H=10,L/D=50 | H=20,L/D=50 |
| 0 | 2.140 | 2.150 | 2.170 | 638 | 633 | 627 |
| 50 | 2.150 | 2.160 | 2.180 | 631 | 626 | 621 |
| 100 | 2.160 | 2.170 | 2.190 | 624 | 619 | 614 |

| Fixed-Free Pile | | | | | | |
|---|---|---|---|---|---|---|
| | Y* | | | M* | | |
| H | V=0,L/D=25 | V=4,L/D=25 | V=6,L/D=25 | V=0,L/D=25 | V=4,L/D=25 | V=6, L/D=25 |
| 0 | 1.0225 | 1.029 | 1.1663 | 103.1691 | 92.4 | 403.2474 |
| 10 | 1.032 | 1.0411 | 1.0465 | 102.4983 | 90.4424 | 119.1688 |
| 20 | 1.0416 | 1.0528 | 1.7035 | 101.8275 | 88.5633 | 341.9241 |
| H | V=0,L/D=50 | V=4,L/D=50 | V=6,L/D=50 | V=0,L/D=50 | V=4,L/D=50 | V=6, L/D=50 |
| 0 | 2.050 | 2.070 | 2.070 | 689 | 661 | 642 |
| 10 | 2.060 | 2.070 | 2.080 | 688 | 659 | 638 |
| 20 | 2.070 | 2.080 | 2.090 | 686 | 656 | 637 |

**Table 3.12** Variation of Y* and M* with L/D under combined loading conditions

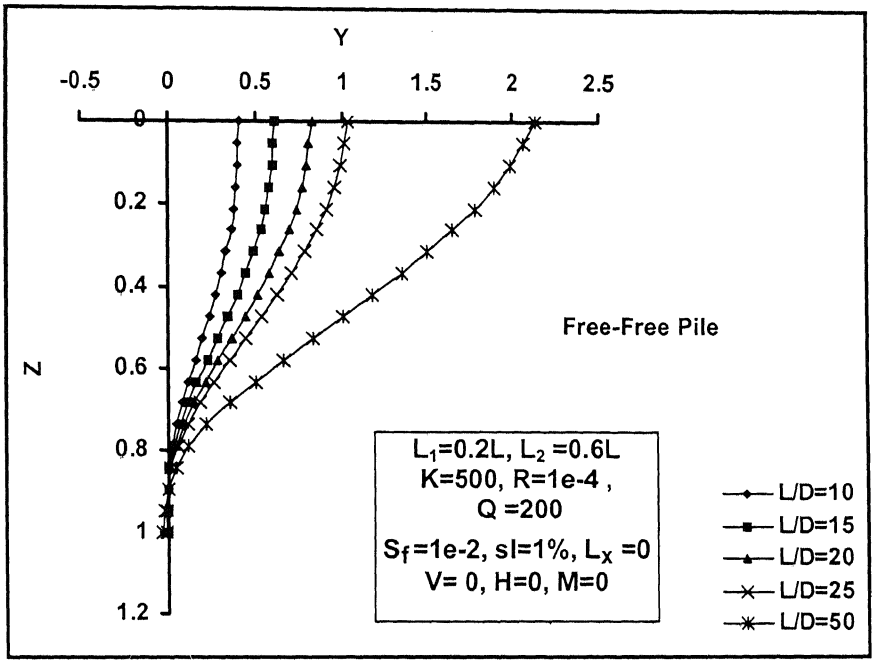


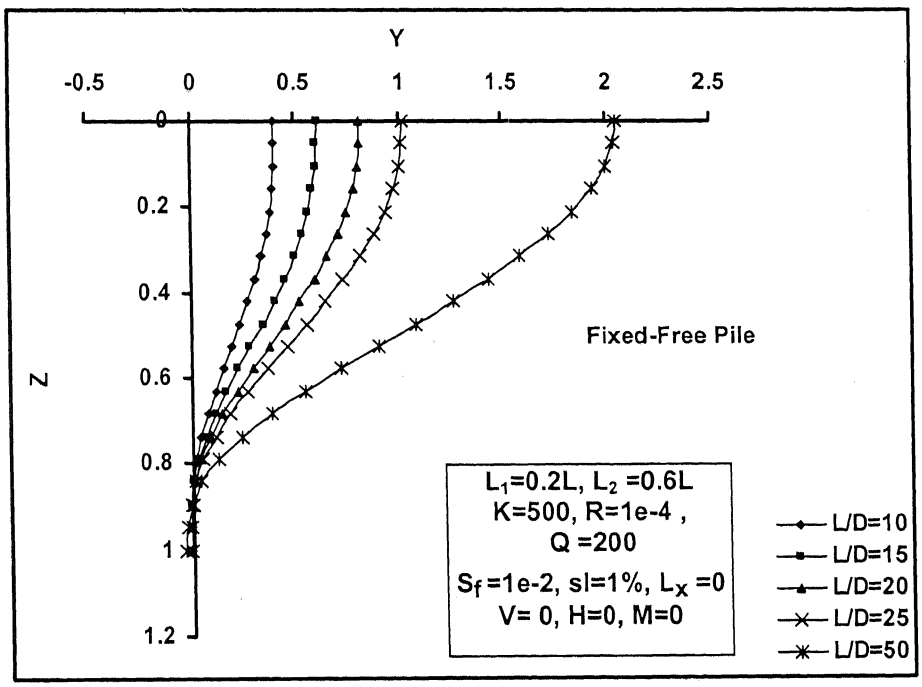


Fig. 3.62 Variation of Y with Z for different L/D

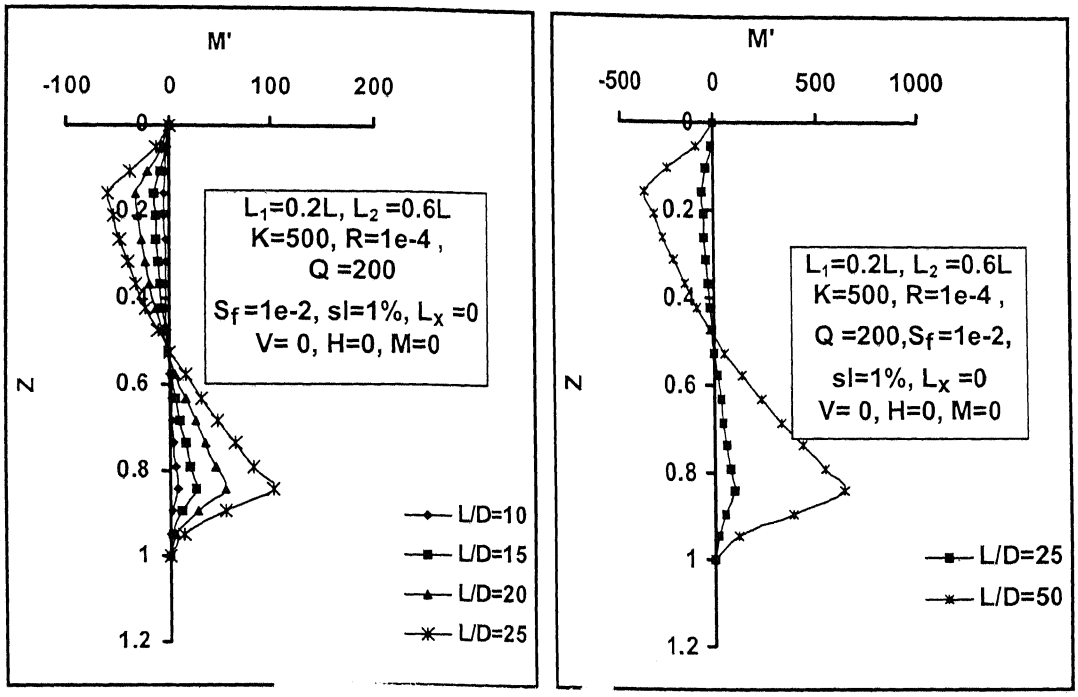


Fig. 3.63 Variation of M' of Free-Free pile with Z for different L/D

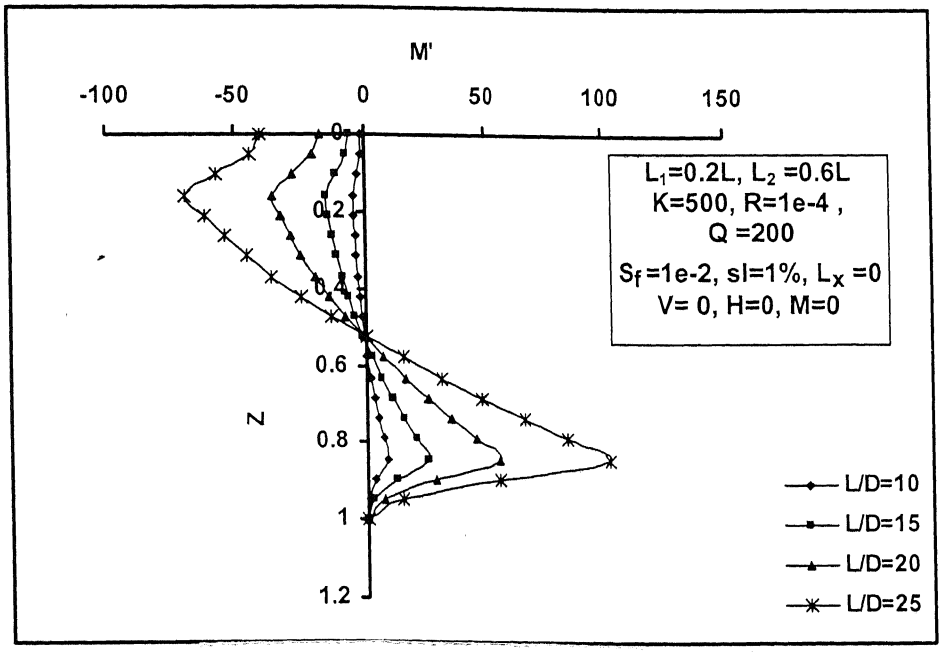


Fig. 3.64 Variation of M' of Fixed-Free pile with Z for different L/D

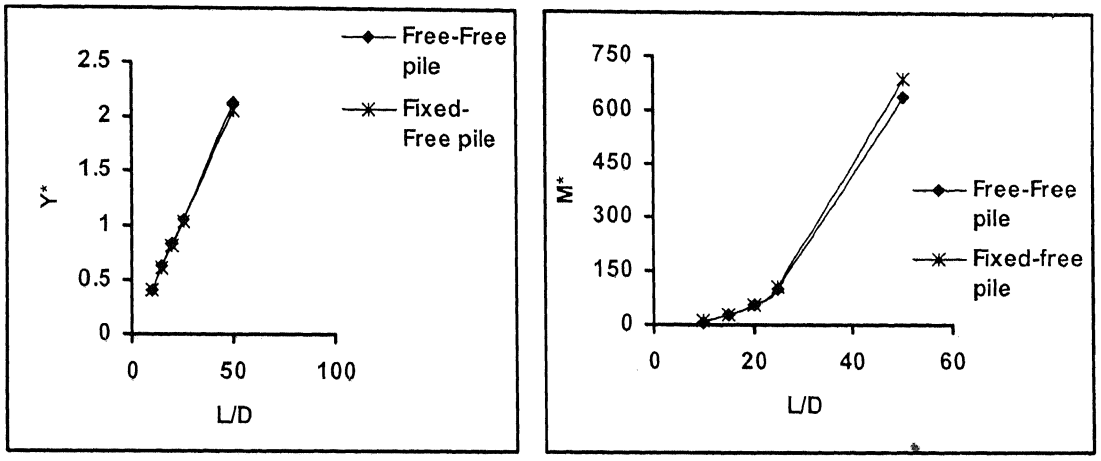


**Fig. 3.65** Effect of L/D on Y* and M*

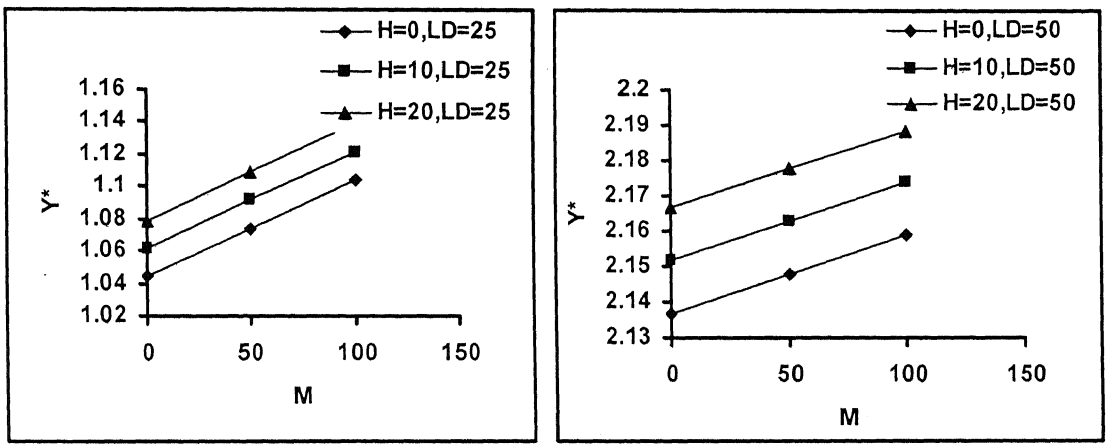


**Fig.3.66** Effect of M on Y* of Free-Free pile for different H and L/D

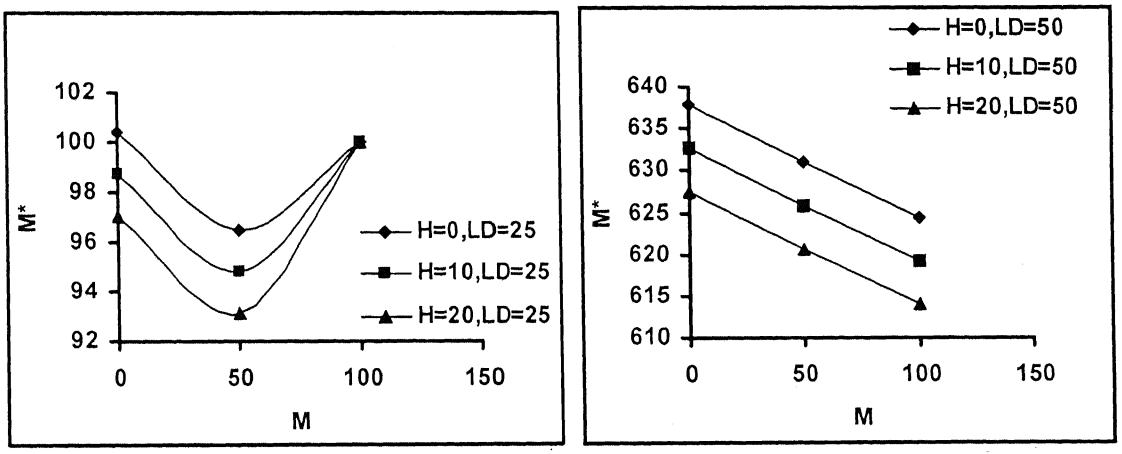


**Fig.3.67** Effect of M on M* of Free-Free pile for different H and L/D

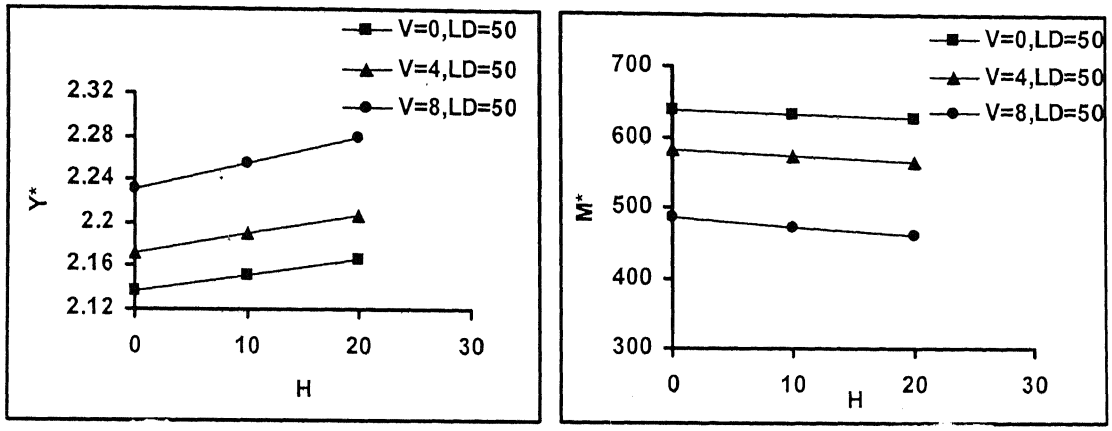


Fig.3.68 Effect of H on Y* and M* of Free-Free pile for different V

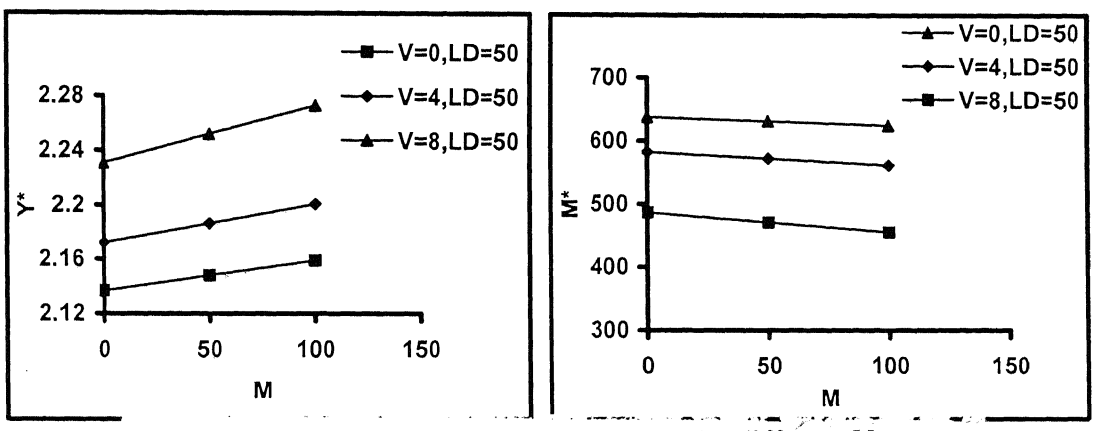


Fig.3.69 Effect of M on Y* and M* of Free-Free pile for different V

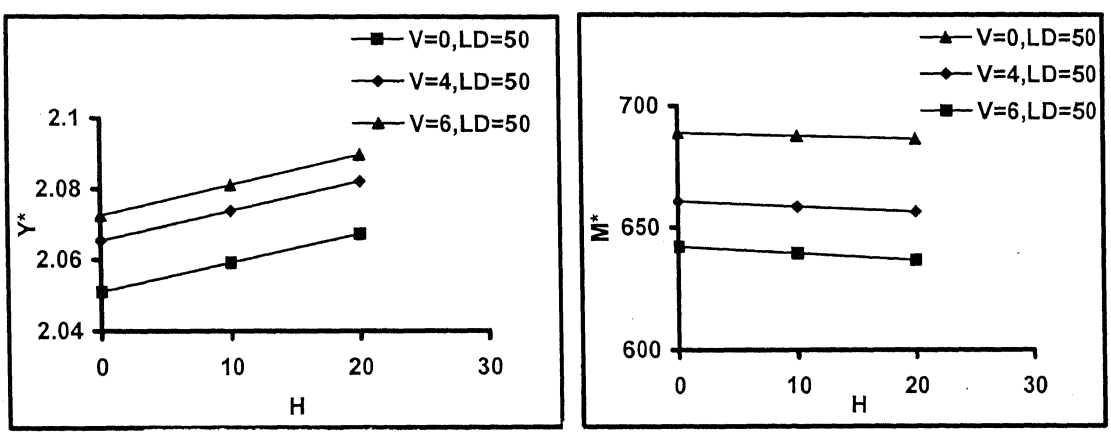


Fig.3.70 Effect of H on Y* and M* of Fixed-Free pile for different V

### 3.5.9 *Effect of gradient of surface topography*

The gradient of the surface topography, sl, has an appreciable influence on the deflection and bending moment of the pile, as the ground displacements are directly proportional to it. The values of Y* and M* at different values of slopes are shown in Table 3.13. The observed behavior is shown in Fig.3.71 and Fig.3.72 indicating that both Y* and M* nonlinearly increased with the slope. This is because the steepness of the slope itself triggers the liquefied soil to spread and subsequently cause the soil layer to move.

| | Free-Free Pile | | Fixed-Free Pile | |
|---|---|---|---|---|
| sl (%) | Y* | M* | Y* | M* |
| 1 | 1.044 | 100.425 | 1.0225 | 103.1691 |
| 10 | 2.2321 | 214.7037 | 2.1861 | 220.5716 |
| 20 | 2.8057 | 269.8855 | 2.748 | 277.2615 |
| 30 | 3.2074 | 308.5245 | 3.1414 | 316.9565 |
| 40 | 3.5268 | 339.2497 | 3.4542 | 348.5214 |
| 50 | 3.7963 | 365.1739 | 3.7182 | 375.1541 |

**Table 3.13** Variation of Y* and M* with slope

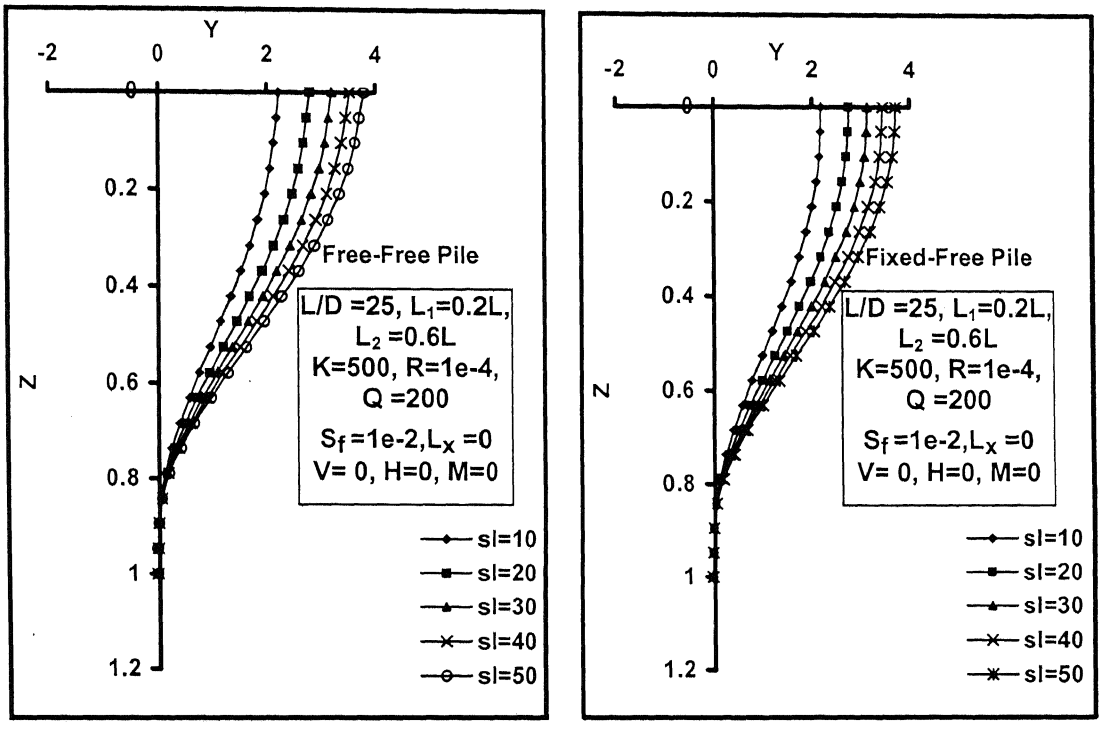


Fig. 3.71 Variation of Y with Z for different sl

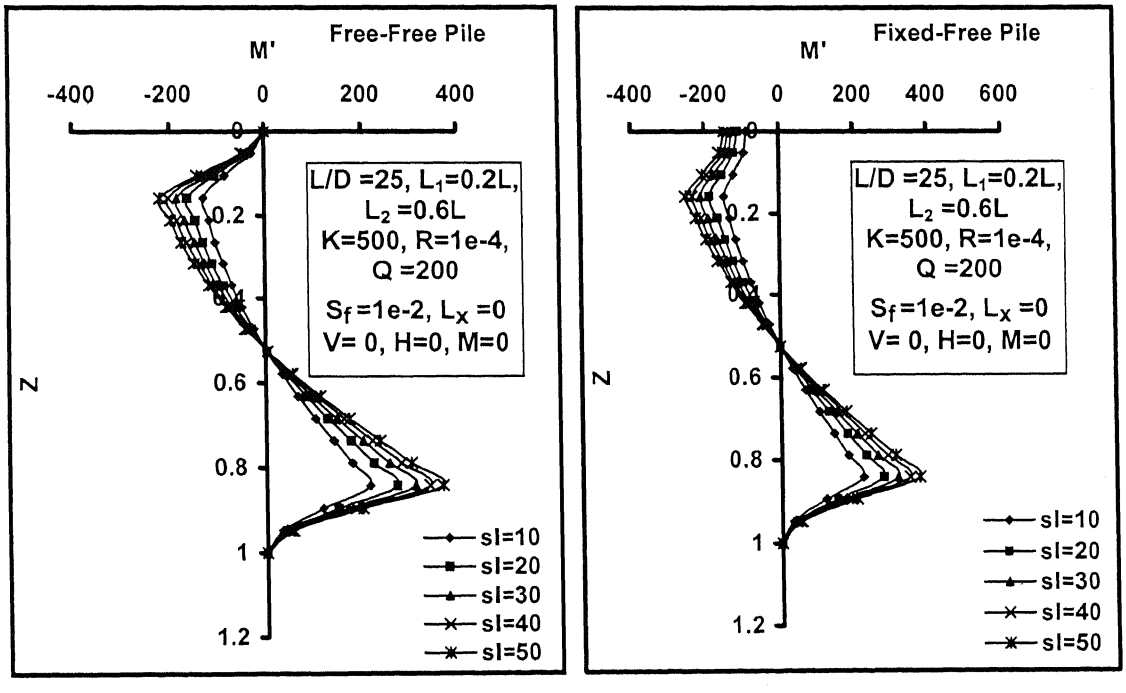


Fig. 3.72 Variation of M' with Z for different sl

### *3.5.10 Effect of depth of liquefaction*

The non-liquefied depth factor, r is varied from 0 to 0.8 and the effect under no external loading condition is shown in Fig.3.73 to Fig.3.75. The embedded depth is taken to be constant throughout the analysis as 20% of the length of the pile. When there is no liquefaction i.e. when r=0.8, the pile shows zero values of Y and M', which validates the correctness of the developed program (Fig.3.73). As the non-liquefied depth factor decreases to zero, i.e. when the liquefaction is starting from the ground surface itself, the Y at the pile top increases to its maximum value, which is around 1.2D compared to zero when there was no soil liquefaction at all. But the Y in liquefied region is more when the non-liquefied depth is larger. This is because the relative displacement of the pile and the soil is more when the non-liquefied depth is larger and this results in the increase of lateral soil pressure. It will lead to the increase of deflection in the liquefied zone and also an increase in the values of M* from 82 to 168, which occurs at Z=0.8 (Fig.3.75). Thus M* increases with r and suddenly drops to zero when r=0.8. For both the end conditions Y* decreases and M* increases with increase in r. Only in the range r=0 to r=0.2, the end condition will influence the flexural behavior of pile. In this range Free-Free pile will have more Y* than that of Fixed-Free pile and reverse is the case for M*. Table 3.14 shows the values of Y* and M* at different depth of liquefaction.

| | Free-Free Pile | | Fixed-Free Pile | |
|---|---|---|---|---|
| r | Y* | M* | Y* | M* |
| 0 | 1.1712 | 82.2762 | 1.1503 | 101.2597 |
| 0.2 | 1.044 | 100.425 | 1.0225 | 103.1691 |
| 0.4 | 0.8319 | 128.573 | 0.831 | 128.6744 |
| 0.6 | 0.5944 | 168.698 | 0.5944 | 168.7142 |
| 0.8 | 0 | 0 | 0 | 0 |

**Table 3.14** Variation of Y* and M* with r under no external loading condition

Under lateral loading, when r is increased from 0 to 0.4, the Y* decreases by 30% for all the combinations of H and M. The figures show similar trend of behavior when the values of r are 0 and 0.4 respectively. The M* initially decreases and then increases with the applied moment factor at r=0. But, in contrast when r=0.4, M* all the time increases with increase in the lateral loads. The lateral soil pressure contributes to the increase in M*. The results are shown in Fig.3.76 and Fig.3.77.

The effect during combined loading condition is given in Fig.3.78 to Fig.3.83.When V and H acts on the Free-Free pile, Y* decreases from 1.3 to 0.84 as r increases from 0 to 0.4 ( Fig.3.78).The critical range of V reduces as r reduces. This is because the supporting capacity of the soil becomes increasingly smaller over greater length with the reduction in r. M* does not show appreciable variation with r, at lower values of V,. But for V greater than 4, M* considerably reduces. The combined loading of V and M also shows the same behavior as that of V and H. Higher M induces more deflection and bending moment. The influence of combined loading in Fixed-Free pile has also been studied (Fig.3.82 and Fig.3.83). At r=0, Y* and M* increases with increase in H and M. At r=0.4, Y* increases with V and H and finally reaches a constant value of 0.84. M* decreases with H as V varies from 0 to 4 beyond which it starts increasing. When V is greater than 4, the negative moments are higher due to the higher relative displacement in the top interface. M* decreases slightly with increase in lateral load. This study signifies the importance of proper densification of soil in liquefiable areas and to have a suitable depth of top non-liquefied soil cover. Also, it has been seen that compared to Free-Free piles Fixed-Free piles are more suitable in sites with sufficient top non-liquefied cover due to reduced deflection and moments. Table 3.15 summarizes quantitatively the effect of r on Y* and M* for both Free-Free and Fixed-Free piles under combined loading conditions as explained earlier qualitatively in the above figures..

| Free-Free Pile | | | | | | | |
|---|---|---|---|---|---|---|---|
| Y* | | | | M* | | | |
| H | V=0,r=0 | V=4,r=0 | V=8,r=0 | H | V=0,r=0 | V=4,r=0 | V=8,r=0 |
| 0 | 1.17 | 1.3277 | 1.3685 | 0 | 82.3 | 128.395 | 438 |
| 10 | 1.2074 | 1.3914 | 1.4197 | 10 | 82.488 | 137.2495 | 453.1941 |
| 20 | 1.2436 | 1.455 | 1.4709 | 20 | 82.6997 | 146.1039 | 468.547 |
| M | V=0,r=0 | V=4,r=0 | V=8,r=0 | M | V=0,r=0 | V=4,r=0 | V=8,r=0 |
| 0 | 1.1712 | 1.3277 | 1.3685 | 0 | 82.2762 | 128.395 | 438 |
| 50 | 1.19 | 1.5583 | 1.3286 | 50 | 71.7438 | 179.6989 | 365.1301 |
| 100 | 1.2088 | 1.8582 | 1.3512 | 100 | 100 | 237.765 | 306.8337 |
| M | H=0,r=0 | H=10,r=0 | H=20,r=0 | M | H=0,r=0 | H=10,r=0 | H=20,r=0 |
| 0 | 1.1712 | 1.2074 | 1.2436 | 0 | 82.2762 | 82.488 | 82.6997 |
| 50 | 1.19 | 1.2262 | 1.2624 | 50 | 71.7438 | 71.9556 | 72.1673 |
| 100 | 1.2088 | 1.245 | 1.2812 | 100 | 100 | 100 | 100 |
| H | V=0,r=0.4 | V=4,r=0.4 | V=8,r=0.4 | H | V=0,r=0.4 | V=4,r=0.4 | V=8,r=0.4 |
| 0 | 0.8319 | 0.841 | 0.861 | 0 | 128.5725 | 120 | 138 |
| 10 | 0.838 | 0.839 | 0.854 | 10 | 128 | 120 | 138 |
| 20 | 0.854 | 0.856 | 0.86 | 20 | 128 | 120 | 138 |
| M | V=0 | V=4,r=0.4 | V=8,r=0.4 | M | V=0 | V=4,r=0.4 | V=8,r=0.4 |
| 0 | 0.832 | .841 | .861 | 0 | 129 | 120 | 138 |
| 50 | 0.848 | .851 | .861 | 50 | 129 | 122 | 139 |
| 100 | 0.874 | .890 | 0.942 | 100 | 129 | 123 | 160 |
| M | H=0,r=0.4 | H=10,r=0.4 | H=20,r=0.4 | M | H=0,r=0.4 | H=10,r=0.4 | H=20,r=0.4 |
| 0 | 0.832 | 0.838 | 0.854 | 0 | 129 | 128.4432 | 129 |
| 50 | 0.848 | 0.864 | 0.880 | 50 | 129 | 129 | 129 |
| 100 | 0.874 | 0.89 | 0.906 | 100 | 129 | 129 | 129 |
| Fixed-Free Pile | | | | | | | |
| H | V=0,r=0 | V=4,r=0 | V=6,r=0 | H | V=0,r=0 | V=4,r=0 | V=6,r=0 |
| 0 | 1.15 | 1.2732 | 1.4043 | 0 | 101 | 102.2793 | 179.1743 |
| 10 | 1.1851 | 1.3138 | 1.466 | 10 | 102.7752 | 104.7137 | 190 |
| 20 | 1.2198 | 1.3543 | 1.5335 | 20 | 104.2906 | 107.148 | 204 |
| H | V=0,r=0.4 | V=4,r=0.4 | V=6,r=0.4 | H | V=0,r=0.4 | V=4,r=0.4 | V=6,r=0.4 |
| 0 | 0.831 | 0.838 | 0.844 | 0 | 128.6744 | 120 | 123 |
| 10 | 0.835 | 0.839 | 0.844 | 10 | 128 | 120 | 122 |
| 20 | 0.844 | 0.844 | 0.844 | 20 | 128 | 119 | 122 |

**Table 3.15** Variation of Y* and M* with r under combined loading condition

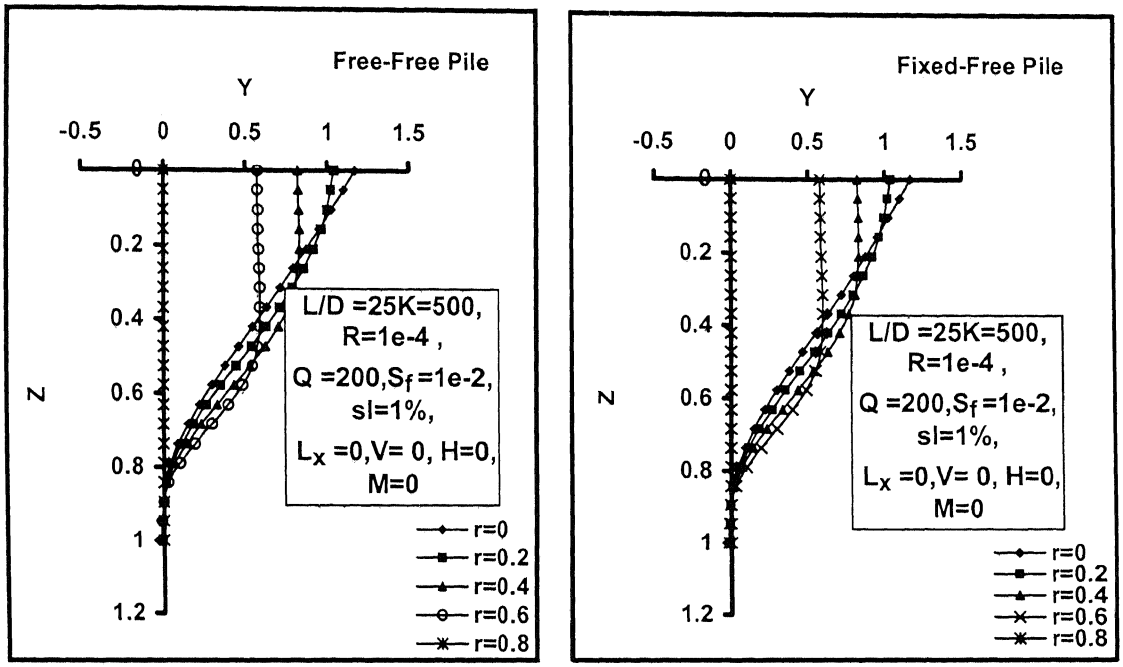


Fig. 3.73 Variation of Y with Z for different r

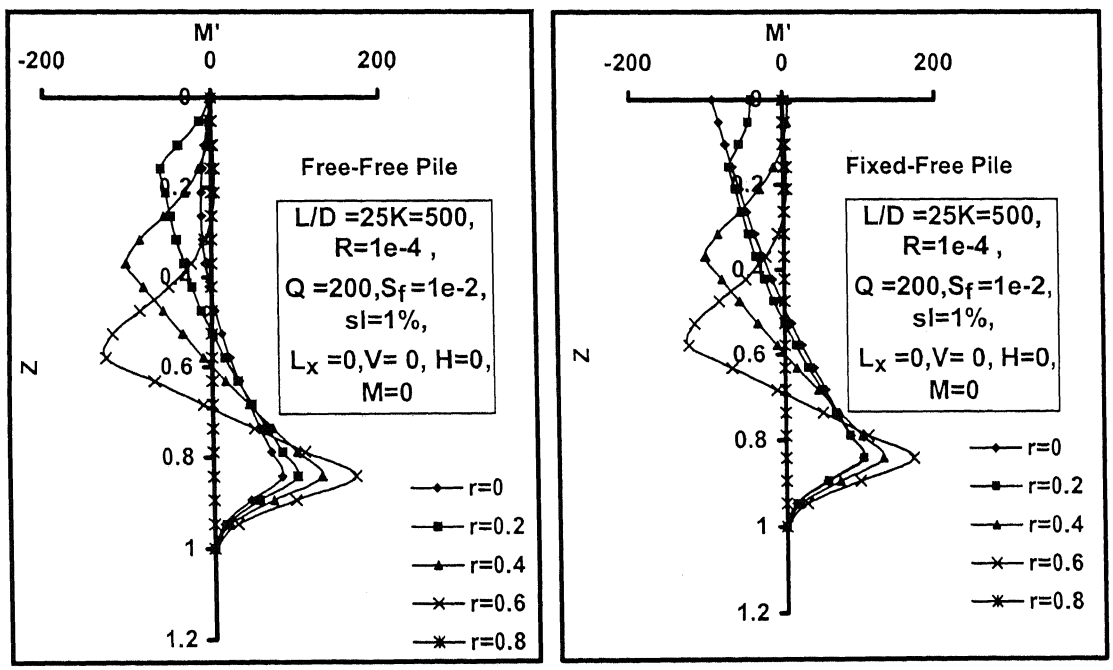


Fig. 3.74 Variation of M' with Z for different r

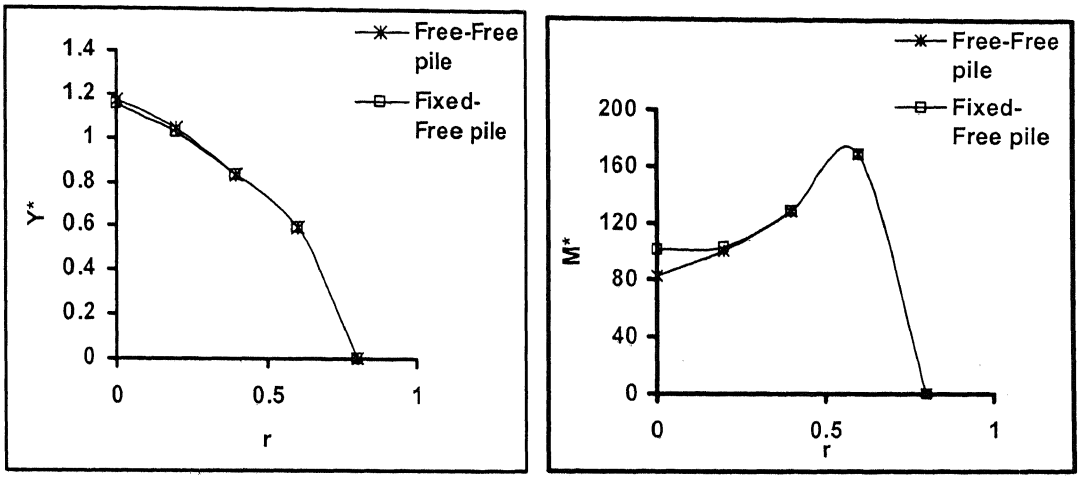


**Fig. 3.75** Effect of r on Y* and M*

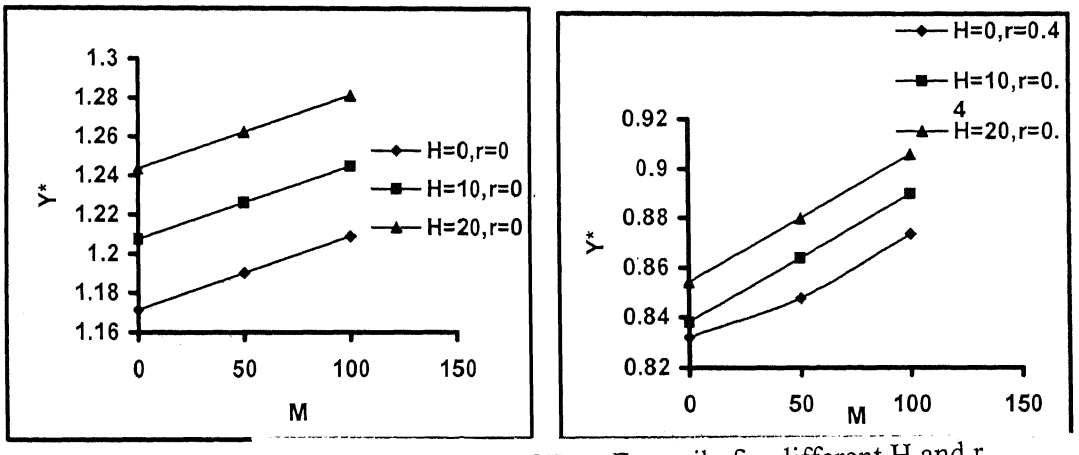


**Fig.3.76** Effect of M on Y* of Free-Free pile for different H and r

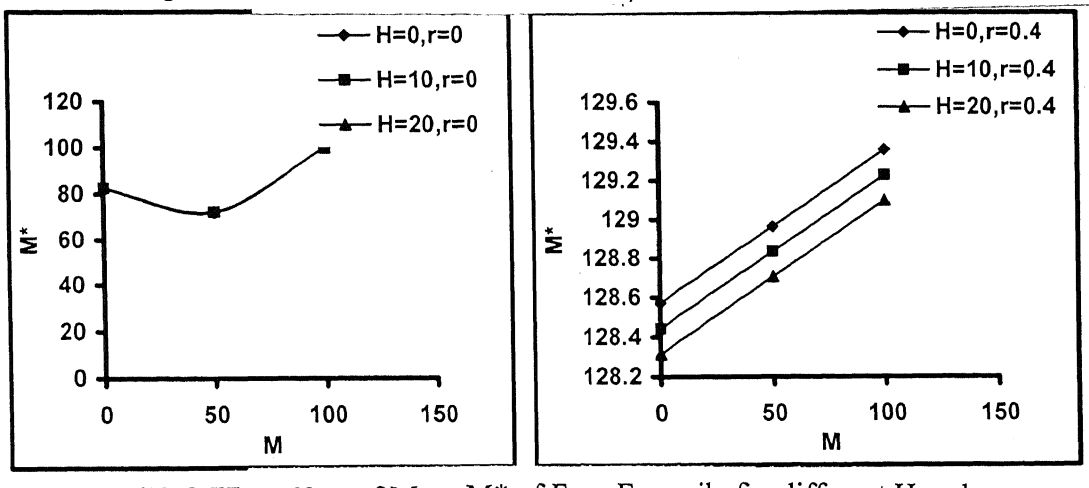


**Fig3.77** Effect of M on M* of Free-Free pile for different H and r

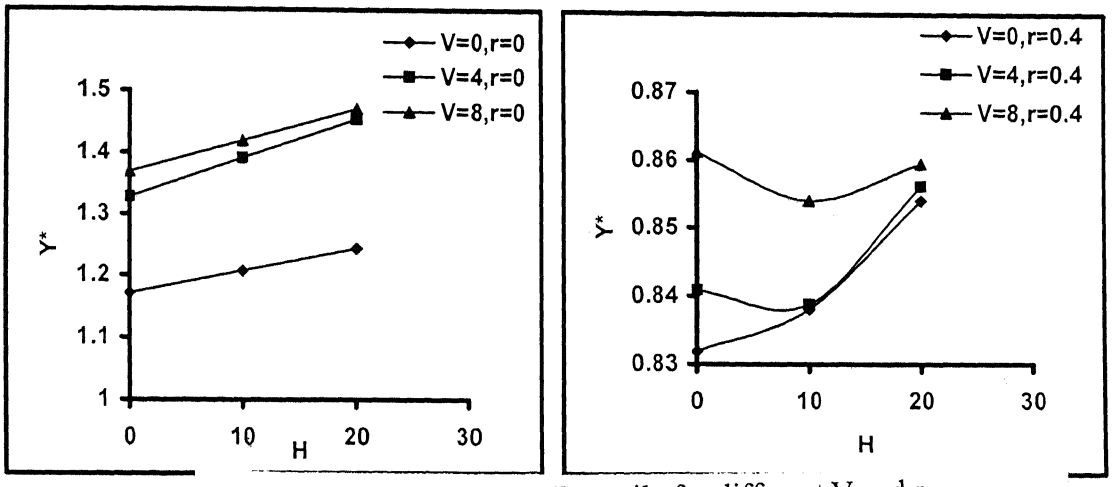


Fig.3.78 Effect of H on Y* of Free-Free pile for different V and r

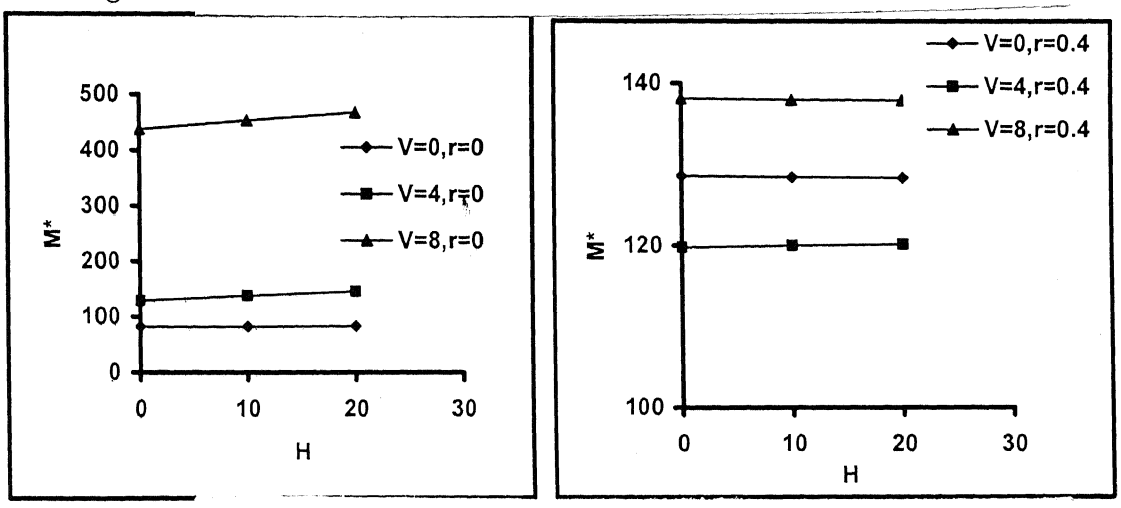


Fig.3.79 Effect of H on M* of Free-Free pile for different V and r

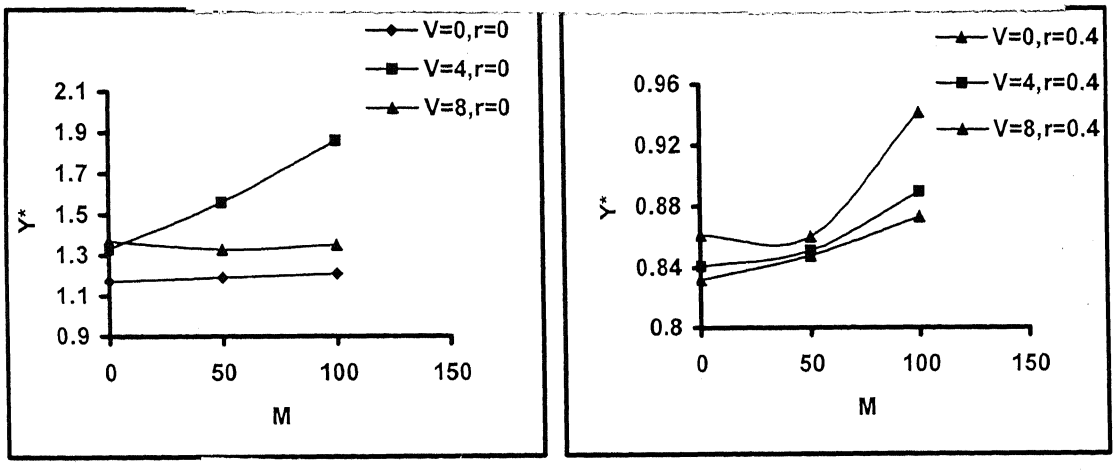


Fig.3.80 I Effect of M on Y* of Free-Free pile for different V and r

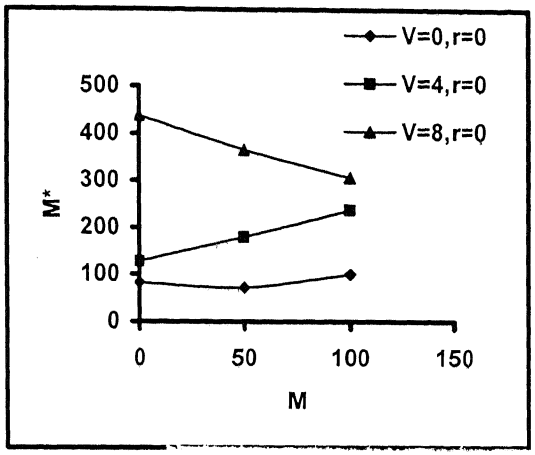


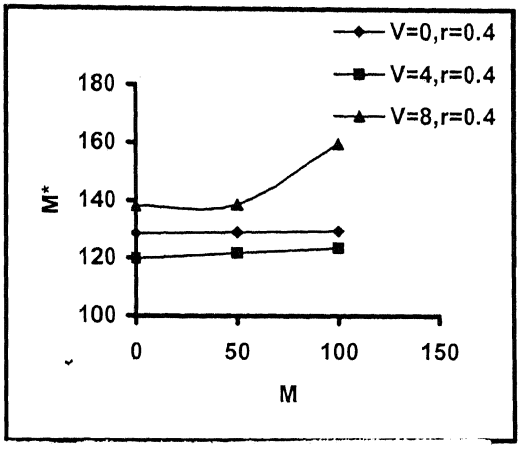


**Fig.3.81** Effect of M on M* of Free-Free pile for different V and r

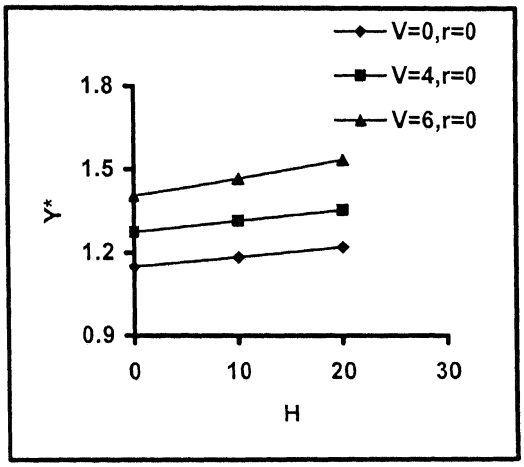


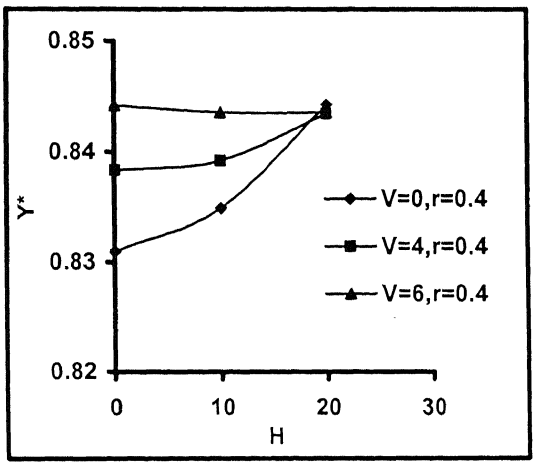


**Fig.3.82** Effect of H on Y* of Fixed-Free pile for different V and r

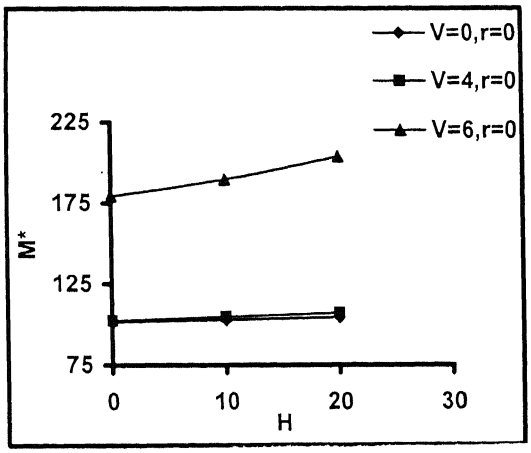


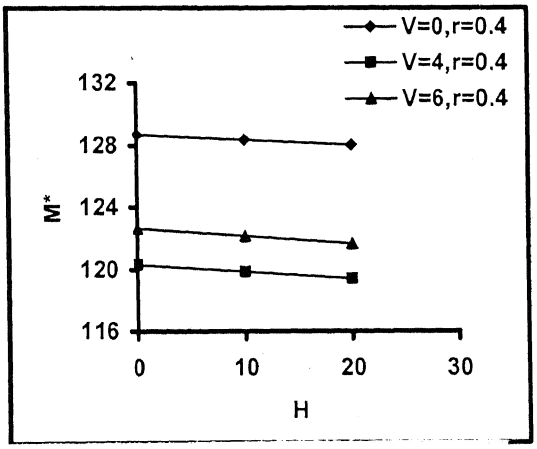


**Fig.3.83** Effect of H on M* of Fixed-Free pile for different V and r

### *3.5.11 Effect of location factor*

The effect of location factor ($L_x$) designated by the ratio of the distance from the waterfront to the total lateral spreading length has been studied. It has been observed from case studies that worst conditions of ground deformation exist near the waterfront. The results of no external loading condition are shown in Fig.3.84 to Fig.3.86. As the distance from waterfront (x) increases Y as well as M' decreases. The values of Y* and M* at different $L_x$ are shown in Table 3.16. The Y* as well as M* shows a nonlinear decrease with increase in $L_x$ with Y* decreasing from 1.04 to 0.03 and M* decreasing from 100 to 3 as $L_x$ increases from 0 to 1 (Fig 3.86).

Under the application of externally applied lateral loads Y* decreases when $L_x$ is increased from 0 to 0.5 (Fig 3.87).The trends of the curves are similar for $L_x$ =0 and $L_x$ =0.5. The M* initially decreases and then increases with applied moment factor when $L_x$ =0. But when $L_x$ =0.5, M* increases with increase in the applied moment and when applied moment exceeds 100, M* becomes equal to M. H does not have a significant effect. The results are shown in Fig.3.87 and Fig.3.88.

The effect during combined loading condition is given in Fig.3.89 to Fig.3.94. In Free-Free pile under the combined loading of V and H, there is appreciable reduction in Y* and M* as $L_x$ increases (Fig 3.89 and 3.90). The lateral spreading force will be lesser at location far away from the water front. Hence the same section of pile can take more external loads than that of at water front. At $L_x$ = 0.5 Y* and M* shows a nonlinear variation with H when V is greater than 4.When V and M acts together, Y* shows an appreciable reduction as $L_x$ increases. M* decreases with $L_x$ only if the axial load and the applied moment are less than the critical range. During the combined loading in farther sites the Fixed-Free pile is more prone to failure at higher values of V. This is because Fixed-Free pile experiences higher deflection and bending moment in the liquefied zone due to high relative displacement between soil and pile.

| | Free-Free Pile | | Fixed-Free Pile | |
|---|---|---|---|---|
| $L_x$ | Y* | M* | Y* | M* |
| 0 | 1.044 | 100.4245 | 1.0225 | 103.1691 |
| 0.2 | 0.522 | 50.2122 | 0.5113 | 51.5845 |
| 0.4 | 0.261 | 25.1061 | 0.2556 | 25.7923 |
| 0.6 | 0.1305 | 12.5531 | 0.1278 | 12.8961 |
| 0.8 | 0.0653 | 6.2765 | 0.0639 | 6.4481 |
| 1 | 0.0326 | 3.1383 | 0.032 | 3.224 |

**Table 3.16** Variation of Y* and M* with $L_x$ under no external loading condition

| Fixed-Free Pile | | | | | | |
|---|---|---|---|---|---|---|
| | Y* | | | M* | | |
| H | V=0,$L_x$=0 | V=4,$L_x$=0 | V=8,$L_x$=0 | V=0,$L_x$=0 | V=4,$L_x$=0 | V=8,$L_x$=0 |
| 0 | 1.0225 | 1.029 | 1.1663 | 103.1691 | 92.4 | 403.2474 |
| 10 | 1.032 | 1.0411 | 1.0465 | 102.4983 | 90.4424 | 119.1688 |
| 20 | 1.0416 | 1.0528 | 1.7035 | 101.8275 | 88.5633 | 341.9241 |
| H | V=0,$L_x$=0.5 | V=4,$L_x$=0.5 | V=8,$L_x$=0.5 | V=0,$L_x$=0.5 | V=4,$L_x$=0.5 | V=8,$L_x$=0.5 |
| 0 | 0.181 | 0.182 | 0.203 | 18.2 | 16.2 | 61.5 |
| 10 | 0.19 | 0.194 | 0.103 | 17.6 | 14.4 | 270 |
| 20 | 0.2 | 0.206 | 0.214 | 16.8963 | 13.6 | 581 |

**Table 3.17** Variation of Y* and M* with $L_x$ under combined loading condition

| Free-Free Pile | | | | | | |
|---|---|---|---|---|---|---|
| | Y* | | | M* | | |
| H | $V=0,L_x=0$ | $V=4,L_x=0$ | $V=8,L_x=0$ | $V=0,L_x=0$ | $V=4,L_x=0$ | $V=8,L_x=0$ |
| 0 | 1.044 | 1.050 | 1.1881 | 100.4245 | 87.0652 | 423 |
| 10 | 1.0615 | 1.100 | 1.1674 | 98.7343 | 78.4786 | 363.6048 |
| 20 | 1.079 | 1.140 | 1.1467 | 97.0441 | 73.0219 | 309.7687 |
| M | $V=0,L_x=0$ | $V=4,L_x=0$ | $V=8,L_x=0$ | $V=0,L_x=0$ | $V=4,L_x=0$ | $V=8,L_x=0$ |
| 0 | 1.044 | 1.050 | 1.1881 | 100.4245 | 87.0652 | 423 |
| 50 | 1.074 | 1.140 | 1.110 | 96.516 | 71.4 | 281 |
| 100 | 1.104 | 1.220 | 1.080 | 100 | 105 | 181 |
| M | $H=0,L_x=0$ | $H=10,L_x=0$ | $H=20,L_x=0$ | $H=0,L_x=0$ | $H=10,L_x=0$ | $H=20,L_x=0$ |
| 0 | 1.044 | 1.0615 | 1.079 | 100.4245 | 98.7343 | 97.0441 |
| 50 | 1.074 | 1.0915 | 1.109 | 96.516 | 94.8258 | 93.1356 |
| 100 | 1.104 | 1.1215 | 1.1391 | 100 | 100 | 100 |
| H | $V=0,L_x=0.5$ | $V=4,L_x=0.5$ | $V=8,L_x=0.5$ | $V=0,L_x=0.5$ | $V=4,L_x=0.5$ | $V=8,L_x=0.5$ |
| 0 | 0.185 | 0.186 | 0.210 | 17.8 | 15.4 | 74.7 |
| 10 | 0.202 | 0.228 | 0.197 | 16.1 | 15.4 | 31.8 |
| 20 | 0.220 | 0.270 | 0.246 | 14.3723 | 32.1 | 69 |
| M | $V=0,L_x=0.5$ | $V=4,L_x=0.5$ | $V=8,L_x=0.5$ | $V=0,L_x=0.5$ | $V=4,L_x=0.5$ | $V=8,L_x=0.5$ |
| 0 | 0.185 | 0.1862 | 0.21 | 17.8 | 15.3911 | 74.7 |
| 50 | 0.2146 | 0.2706 | 0.2812 | 50 | 54.3144 | 110.1491 |
| 100 | 0.2446 | 0.3551 | 0.5746 | 100 | 109.5753 | 258.7872 |
| M | $H=0,L_x=0.5$ | $H=10,L_x=0.5$ | $H=20,L_x=0.5$ | $H=0,L_x=0.5$ | $H=10,L_x=0.5$ | $H=20,L_x=0.5$ |
| 0 | 0.185 | 0.2021 | 0.2196 | 0.178 | 16.0625 | 14.3723 |
| 50 | 0.2146 | 0.2321 | 0.2496 | 50 | 50 | 51.749 |
| 100 | 0.2446 | 0.2621 | 0.2796 | 100 | 100 | 100 |

**Table 3.17** Variation of Y* and M* with $L_x$ under combined loading condition (contd)

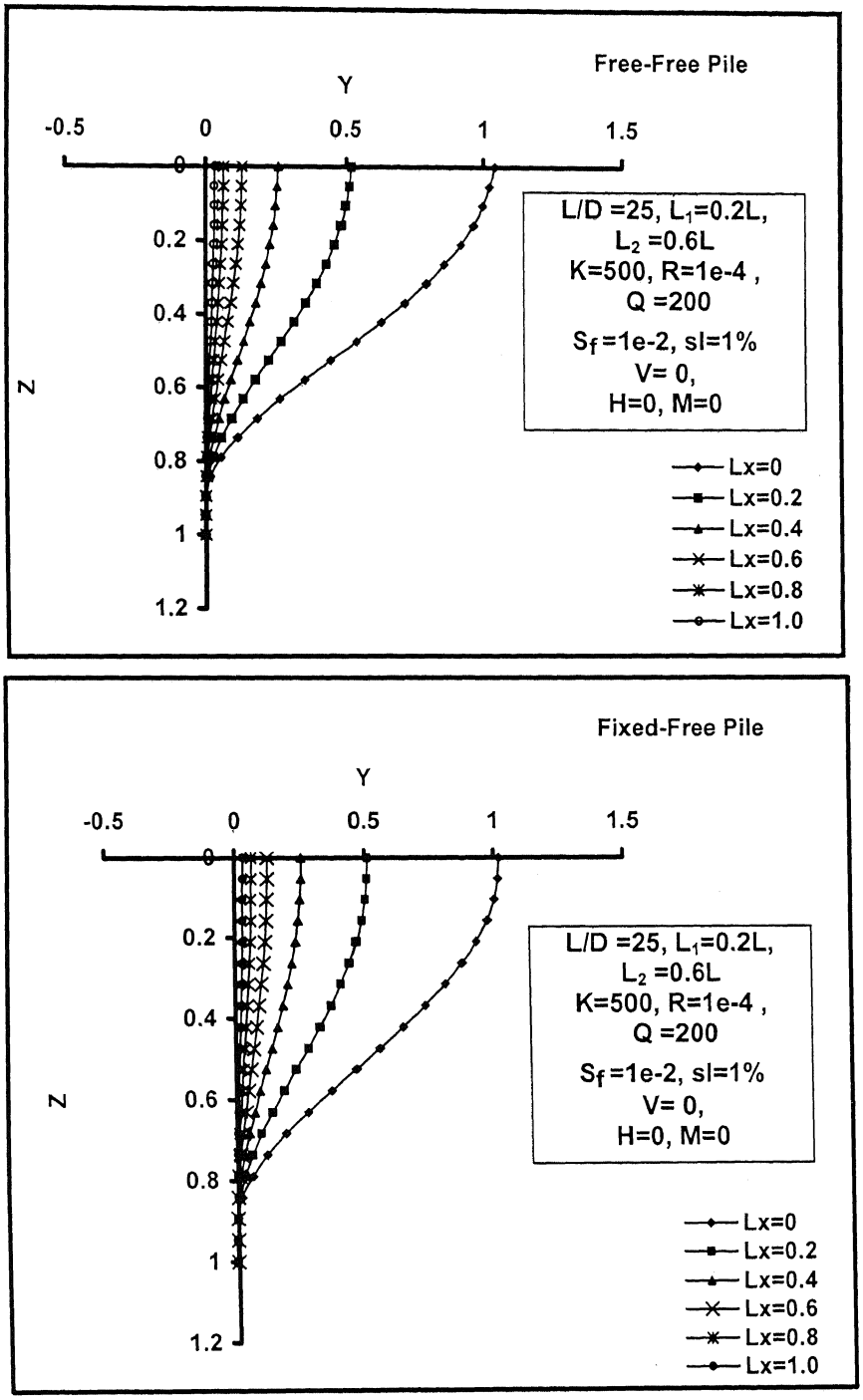


Fig. 3.84 Variation of Y with Z for different $L_x$

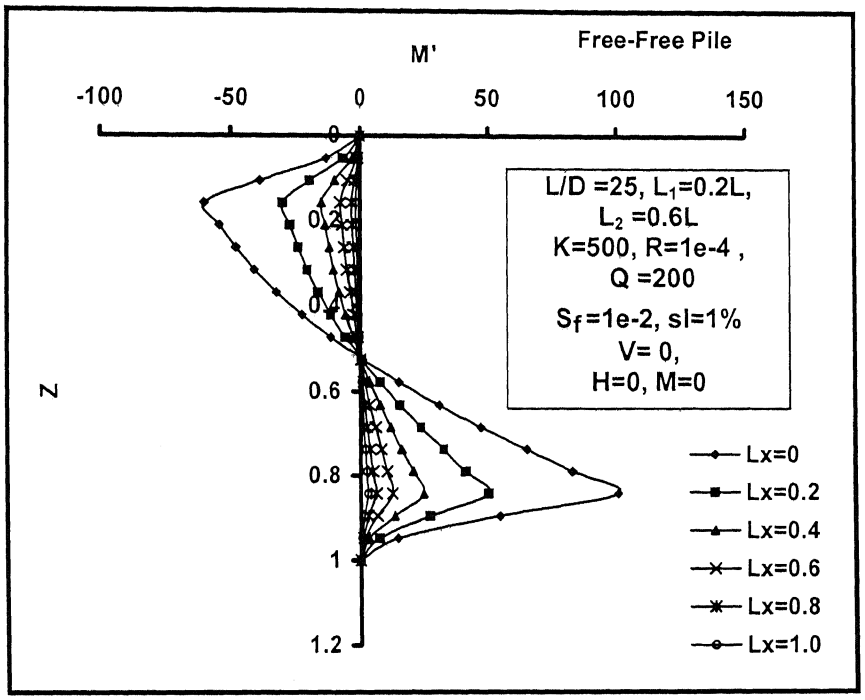


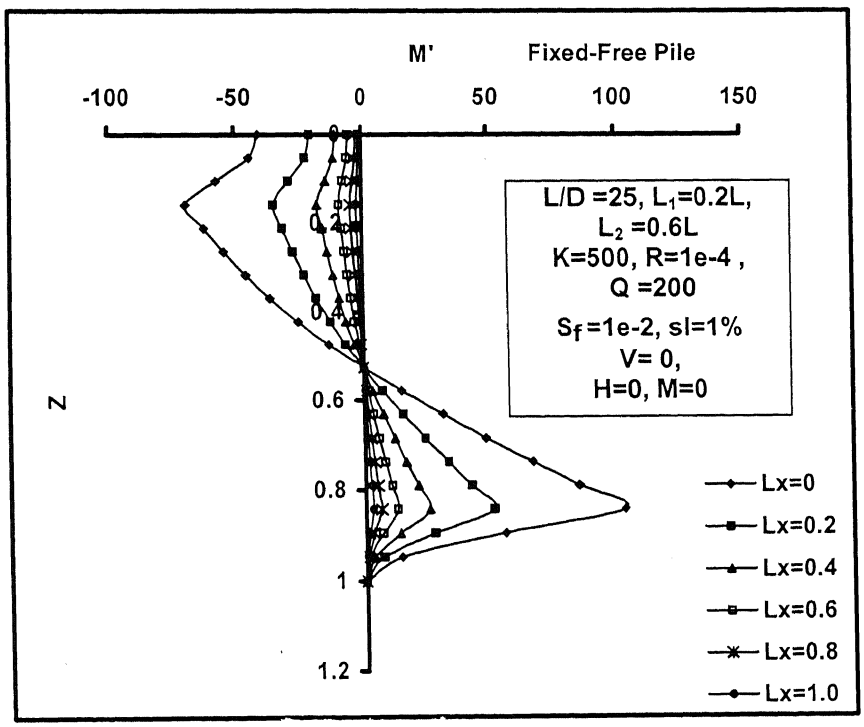


Fig. 3.85 ] Variation of M' with Z for different $L_x$

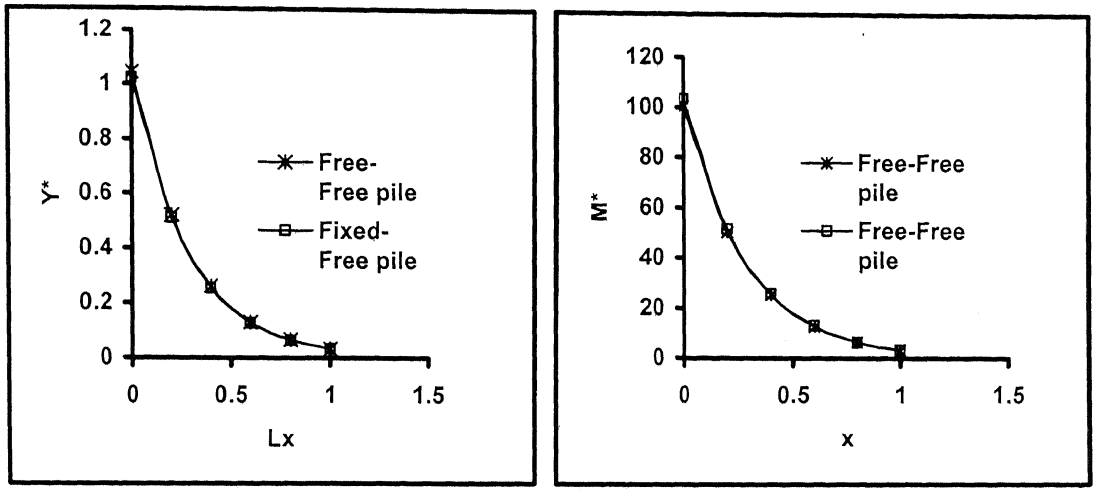


Fig. 3.86 Effect of $L_x$ on Y* and M*

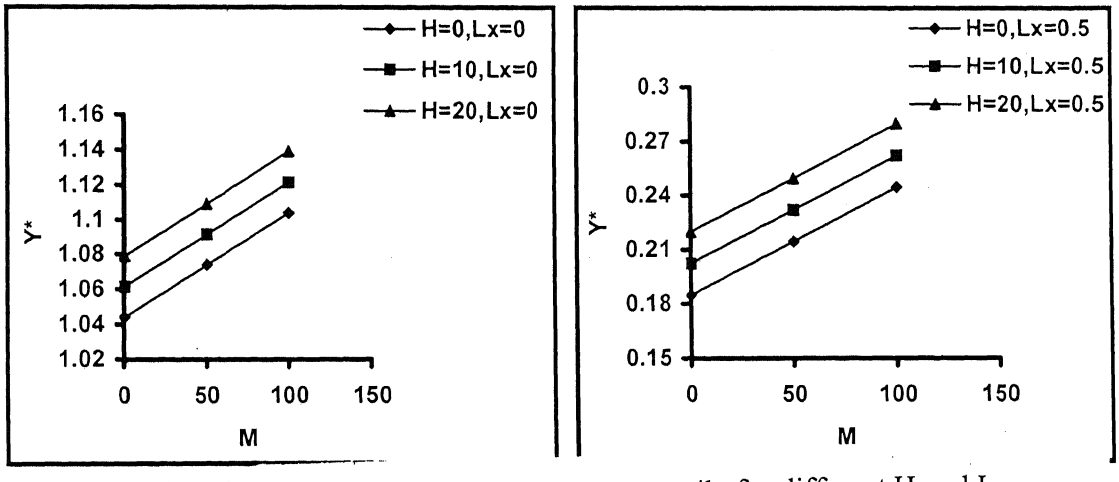


Fig.3.87 Effect of M on Y* of Free-Free pile for different H and $L_x$

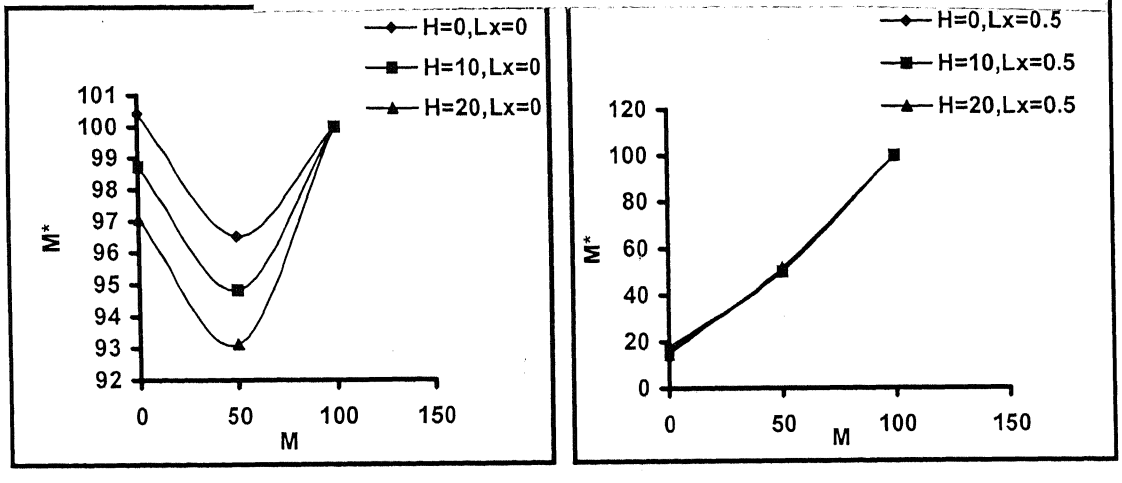


Fig.3.88 Effect of M on M* of Free-Free pile for different H and $L_x$

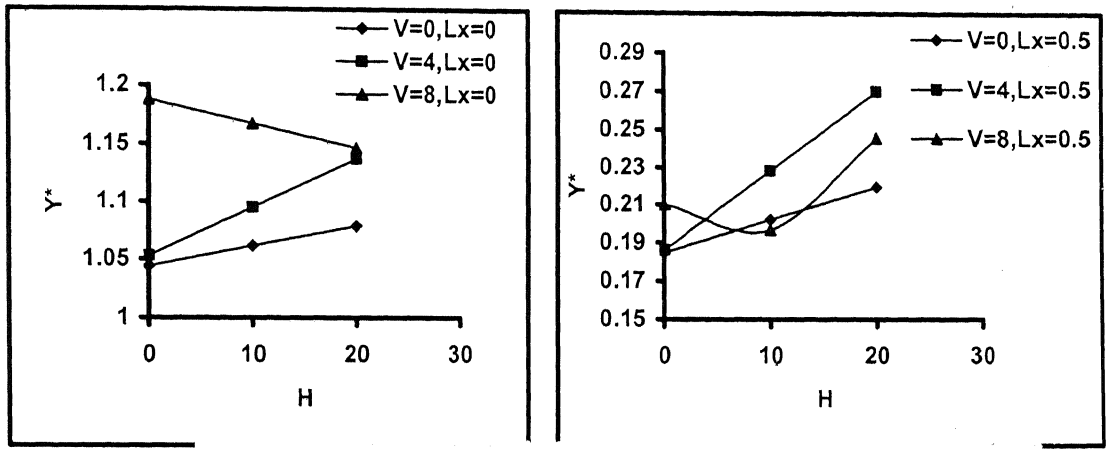


Fig.3.89 I Effect of H on Y* of Free-Free pile for different V and $L_x$ )

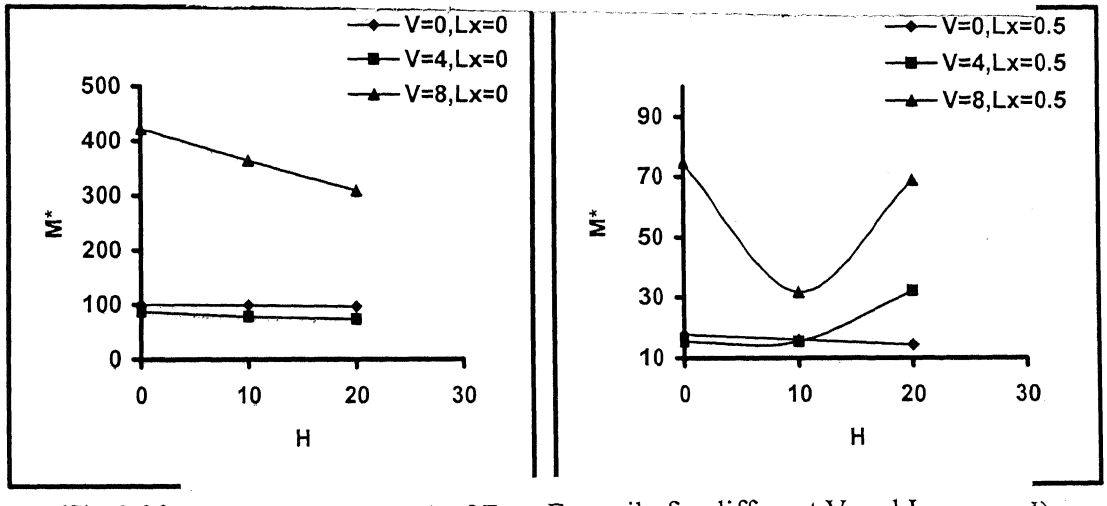


Fig.3.90 Effect of H on M* of Free-Free pile for different V and $L_x$ I)

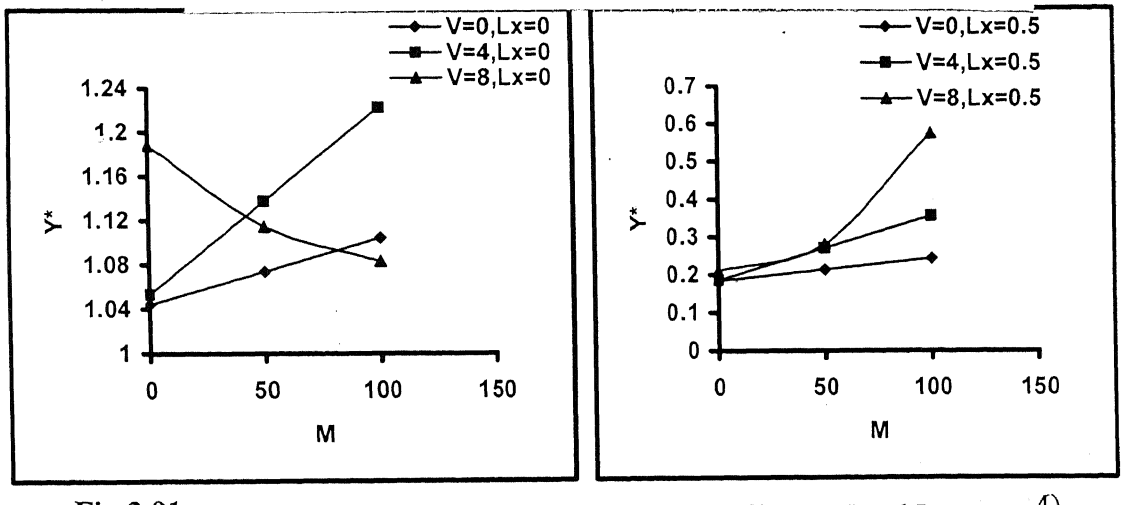


Fig.3.91 Effect of M on Y* of Free-Free pile for different V and $L_x$ 1)

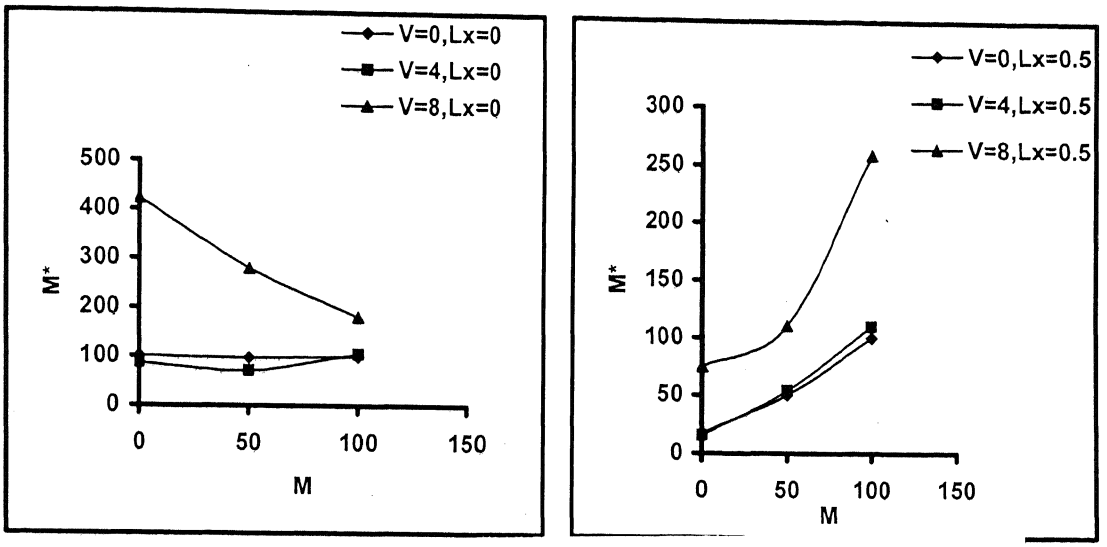


Fig.3.92 Effect of M on M* of Free-Free pile for different V and $L_x$

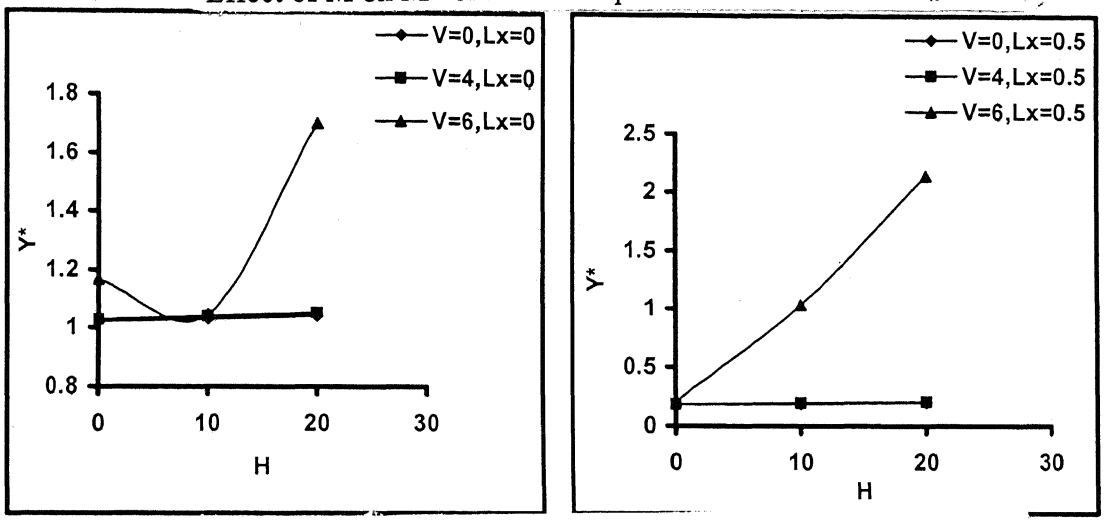


Fig.3.93 Effect of H on Y* of Fixed-Free pile for different V and $L_x$

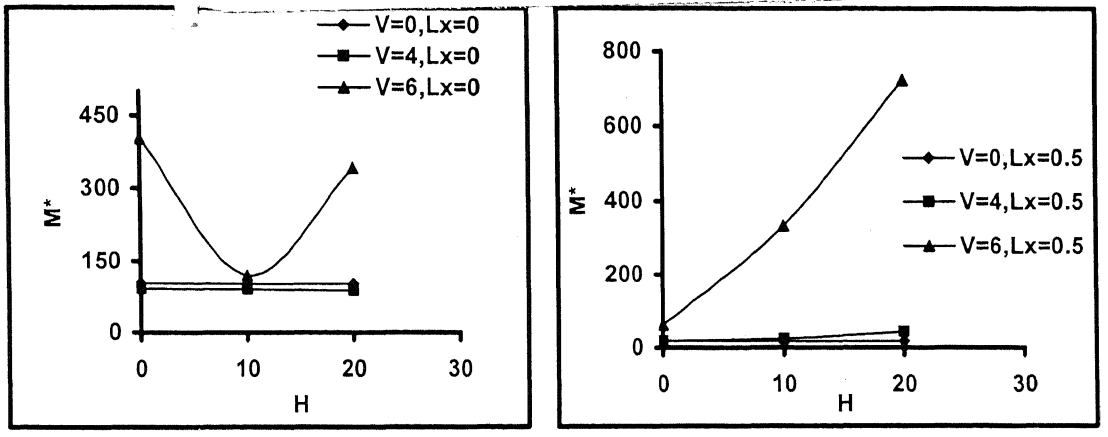


Fig.3.94 Effect of H on M* of Fixed-Free pile for different V and $L_x$

### *3.5.12 Effect of boundary conditions*

The effect of various boundary conditions on the flexural behavior of pile in liquefiable areas has been studied and the results are shown in Fig.3.95 and Fig.3.96. The analysis were carried out for a value of V=2 and H=10.It has been observed that Free-Free pile and Fixed-Free pile with sway shows the maximum head deflection of 1.07D and 1.04D respectively , the values not differing by no more than 2.88%. The bending moment diagram also shows the same pattern of variation. M* is at the bottom interface (Z=0.8) This M* are 86 and 92 for Free-Free pile and Fixed-Free pile with sway respectively the difference being only 6.9%.

The piles with other end conditions show a different behavior. The Y* which occurs just below the top interface (Z=0.3), increases from 2.4 to 2.6 (% difference of only 8%) as the degrees of freedom reduces. M* is around 5000 which occurs at the pile head. Free-Free pile and Fixed-Free pile with sway show this type of behavior at higher external loads. This may be because pile section is not capable to withstand this loading condition and the moments induced due to the fixities.

Also it has been noticed that, at these stages pile deflection in the liquefied zone is very high compared to that of the ground displacement and M* is not occurring at the interfaces which are very rare phenomena. If pile deflection is more compared to the soil displacement then the direction of the force to the pile body is reversibly oriented and the basic assumption of the liquefied soil dragging the pile would become invalid.

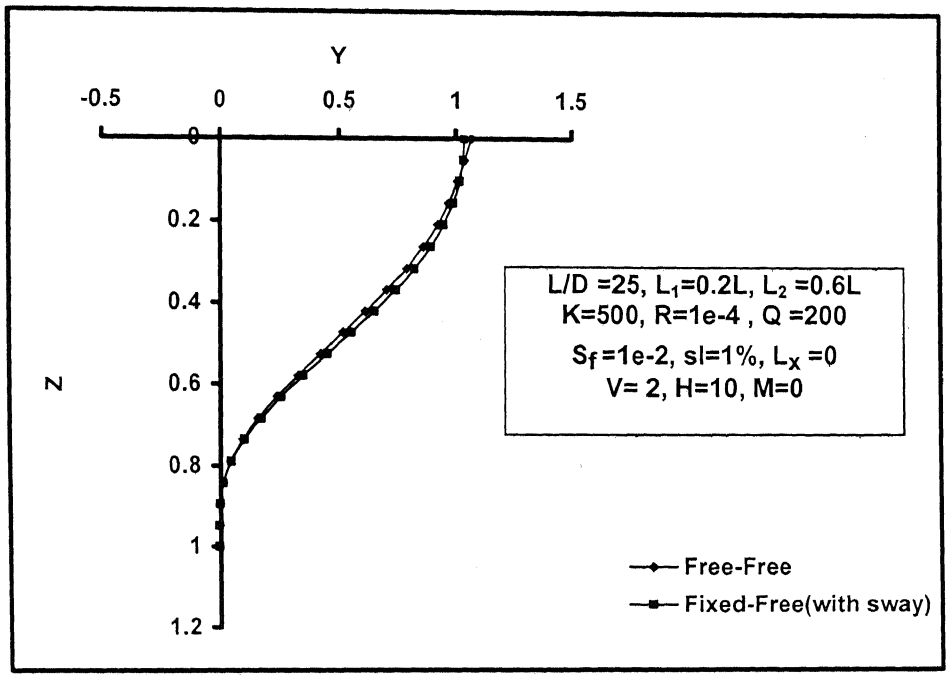


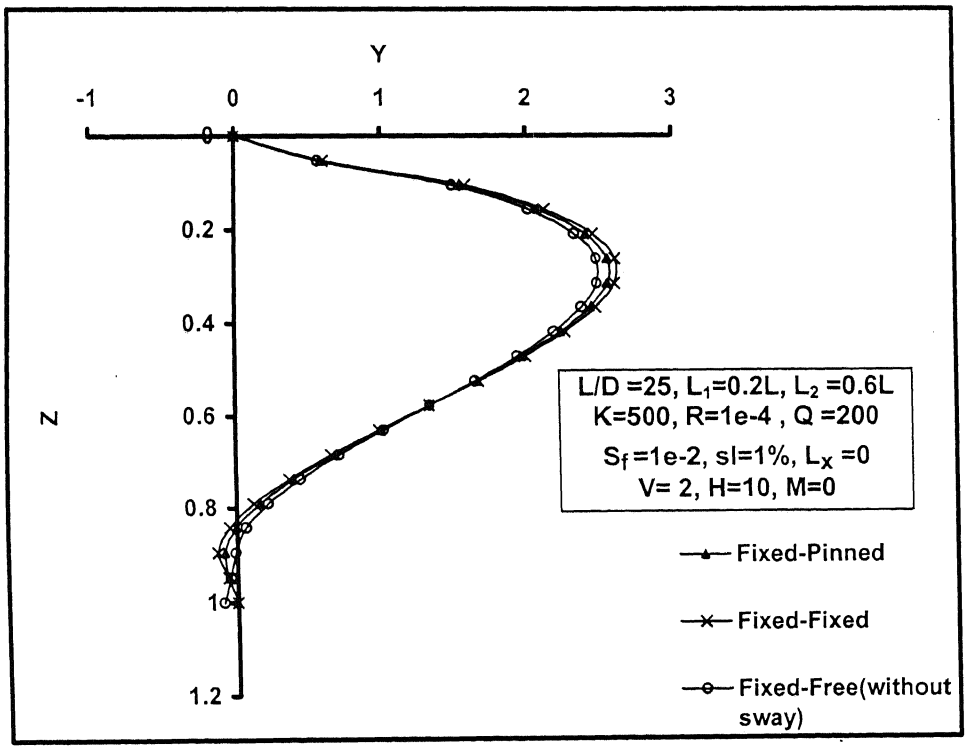


Fig.3.95 I Variation of Y with Z for different boundary conditions

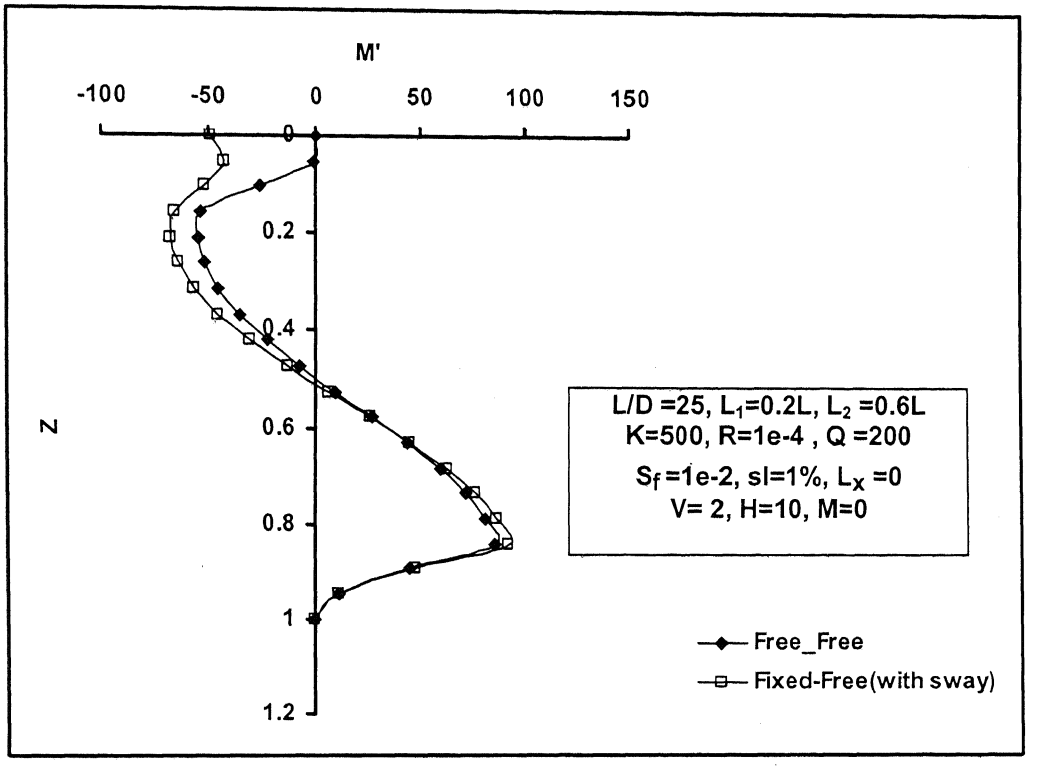


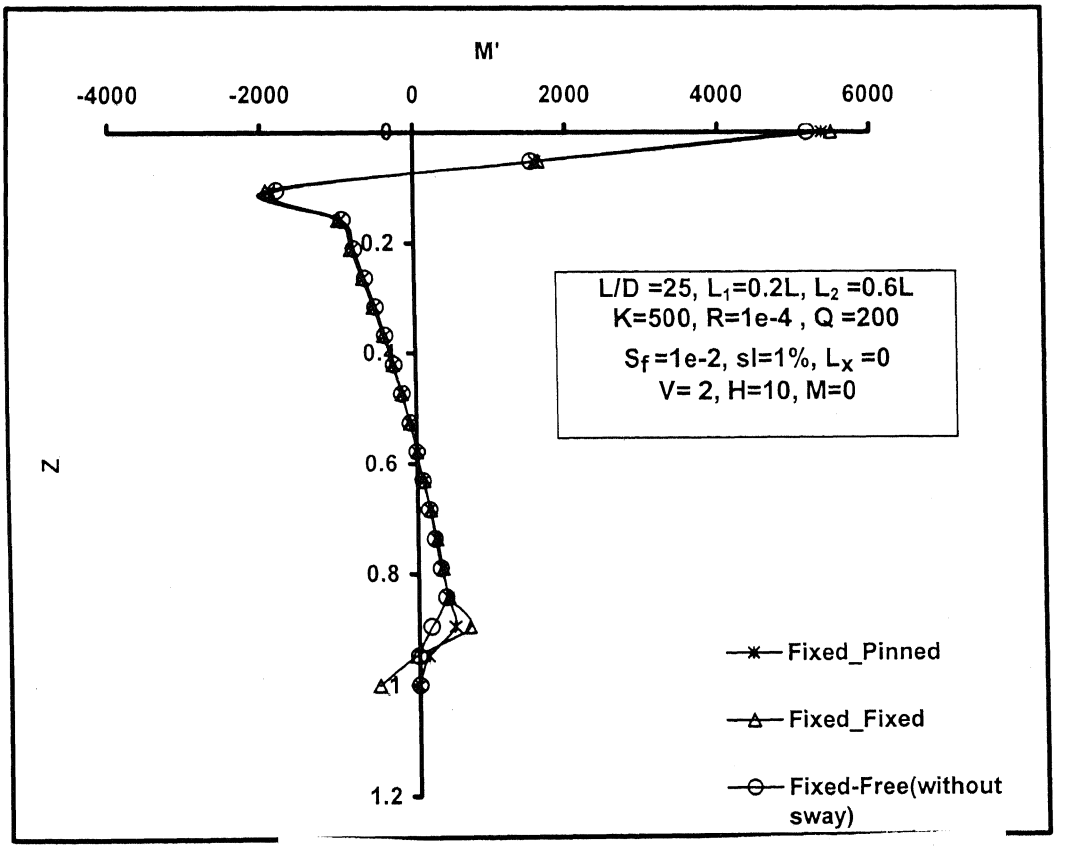


**Fig.3.96** Variation of M' with Z for different boundary conditions

# Chapter 4

# CONCLUSIONS

## 4.1 Inferences

The axial load has a significant importance on the response of pile foundations in lateral spreading areas. Several failures have been documented where soil liquefied during earthquakes. A pile which is otherwise safe under normal conditions may fail when it looses support from the surrounding soils due to either partial or full soil liquefaction. In addition to the loss of support the piles may experience large drag force due to the moving soil especially for riverfront structures. As the vertical load factor reaches a critical value, the pile may fail due to buckling. In the present study, the critical value of the vertical load factor is 7 and 6 for Free-Free pile and Fixed-Free pile respectively. For the given set of soil and pile properties considered in the present analysis, the predicted behavior of pile is not reliable when V exceeds 8.5. The developed bending moment will be very high at critical loading and it may exceed the yield moment of the section and hence the failure can take place. Therefore, the current method of pile design based on bending mechanism is not appropriate and for the safe design, consideration of axial loads also is very important.

Such a study had been undertaken in the present thesis, the details of which were presented in Chapter 3 and the following inferences are made from the results and discussions described presented there in.

1. The lateral loading affects mainly the pile head deflection. The 25% increase in lateral loading results in the 4% increase of head deflection and 4% decrease in bending moment.
2. Under combined loading, the lateral loads reduce the effect of axial load, if the vertical load factor is less than the critical value.
3. The variation of stiffness factor seems to have negligible effect on the flexural behavior of the piles. But it may affect if we consider any other axial load distribution profile.

4. The pile flexibility factor has an important influence on the pile deformation and it affects the critical load factor also. Increase in pile flexibility factor causes increase in deflection and bending moment under all loading and end conditions.

5. The ratio of the soil modulus to the undrained strength of the soil, Q, affects the pile behaviour in different ways under different conditions of loading. The force exerted by the laterally spreading soil manifest in increasing the bending moment only. Under lateral and combined loading, it decreases deflection and increases the bending moment.

6. Slenderness has an immense effect on the deformation and bending pattern of the piles in liquefiable areas. The pile should have a minimum diameter to keep the deflection and bending moment within permissible values. In the present study critical slenderness ratio is 25. When L/D = 50, the maximum deflection is more than twice the diameter.

7. The deflection and bending moment of the pile in lateral spreading areas are directly proportional to the gradient of surface topography. As the gradient varies from 1% to 50%, the maximum nondimensional deflection and bending moment coefficient increases by three times.

8. The depth of top non liquefied layer plays an important role in the flexural behaviour of piles in liquefiable areas. As the top nonliquefied depth increases from zero to 40% of the length of the pile, then the reduction in maximum deflection is around 30%. The densification of the soil in the liquefiable areas and a proper top nonliquefied soil cover will cause an appreciable reduction in the destruction.

9. The piles near water front suffer more damage and hence the design should take care of the location factor also. The Free-Free piles located at places away from waterfront (i.e. at $L_x$=0.5 in the present study) are experiencing 70% lesser deflection and 50% lesser bending moment compared to that at the waterfront.

10. The boundary conditions seriously affect the response of pile foundations subjected to any type of loading. The Fixed-Free pile with sway is found to be suitable in areas with sufficient top non-liquefiable layer. But a generalized conclusion can not be done on the

suitability of any particular end condition under all types of loading and soil profile condition. A proper choice depends on all the factors stated above.

11. The developed computer program can be used effectively to predict the deflection and bending moment of the piles under various conditions of loading, soil profile, and pile characteristics. There is a reasonable compliance between the predicted results and the field observations. The predicted maximum pile head deflection is exactly identical with the field observations. The predicted maximum bending moment has only 4% variation from the field observation and the predicted values are on the conservative side.

## 4.2 Scope of future work

More work is needed, combining centrifuge model experiments, case histories and analytical studies to improve the present understanding and to eliminate the uncertainties about actual physical mechanisms involved. Relationships should be developed to find the variation of stiffness degradation parameter with various aspects of soil properties and earthquake intensities. The effect of axial load and the relation between critical load and various influencing parameters have to be developed to ensure safe and economic design of piles in lateral spreading soils. Elasto-plastic analysis of the soil-structure interaction problem may be conducted.

# REFERENCES


1. Abdoun,T., and Dobry,R. (2002). "Evaluation of pile foundation response to lateral spreading." *Soil Dynamics and Earthquake Engineering,* 22, pp. 1051-1058.
2. Barlett,S.F., and Youd,T.L. (1995). "Empirical prediction of liquefaction induced lateral spread." *Journal of Geotechnical Engineering,* Vol.121, No.4, pp. 316-329.
3. Basudhar,P.K., Mishra,S.K., Maheshwari,P., and Das,S.K., (2002). "Flexural analysis of laterally loaded piles under liquefied soil conditions." *Proceedings Indian Geotechnical Conference, Geotechnical Engineering: Environmental Challenges.* Allahabad, India, pp.435-440.
4. Berrill,J.B., Christensen,S.A., Keenan,R.P., Okadas,W., and Pettinga,J.R., (2001). "Case study of lateral spreading forces on a piled foundation." *Geotechnique* 51, No.6, pp.501-517.
5. Bhattacharya,S., and Bolton,M.D., (2004). "A fundamental omission in seismic pile design leading to collapse." *Proceedings of the 11$^{th}$ International Conference on Soil Dynamics and Earthquake Engineering.* Berkeley, Vol.1, pp.820-827.
6. Bhattacharya,S., (2004). "A method to evaluate the safety of the existing piled foundations against buckling in liquefiable soils." *First International Conference on Urban Earthquake Engineering.* Tokyo, Japan, pp.339-346.
7. Bhattacharya,S., and Tokimatsu,K., (2004). "Essential criteria for design of piled foundations in seismically liquefiable areas." *Proceedings of the 39$^{th}$ Japan National Conference on Geotechnical Engineering.* Niigata.
8. Chaudhury,D., Toprak,S., and O'Rourke,T.D., (1995). "Pile response to lateral spread: a benchmark case." *Proceedings of the 4$^{th}$ U.S Conference.* San Francisco, California, pp.755-762.
9. Cubrinovski,M., Ishihara,K., and Furukawazono,K., (1999). "Analysis of full scale tests on piles in deposits subjected to liquefaction." *Proceedings of the 2$^{nd}$ International Conference on Earthquake Geotechnical Engineering.* Lisbon, Portugal, pp.567-572.
10. Finn,W.D.L., and Fujita,N. (2002). "Piles in liquefiable soils: seismic analysis and design issues." *Soil Dynamics and Earthquake Engineering,* 22, pp. 731-742.

11. Finn,W.D.L., (2004). "Urban earthquake engineering: foundation characterization for perfoemance based design." *First International Conference on Urban Earthquake Engineering.* Tokyo, Japan, pp.311-330.

12. Ishihara,K., (1997). "Geotechnical aspects of the 1995 Kobe earthquake." *Proceedings of the 14th International Conference on Soil Mechanics and Foundation Engineering.Terzaghi Oration.* Hamburg, pp.2047-2073.

13. Ishihara,K., and Cubrinovski,M., (1998). "Soil-pile interaction in liquefied deposits undergoing lateral spreading." *Geotechnical Hazards* (eds. By Maric, B. et al.). Balkema, pp.51-64.

14. Imamura,S., Hagiwara,T., Tsukamoto,Y., and Ishihara,K., (2004). "Response of pile groups against seismically induced lateral flow in centrifuge model tests." *Soils and Foundations,* Vol.44, No.3, pp.39-55.

15. Kawakami,T., Suemasa,N., Hamada,M., Sato,H., and Katada,T., (1994). "Experimental study on mechanical properties of liquefied sand." *Technical Report NCEER-94-0026,* NCEER, Buffalo, NY, pp.285-299.

16. Klar,A., Baker,R., and Frydman,S. (2004). "Seismic soil-pile interaction in liquefiable soil." *Soil Dynamics and Earthquake Engineering,* 24, pp. 551-564.

17. Mishra,S.K., (1992). "Analysis of laterally loaded piles under liquefied soil conditions." MTech Thesis, Indian Institute of Technology, Kanpur.

18. Miyajima,M., and Kitaura,M., (1994). "Experiments on force acting on underground structures in liquefaction-induced ground flow." *Technical Report NCEER-94-0026,* NCEER, Buffalo, NY, pp.445-455.

19. O'Rourke,T.D., Meyersohn,W.D., Shiba,Y., and Chaudhuri,D., (1994). "Evaluation of pile response to liquefaction-induced lateral spread." *Technical Report NCEER-94-0026,* NCEER, Buffalo, NY, pp.457-479.

20. Poulos,H.G., and Davis,E.H (1980). "Pile Foundation Analysis and Design", John Wiley and Sons, Inc, New York.

21. Sarma,C.R., (1983). "Analysis of single piles subjected to axial, lateral and combined loading." PhD Thesis, IIT Kanpur.

22. Tokimatsu,K., Oh-oka,H., Satake,K., Shamoto,Y., and Asaka,Y., (1998). "Effects of lateral ground movements on failure patterns of piles in the 1995 Hyogoken-Nambu

earthquake." *ASCE Geotechnical Earthquake Engineering and Soil Dynamics 3rd Conference*, pp.1175-1186.

23. Tokimatsu,K., (1999). "Performance of pile foundations in laterally spreading soils." *Proceedings of the 2nd International Conference on Earthquake Geotechnical Engineering.* Lisbon, Portugal, pp.957-964.
24. Tsukamoto,Y., Ishihara,K., Yamabe,S., and Hyodo,J., (1999). "Behaviour of piles in the liquefied deposit undergoing lateral spreading." *Proceedings of the 2nd International Conference on Earthquake Geotechnical Engineering.* Lisbon, Portugal, pp.377-382.
25. Sento,N., Goto,K., Namba,S., Kobayashi,K., Oh-oka,H., and Tokimatsu,K., (1999). "Case study for pile foundation damaged by soil liquefaction at inland site of artificial island." *Proceedings of the 2nd International Conference on Earthquake Geotechnical Engineering.* Lisbon, Portugal, pp.625-630.
26. Tokimatsu,K., and Suzuki,H., (2004). "Effects of dynamic soil-structure interaction on pile stress in large shaking table tests." *First International Conference on Urban Earthquake Engineering.* Tokyo, Japan, pp.331-338.
27. Tamari,Y., and Towhata,I., (2003). "Seismic soil-structure interaction of cross sections of flexible underground structures subjected to soil liquefaction." *Soils and Foundations,* Vol.43, No.2, pp.69-87.
28. Zhang,G., Robertson,P.K., and Brachman,R.W.I., (2004). "Estimating liquefaction induced lateral displacements using the standard penetration test or cone penetration test." *Journal of Geotechnical and Geoenvironmental Engineering,* Vol.130, No.8, pp.861-871.

# APPENDIX

***Development of finite difference equations.***

$$E_p I_p \frac{d^4 y}{dz^4} + \frac{d}{dz}\left[P_z \frac{dy}{dz}\right] + k_h D(y - g(z,x)) = 0$$

This equation can be written as follows

$$E_p I_p \frac{d^4 y}{dz^4} + \left[\frac{dP}{dz} \cdot \frac{dy}{dz}\right] + \left[P \cdot \frac{d^2 y}{dz^2}\right] + k_h D(y - g(z,x)) = 0$$

For node i the above equation can be written in central difference form as follows

$$\frac{E_p I_p n^4}{L^4}\left[y_{i-2} - 4y_{i-1} + 6y_i - 4y_{i+1} + y_{i+2}\right] +$$
$$\frac{n^2}{4L^2}(P_{i+1} - P_{i-1})(y_{i+1} - y_{i-1}) + \frac{n^2}{L^2} P_i (y_{i-1} - 2y_i + y_{i+1})$$
$$+ k_h D(y - g) = 0$$

$$\frac{E_p I_p n^4}{L^4}\left[y_{i-2} - 4y_{i-1} + 6y_i - 4y_{i+1} + y_{i+2}\right] +$$
$$= \frac{Pn^2}{L^2}\left\{\frac{1}{4P}(P_{i+1} - P_{i-1})(y_{i+1} - y_{i-1}) + \frac{P_i}{P}(y_{i-1} - 2y_i + y_{i+1})\right\}$$
$$+ k_h D(y - g) = 0$$

$$\frac{E_p I_p n^4}{L^4}\left[y_{i-2} - 4y_{i-1} + 6y_i - 4y_{i+1} + y_{i+2}\right] +$$
$$= \frac{Pn^2}{L^2}\left\{\left(\frac{\alpha_{i+1} - \alpha_{i-1}}{4}\right)(y_{i+1} - y_{i-1}) + \alpha_i (y_{i-1} - 2y_i + y_{i+1})\right\}$$
$$+ k_h D(y - g) = 0$$

$$\frac{E_p I_p n^4}{L^4}\left[y_{i-2} - 4y_{i-1} + 6y_i - 4y_{i+1} + y_{i+2}\right] +$$
$$= \frac{Pn^2}{L^2}\left[\left\{\alpha_i - \frac{(\alpha_{i+1} - \alpha_{i-1})}{4}\right\} y_{i-1} - 2\alpha_i y_i + \left\{\alpha_i + \frac{(\alpha_{i+1} - \alpha_{i-1})}{4}\right\} y_{i+1}\right]$$
$$+ k_h D(y - g) = 0$$

***Boundary conditions and the respective finite difference equations***

*Free-Free end condition*

Considering the free-free boundary conditions at the pile head and tip,

$E_p I_p y'' = M_T$, *at* $z=0$

$E_p I_p y'' = 0$, *at* $z=L$

Hence

$$E_p I_p \left(\frac{d^2 y}{dz^2}\right)_{i=1} = \frac{E_p I_p n^2}{L^2}(y_0 - 2y_1 + y_2) = M_T$$

*or*

$$y_0 = \frac{M_T L^2}{E_p I_p n^2} + 2y_1 - y_2$$

$$E_p I_p \left(\frac{d^2 y}{dz^2}\right)_{i=n+1} = \frac{E_p I_p n^2}{L^2}(y_n - 2y_1 + y_{n+2}) = 0$$

*or*

$$y_{n+2} = 2y_{n+1} - y_n$$

Using these values of $y_0$ and $y_{n+2}$, the differential equations at the nodes 2 and n can be written as

At node i=2,

$$\frac{E_p I_p n^4}{L^4}[-2y_1 + 5y_2 - 4y_3 + y_4] +$$

$$\frac{Pn^2}{L^2}\left[\left\{\alpha_2 - \frac{(\alpha_3 - \alpha_1)}{4}\right\} y_1 - 2\alpha_2 y_2 + \left\{\alpha_2 + \frac{(\alpha_3 - \alpha_1)}{4}\right\} y_3\right]$$

$$+ k_{h2} D(y_2 - g_2) + \frac{M_T n^2}{L^2}$$

At node i=n,

$$\frac{E_p I_p n^4}{L^4}\left[y_{n-2}-4y_{n-1}+5y_n-2y_{n+1}\right]+$$

$$\frac{Pn^2}{L^2}\left[\left\{\alpha_n-\frac{(\alpha_{n+1}-\alpha_{n-1})}{4}\right\}y_{n-1}-2\alpha_n y_n+\left\{\alpha_n+\frac{(\alpha_{n+1}-\alpha_{n-1})}{4}\right\}y_{n+1}\right]$$

$$+k_{h(n)}D(y_n-g_n)=0$$

*Fixed-Free (with sway) end condition*

In this case pile head is fixed against rotation but sway is allowed and the pile tip has free boundary condition.

$E_p I_p y' = 0$, *at* $z=0$

$E_p I_p y'' = 0$, *at* $z=L$

Hence $\left(\frac{dy}{dz}\right)_{i=1} = (y_2 - y_0) = 0, \therefore\ y_0 = y_2$

Using this value of $y_0$, the differential equations at the nodes 2 can be written as

At node i=2,

$$\frac{E_p I_p n^4}{L^4}\left[4y_1+7y_2-4y_3+y_4\right]+$$

$$\frac{Pn^2}{L^2}\left[\left\{\alpha_2-\frac{(\alpha_3-\alpha_1)}{4}\right\}y_1-2\alpha_2 y_2+\left\{\alpha_2+\frac{(\alpha_3-\alpha_1)}{4}\right\}y_3\right]$$

$$+k_{h2}D(y_2-g_2)=0$$

*Fixed-Free (with no sway) end condition*

In this case pile head is fixed against rotation and sway is also restricted and the pile tip has free boundary condition.

$E_p I_p y' = 0$ & $E_p I_p y = 0$, *at* $z=0$

$E_p I_p y'' = 0$, *at* $z=L$

Hence, $\left(\frac{dy}{dz}\right)_{i=1} = (y_2 - y_0) = 0, \therefore\ y_0 = y_2, \& y_1 = 0$

For node i=2,

$$\frac{E_p I_p n^4}{L^4}[7y_2 - 4y_3 + y_4] +$$

$$\frac{Pn^2}{L^2}\left[-2\alpha_2 y_2 + \left\{\alpha_2 + \frac{(\alpha_3 - \alpha_1)}{4}\right\} y_3\right]$$

$$+k_{h2} D(y_2 - g_2) = 0$$

*Fixed-Pinned end condition*

In this case pile head is fixed against rotation and sway is also restricted and the pile tip is supported.

$E_p I_p y' = 0$ & $E_p I_p y = 0$, *at* $z=0$

$E_p I_p y'' = 0$ & $E_p I_p y = 0$, *at* $z=L$

Hence

$$y_{n+1} = 0$$

$$E_p I_p \left(\frac{d^2 y}{dz^2}\right)_{i=n+1} = \frac{E_p I_p n^2}{L^2}(y_n - 2y_{n+1} + y_{n+2}) = 0$$

$$\therefore y_{n+2} = -y_n$$

For node i=n,

$$\frac{E_p I_p n^4}{L^4}[y_{n-2} - 4y_{n-1} + 5y_n] +$$

$$\frac{Pn^2}{L^2}\left[\left\{\alpha_n - \frac{(\alpha_{n+1} - \alpha_{n-1})}{4}\right\} y_{n-1} - 2\alpha_n y_n\right]$$

$$+k_{h(n)} D(y_n - g_n) = 0$$

*Fixed-Fixed end condition*

In this case pile head is fixed against rotation and sway is also restricted and the pile tip is also fixed.

$E_p I_p y' = 0$ & $E_p I_p y = O$, at $z=0$

$E_p I_p y' = 0$ & $E_p I_p y = 0$, at $z=L$

Hence

$$y_{n+1} = 0$$

$$(y_{n+2} - y_n) = 0 \therefore y_{n+2} = y_n$$

For node i=n,

$$\frac{E_p I_p n^4}{L^4}\left[y_{n-2} - 4y_{n-1} + 7y_n\right] +$$

$$\frac{Pn^2}{L^2}\left[\left\{\alpha_n - \frac{(\alpha_{n+1} - \alpha_{n-1})}{4}\right\} y_{n-1} - 2\alpha_n y_n\right]$$

$$+k_{h(n)} D(y_n - g_n) = 0$$